UNIVERSITY OF OKLAHOMA

GRADUATE COLLEGE

LOW-MOLECULAR-WEIGHT BRANCHED POLYETHYLENIMINES: MULTIFUNCTIONAL BETA-LACTAM POTENTIATORS AGAINST RESISTANT GRAM-NEGATIVE PATHOGENS

A DISSERTATION

SUBMITTED TO THE GRADUATE FACULTY

in partial fulfillment of the requirements for the

Degree of

DOCTOR OF PHILOSOPHY

By

HANNAH RUTH PANLILIO LAMB

NORMAN, OKLAHOMA

2022

LOW-MOLECULAR-WEIGHT BRANCHED POLYETHYLENIMINES: MULTIFUNCTIONAL BETA-LACTAM POTENTIATORS AGAINST RESISTANT GRAM-NEGATIVE PATHOGENS

A DISSERTATION APPROVED FOR THE

DEPARTMENT OF CHEMISTRY AND BIOCHEMISTRY

BY THE COMMITTEE CONSISTING OF

DR. CHARLES V. RICE (CHAIR)

DR. CHRISTINA BOURNE

DR. KARA DE LEON

DR. LAURA-ISOBEL MCCALL

Dedication

Dedicated to my *parents*. Thank you for your sacrifice that I may have a bright future.

Salamat pu.

I thank and praise you, God of my ancestors:
You have given me wisdom and power,
you have made known to me what we asked of you,
you have made known to us the dream of the king.
Daniel 2:23

Acknowledgements

This work was envisioned and made to completion with the help and support of many people in my life. I would like to express my deepest gratitude to my research advisor, Dr. Charles V. Rice, for his mentorship and guidance throughout my graduate studies. Dr. Rice challenged me to be a better scientist while encouraging me to be a better person. I would also like to acknowledge Toni Rice for her support and wisdom. Toni and Dr. Rice truly became my secondary parents, I am very grateful.

I would also like to thank the Rice Research Group and everyone who has been a part of it. A special thanks is directed to Dr. Anh Lam who trained me *very* well in my initial years of graduate school. I learned a variety of techniques and critical thinking skills from her. I would also like to thank the graduate students in the lab: Neda Heydarian, Tristan Haight, William Best and Chase Roedl. Thank you for the opportunity to share ideas with you. An immense gratitude is also owed to the army of undergraduate students in the Rice Lab. I would like to specifically mention Jennifer Pusavat, Andrew Neel, and Maya Ferrell for all the contributions they have made in this work.

Besides my advisor and research group, I would also like to thank my committee members and professors for the scientific guidance they have extended. I would like to thank Dr. Christina Bourne for her very helpful insights about this work, Dr. Laura-Isobel McCall for helping me think about the details of my project often, and Dr. Kara De León for sharing her expertise in microbiology. I would also like to thank former members of my committee, Dr. George Richter-Addo and Dr. Bradley Stevenson. Thank you for helping me develop my project and ask the right questions. Thank you also to Dr. Tingting Gu and Dr. Preston Larson for all their help with light

and electron microscopy. I would like acknowledge Dr. Phil Bourne in the Protein Production Core for helping me develop and troubleshoot my ITC experiments. Thank you to Dr. Rama Kothapalli and Dr. Susan Nimmo as well; they were very helpful mentors in my graduate studies.

My family and friends helped me live a full life while in graduate school. Friendships helped me run the marathon of graduate school with endurance. Hence, I want to specifically mention the people who I ran with. I would like to thank Danya Dean, for the friendship, the encouragements, and the joy that she brought. A special thanks to Leena Nabulsi, for her passion for the Lord. Thank you to Sarah Mauer for the life-giving conversations when I felt like giving up. Thank you also to Jenna Mann for the way she listens and exhorts. I would also like thank my parents for immigrating to the U.S. and sacrificing their lives so that I can have a better future. I thank my family in the Philippines for always being supportive of my dreams.

This acknowledgement section would not be complete without mentioning my deep sense of gratitude to my husband, Zachary Lamb. Thank you for letting me practice my presentations with you and letting me talk about research *a lot*. Thank you for keeping me upright when graduate school got difficult and for rejoicing with me in seasons of celebration. I could not have done all this work without your encouragement and support.

Lastly—and most certainly not the least, I would like to thank God. Thank you for your abundant grace in my life.

List of Tables

List of Figures

Abstract

Antibiotic resistance is a simmering threat to the global public health system. Currently, it is estimated by the Centers for Disease Control and Prevention that at least 2.8 million people in the US get infected with antibiotic resistant bacteria annually. Among these resistant pathogens are the multidrug resistant (MDR) *Pseudomonas aeruginosa* and carbapenem-resistant *Enterobacteriaceae* (CRE). These resistant pathogens employ various mechanisms such as developing biofilms, transferring genetic elements to convey resistance genes (i.e via extracellular DNA), and employing beta-lactamase enzymes to degrade or evade existing antibiotics. To combat these pathogens, much focus is directed toward identifying new antibiotic classes and modifying known antibiotic scaffolds through high throughput screenings and synthesis. However, these efforts are still moving very slowly. Hence, there is a crucial need for new strategies in battling these life-threatening infections. One way to address this issue is by implementing a co-treatment approach where an anti-resistant potentiator compound is co-administered with existing drugs. Findings from our lab suggest that low-molecular weight branched polyethylenimine (600 Da BPEI) and its poly(ethylene glycol) (PEG)ylated derivative (PEG-BPEI) can potentiate existing beta-lactams and disrupt biofilms. These multi-function potentiators have the ability to chelate essential metal ions involved in the beta-lactamase functions, bind eDNA, improve the uptake of antibiotics, and dissolve mature biofilms. Furthermore, previous findings suggest that 600 Da BPEI can suppress the production of the proinflammatory cytokine IL-8 in human epithelial keratinocytes. Thus, these potentiators may simultaneously work as anti-inflammation and infection prevention agents. These results expand the possible utility of 600 Da BPEI and its derivative, PEG-BPEI, as clinically useful broad-spectrum wound healing agents

Chapter 1: "What is a biofilm and why does it matter?"

Background and Significance

A global health crisis is growing due to antibiotic resistance. Antibiotics were first prescribed to treat severe infections after Alexander Fleming discovered penicillin in the 1940's. Over time, various classes of antibiotics that target different bacterial machineries were introduced to the market. However, in recent years, the rate of discovery of new antibiotic classes has stagnated whereas the rate of antibiotic consumption has continued to increase[1]. As a result, antibiotic resistance can emerge as bacteria respond to therapeutic treatments. The Centers for Disease Control and Prevention reports that at least 2.8 million people get infected and at least 35,000 die because of antibiotic resistant bacteria in the United States annually[2]. In Europe, an estimated number of 25,000 deaths are associated to antibiotic resistant bacteria[3]. Greater than 30,000 deaths per year are reported in countries like Thailand as well as increasing variants of antibiotic resistant bacteria emerging in South America, the Middle East, and Asia [4]. In addition to these statistics, neonatal sepsis attributed to antibiotic resistance are increasing in Tanzania and Mozambique, and approximately 58,000 neonatal sepsis deaths related to antibiotic resistance are reported in India[5].

Bacteria have acquired different resistance mechanisms to overcome clinical treatments and one of these is the development of biofilms. Biofilms are dynamic communities of bacterial organisms encapsulated in a thick matrix of extracellular polymeric substance (EPS) that affixes the cells in close proximity to each other and facilitates the transfer of nutrients, waste, quorum sensing, and genetic material[6-7]. Bacteria in biofilms have stronger resilience compared to

planktonic bacteria because the biofilm EPS serves as a physical shield against potential dangers in their environment (i.e. antibiotics, antibacterial agents, shear stress). Bacterial aggregation and eventual biofilm maturation occur in different stages and require species-specific conditions[7]. The first step of biofilm formation involves bacteria adhering on to a surface (either biotic or abiotic)—a step driven by a delicate balance of attractive or repelling forces. Bacterial adhesion on an abiotic surface is primarily driven by non-specific (i.e. hydrophobic interactions) forces while adhesion to biotic surfaces is usually driven by molecular mechanisms (i.e adhesins, lectins, etc.)[8]. The non-specific initial attachment is reversible, which allows the bacteria to return to the planktonic population[9]. In addition, electrostatic interactions can cause charge-charge attraction or repulsion between the cells and surface. Irreversible attachment can be achieved by species-specific adhesins on the cell surface that bind to the substrate and withstand detaching forces. After attachment, cell-to-cell adhesion occurs as adjacent cells are connected by various EPS components [7]. These physio-chemical interactions (hydrogen bonding, Van der Waals, electrostatic, etc.) between cells and EPS components create a stable biofilm matrix. As cell-to-cell adhesion increases, biofilm proliferation enables a dynamic biofilm community to grow, and as the biofilms develop to maturity, cell dispersal becomes possible. Cell dispersal is achieved by shedding of daughter cells of actively growing cells, nutrient deficiency, quorum sensing (QS), and/or shear stress[6]. Controlled cell-dispersal allows bacteria to scatter in a free-floating planktonic state and establish other biofilm populations elsewhere. Controlled dispersal benefits the pathogens and their ability to invade and overrun the host's immune responses. Moreover, bacteria can also respond to their environment and gauge whether it is more beneficial to reside in the biofilm or join the planktonic population[7]. Through the development of these biofilms, resilience against antimicrobial agents increases, making pathogens difficult to eliminate. Therefore, advances in understanding the

structure and molecular mechanisms of biofilm organization are critical in the fight against these deadly pathogens[10].

Biofilm Components

The EPS of biofilms is composed of proteins, exopolysaccharides, extracellular DNA (eDNA), RNA, water, secondary metabolites (e.g. pyocyanin, rhamnolipids), and, in some cases, iron-scavenging siderophores [11-13]. These components assemble into a rigid matrix that protects the encased bacterial cells (Figure 1). Biofilm matrix proteins help cells attach to surfaces, stabilize the biofilm, and modulate the structure of the matrix[14]. Exopolysaccharides are natural polymers composed of biomacromolecules that can have positive or negative charges. Exopolysaccharides like poly N-acetylglucosamine (PNAG) and alginate are crucial to intercellular adhesion, structural support, and protection from the environment[15-17]. Some exopolysaccharides are pathogen-specific. *Pseudomonas aeruginosa* can encode exopolysaccharides, Pel and Psl, in their biofilms, which are important in cell-cell and cell-surface interactions[17]. However, exopolysaccharides (i.e. Pel, Psl) are not necessarily required for *all* biofilms; some strains of *P. aeruginosa* were reported to produce exopolysaccharide-independent biofilms[18]. Such biofilms were mediated with extracellular DNA and "other" biofilm components. Extracellular DNA was reported to be required in the initial establishment of *P. aeruginosa* biofilms but not in *Neisseria meningitidis* and *Listeria monocytogenes*[19]. Extracellular DNA are extracellular nucleic acid biopolymers critical to the integrity of the biofilm matrix by stabilizing charges, providing structural rigidity, and protecting the matrix from host defense responses. Lastly, the secondary metabolites and RNA found in the biofilm matrix are linked to nutrient maintenance, housekeeping, gene expression and biofilm fitness[13, 20].

Purpose of this Review

Recently, the importance of eDNA in biofilm formation, cell-to-cell adhesion, cell signaling, and maintaining the structural stability of the biofilm matrix was better recognized. Its significance was overlooked until 2002, when Whitchurch et al. used DNAse I to disrupt biofilms of *P. aeruginosa*[21]. Disrupting biofilms allowed antibiotics to reach the cells, which resulted in enhanced bactericidal efficiency. Since then, eDNA has become the focus of many research efforts. In a 2015 review by Okshevsky et al., the importance of eDNA in biofilms was highlighted along with detailed descriptions of its production, adhesion, and role in microbial biofilms[22]. In addition, the review suggested that researchers should examine strategies that destabilize the interactions between eDNA and other biomolecules in the biofilm matrix to disrupt biofilms. Over the last five years, additional work has been done to investigate and target eDNA interactions in biofilms. In this review, we will include recent developments, emphasizing potential routes that can be employed to disrupt biofilms. We will focus on works that used eDNA as a target and those that elucidated the interactions of eDNA with other biofilm components.

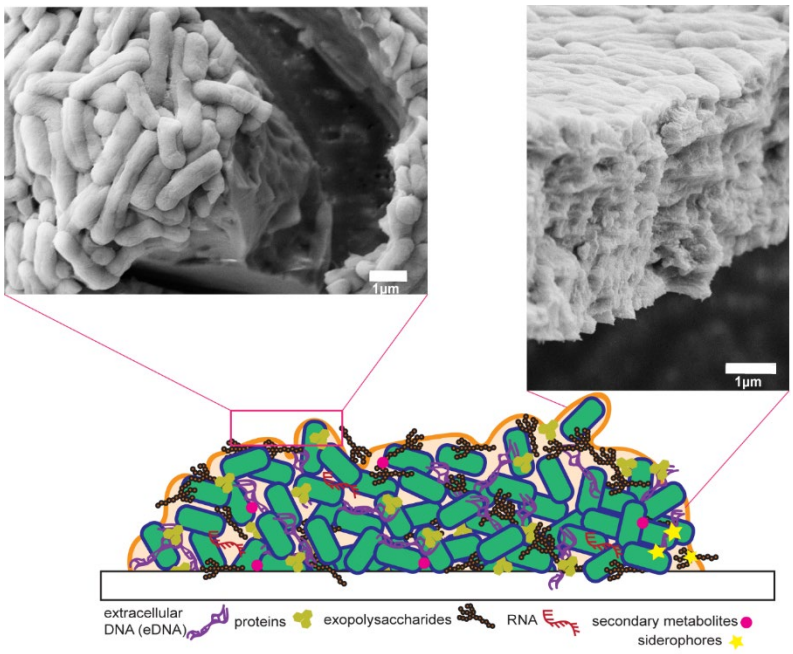

Figure 1. Illustration of a biofilm of bacterial cells (green) showing proteins, exopolysaccharides, RNA, secondary metabolites, siderophores, and eDNA in the matrix. Scanning Electron Microscopy images of *Escherichia coli* biofilms show high density

Extracellular DNA (eDNA) in Biofilms:

Extracellular DNA vs chromosomal DNA

Deoxyribonucleic acid (DNA) is a ubiquitous molecule that contains genetic material of living cells. The DNA of a bacterial cell is packaged as either linear or a single-looped double-stranded molecule called the genome. This chromosomal DNA, which is usually found in the cell, is also referred to as genomic DNA (gDNA). In addition to gDNA, bacteria also have small circular DNA called plasmids. Plasmids are extrachromosomal stretches of DNA that replicate distinctly from the gDNA. Furthermore, DNA can exist outside the cell; “eDNA” is a term generally used to denote DNA not enclosed in the cell. However, for the purposes of this review, we use the term “eDNA” to indicate genetic material within the biofilm matrix.

Genomic DNA and eDNA may originate from the same cell, but they are not always structurally or compositionally identical. Upon release to the biofilm environment, DNA may or may not undergo structural fragmentations that can alter its function. For example, explosive lysis of *P. aeruginosa* causes the release of intact (non-fragmented) eDNA[23]. Cell lysis refers to the breaking down of the cell membrane caused by environmental stress or other triggers. Lysis happens when the bacterial cell wall is weakened allowing osmotic pressure to rupture the cell membrane[24]. In a study conducted by Deng et al., it was observed that hyperbiofilm-forming Rugose small colony variants (RSCV) of *P. aeruginosa* cells release mostly fragmented eDNA. These RSCV isolated from chronic infections exhibit high resistance to antibiotics and are mostly unaffected by DNA enzymatic treatment (DNase I). In this study, it appears that biofilms form more abundantly around fragmented eDNA than around intact eDNA. In addition, when digested genomic DNA was added on the ATCC strain PAO1, biofilm formation was enhanced. Deng et al. attributed this enhancement to the increased interaction of fragmented eDNA with biofilm matrix proteins. Nevertheless, the specific fragmentation mechanism of eDNA—whether it occurs inside the cell or outside the cell within the biofilm matrix—still remains unclear and requires further investigation[25]. Similarly, in *Acinetobacter* sp., eDNA originates from genomic DNA, but the two types of eDNA are not structurally identical[26]. Using Random Amplification of Polymorphic DNA (RAPD) analysis, gDNA and eDNA extracted enzymatically were compared. This analysis revealed different patterns of DNA bands between the two yet having identical genomic sequences. This further suggests that gDNA is released through cell lysis but may undergo physical/chemical changes. These eDNA structural differences may be caused by environmental stresses or other interactions in the biofilm that can degrade the nucleic acids. For compositional similarity, chemical analysis of *P. aeruginosa* biofilms revealed no distinction

between eDNA and genomic DNA[27] but when comparing eDNA and genomic DNA of multi-species biofilms, differences in composition were observed[28]. Overall, these studies suggest that, although eDNA and gDNA show structural differences, their compositional similarities (primary sequences) indicate that eDNA likely originates from the bacteria themselves.

eDNA in Gram-positive bacteria

Extracellular DNA is important for Gram-positive *Staphylococcus* biofilms. Most, if not all, strains of *Staphylococcus aureus* have eDNA in their biofilms with varying levels depending on culture conditions[29]. Similarly, in a closely related species, *Staphylococcus epidermidis*, eDNA is also important in biofilm-formation. In a review by Montanaro et al., comparison of two clinical isolates of *S. epidermidis* from implant infections showed that a biofilm-forming strain (RP62A) produce more eDNA relative to the weak-biofilm-forming one (ATCC 12228) after 72 hrs[30]. Comparing these two *Staphylococcal* species, it was reported that more eDNA was produced in *S. epidermidis* biofilms after 24 hours in comparison to *S. aureus*[31]. Further comparison of the two species shows that there is a time-based differential production of eDNA between them. The difference in eDNA production is due to the mechanism of eDNA release of each species—*S. aureus* bacterium releases eDNA through cell lysis, whereas *S. epidermidis* bacterium uses an autolysin protein (AtlE) for eDNA release[31-32]. This means that eDNA in *S. epidermidis* biofilms is released earlier compared to *S. aureus* biofilms. The early release of eDNA may cause the difference in observed eDNA concentrations.

Extracellular DNA is also critical for other Gram-positive bacteria. In addition to the *Staphylococcus* genus, the biofilms of another Gram-positive bacterium, *Bacillus licheniformis,* are composed mainly of polymers and eDNA[33]. Biofilms of *Listeria monocytoge*nes also contained eDNA, with higher concentrations observed in diluted media compared to nutrient-rich media.

Cell lysis and subsequent eDNA release are triggered by low-nutrient concentrations of media that create low ionic strength environments[19]. Pathogens likely release eDNA to help scavenge nutrients in order to survive. Similar importance of eDNA was also noted for *Streptococcus intermedius*[34], *Streptococcus mutans*[35], and *Clostridioides difficile*[36] biofilms.

eDNA in Gram-negative bacteria

Similar to Gram-positive bacteria, eDNA is also important for Gram-negatives. The importance of eDNA was noticed by Whitchurch et al., who discovered that eDNA is an essential component of the Gram-negative, *P. aeruginosa* biofilms[37]. This finding was further confirmed after identifying eDNA as an abundant component of the flow-grown EPS of *P. aeruginosa* biofilms[38]. Additionally, the amount of eDNA was positively correlated with the biomass thickness of *Burkholderia pseudomallei* biofilms, regardless of the ratio of living and dead bacterial cells within the biofilms. This finding suggests that it is not only through cell death/lysis that eDNA is released[39]. Uropathogenic *E. coli* (UPEC) also incorporate eDNA in their biofilms, of which bacterial DNA-binding protein (DNABII) are also critical components[40].

eDNA production and release

Biofilm eDNA is secreted in various ways (Figure 2), and different microorganisms have different modes of releasing eDNA. Most eDNA production mechanisms in bacterial organisms is lysis-related [41]. Lysis is the most obvious route of releasing DNA since the bacterial genome is often stored within the cytoplasm. Furthermore, a bacterial cell population can control this lytic process. Autolysis is a self-mediated destruction of the cell by its own enzymes (i.e. lysosomal enzymes like gelatinase, serine protease, autolysins), which can be beneficial to the overall population of surviving species[42-43]. In addition to lysis, eDNA can also be released into the biofilm

matrix via membrane vesicles[44]. This phenomenon is not surprising since bacteria usually use membrane vesicles to transport macromolecules (i.e. DNA, RNA, proteins, etc.)[45]. In addition, prophage-mediated eDNA release was reported where lysogenic phages caused lysis of planktonic *Streptococcus pneumoniae* releasing more eDNA into the biofilm matrix [46]. In this study, about six-fold increase in eDNA was observed in strains carrying prophages and phage lysins. Spontaneous phage induction contribute greatly to the abundance and localization of eDNA in these biofilms[46]. Similarly, autolysis does not seem to occur for *Bacillus subtilis*. Early competence genes are found to regulate eDNA release for undomesticated *B. subtilis* cells, and eDNA production is controlled by the ComX-ComP-ComA system[47]. In the same study, *B. subtilis* cells were transformed by eDNA suggesting the function of eDNA in horizontal gene transfer and social behavior. In addition to these mechanisms, many unknown pathways of eDNA production still need to be identified.

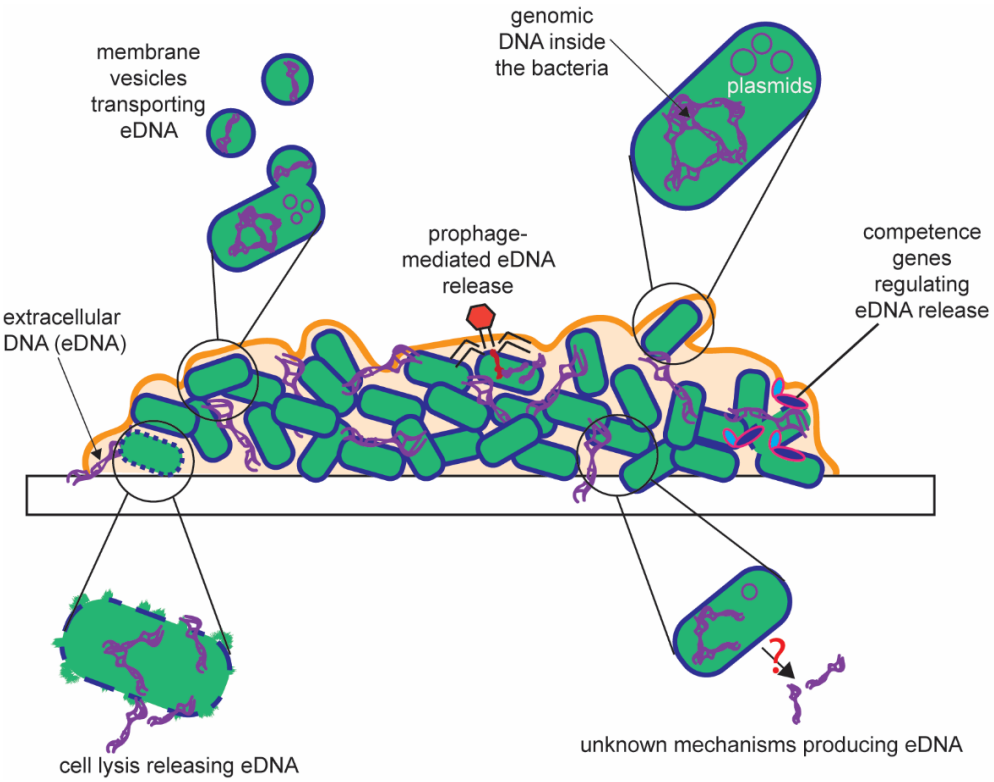

Figure 2. Illustration of eDNA in biofilms of bacterial cells (green) and how it is secreted into the biofilm matrix. Exopolysaccharides and other biofilm components not shown for simplicity

For many bacterial species, autolytic eDNA release is reported to be facilitated by Quorum Sensing (QS). QS regulates bacterial communication within the biofilm, which relies on signaling molecules that are detected by the surrounding bacterial population[48]. For *Staphylococcus epidermidis*, QS-dependent eDNA secretion is mediated by autolysins[49] and for *Enterococcus faecalis*, by both gelatinase (GelE) and serine protease (SprE) [43]. Large amounts of eDNA were also observed to be released in *P. aeruginosa* biofilms through a QS-dependent mechanisms involving N-acyl-L-homoserine lactones (AHL) and the *Pseudomonas* quinolone signal (PQS) in planktonic cell cultures[27]. In a recent study, it was reported that 4-hydroxy-2-alkylquinolines (HAQs) molecules and PrrF small noncoding RNAs both play important roles in signaling eDNA

release within *P. aeruginosa* biofilms[50]. According to their findings, sub-MIC (below the minimum inhibitory concentration) exposure to tobramycin, led to increased levels of HAQs in *P. aeruginosa* H103 strain, and the *ΔprrF* mutant released less eDNA compared to the wild type strain. One of the HAQ's observed in this study is 2-n-heptyl-4-hydroxyquinoline-N-oxide (HQNO), a *P. aeruginosa* QS-regulated molecule, that disrupts the flow of electrons through the respiratory chain[51]. HQNO induces the production of reactive oxygen species (ROS), which results to cell membrane damage and consequent eDNA release[50]. QS also regulates the production of phenazines in *P. aeruginosa* species. Phenazines are nitrogen-containing heterocyclic compounds produced by bacteria with a wide array of biological functions (e.g. electron shuttles, cell signaling molecules, etc.)[52]. One phenazine to take note of is pyocyanin (PYO), which is activated by the LasR/LasI and RhlR/RhlI QS systems[52]. PYO is reported to promote *P. aeruginosa* biofilm formation by also producing ROS such as H_2O_2, which results to cell lysis and subsequent eDNA release[53]. Lastly, for *Pseudomonas putida* biofilms, recent findings suggest that eDNA release is induced under Cu^{2+} stress. The amount of eDNA produced in the biofilm is increased significantly, which is attributed to increase copper resistance [54]. This response shows social behavior and the ability of the bacterial population to detect and react to its environment.

It is widely accepted eDNA originates from chromosomal DNA but it is also proposed that, for infectious biofilms that develop *in vivo*, eDNA also comes from the host [55-57]. For example, human neutrophils were shown to enhance the formation of *P. aeruginosa* biofilms by a. decreasing the number of viable bacteria in the first 4 h of incubation, which increases nutrient availability for the surviving more-fit bacteria, and b. providing actin and DNA to the biofilm matrix, which enhances polymerization[56]. On another hand, it was recently observed that *P. aeruginosa* grown in murine implants formed biofilms with eDNA only localizing outside the

matrix rather than inside the biofilm[58]. This observation greatly challenges many of the *in vitro* studies mentioned in this review that show localization of eDNA within the matrix. In this study, polymorphonuclear leukocytes (PMNs), a type of immune cells, showed cell membraned damage due to exposure to the infectious bacteria[58]. Based on their observations, the authors suggest that PMN-derived (or host-derived) DNA is not incorporated into the biofilms *in vivo*. Instead, the eDNA from necrotic PMN of the host aggregates outside the biofilms. Further investigations and comparisons still need to address this gap in our knowledge. It could be that DNA of PMNs inhibit eDNA release or simply that eDNA is less detectable than PMN DNA.

Identifying specific eDNA release mechanisms of pathogens is important in understanding its role in the biofilms. For example, the production of eDNA is different between the two Staphylococcal species, *S. aureus* and *S. epidermidis*. It was previously reported that eDNA is a major structural component of mature *S. aureus* biofilms but only a minor component for *S. epidermidis*. In the same study, DNAse I treatment inhibited biofilm formation of both *Staphylococcal* strains but detached only the 24-hr old pre-formed *S. aureus* biofilms and not the 24-hr old pre-formed *S. epidermidis* biofilms[59]. The observed results resulted to an assumption that eDNA is not a substantial component of mature *S. epidermidis* biofilms. However, in another study, Qin et al. dispersed about half of the 6-hr old pre-formed *S. epidermidis* biofilms while also using DNAse I[49]. Qin et al. also gave further evidence that the eDNA release in *S. epidermidis* is mainly mediated by the autolysin protein, AtlE. As discussed previously, eDNA is released earlier in *S. epidermidis*; therefore, dispersal of its young biofilms with DNAse treatments is more effective. Moreover, this finding emphasizes the significance of understanding eDNA release mechanisms in applying antibiofilm treatments.

Investigations were also conducted to understand if increased eDNA production meant abundant biofilm formation. Tang et al. found no correlation between the two, but they still proposed that eDNA is important to the biofilms even in low concentrations[60]. Regardless of the quantity, the importance of eDNA in the initial adhesion and biofilm formation is observed throughout various bacterial genera.

Known Functions of eDNA

Extracellular DNA aids in the structural integrity of the biofilm matrix, as wells as bacterial adhesion, metal chelation, metabolic vitality, antibiotic resistance, and horizontal gene transfer (Figure 3). It is critical in bacterial attachment and aggregation of biofilms on surfaces especially in the early stages of biofilm formation[61-62]. It is hypothesized that eDNA increases the hydrophobicity of the cell envelope, which allows the cells to adhere more easily to surfaces[62]. Other than serving as a biofilm adhesive, eDNA was also observed to promote biofilm dispersion by preventing swarmer motile cells to settle in the existing biofilm[63]. When eDNA interacts with the "sticky" surface-binding regions of the cells, dispersal of bacterial population become possible, and allows them to form bacterial population to form new biofilms elsewhere. Another function of eDNA is facilitating phenazine (i.e. PYO) retention and redox recycling for extracellular electron transfer (EET) in the biofilm [64]. This finding highlights the function of eDNA in the overall biofilm fitness. EET and redox cycling allow metabolic vitality to bacterial populations within the biofilm that lack access to electron acceptors and donors[64]. Additionally, eDNA can chelate cations activating resistance mechanisms in *P. aeruginosa* strains[65]. By chelating divalent metal ions that stabilize the LPS layer of Gram-negative bacteria, LPS modifications are triggered thereby "hiding" the bacteria from host defense systems and antibiotics [66]. Furthermore, eDNA

contributes to antibiotic resistance by directly inactivating cationic antibiotics[55, 67]. Besides physio-chemical interactions, eDNA also participate in horizontal gene transfer, which is the non-sexual transfer of genetic information between genomes[47, 68]. This process is important in the virulence and the evolutionary fate of the bacterial population.

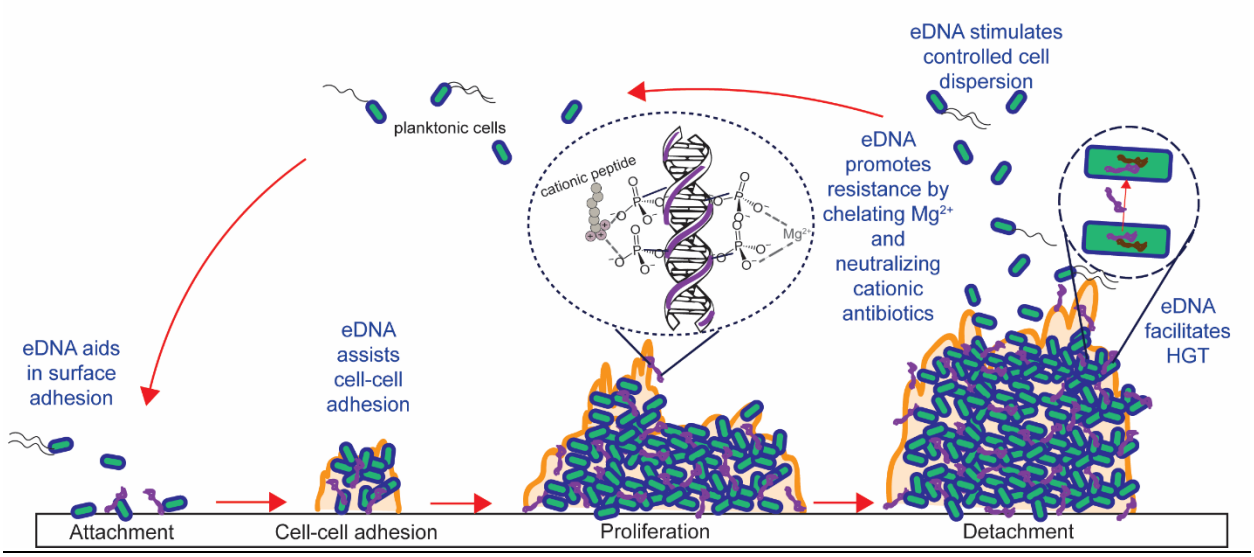

Figure 3. Life cycle of biofilms depicting functions of eDNA in the attachment, cell-cell adhesion, biofilm proliferation, detachment/dispersion, antibiotic resistance, and horizontal gene transfer (HGT).

Structural and chemical modifications of DNA

DNA, in general, can exist in different structural conformations: A-DNA, B-DNA, and Z-DNA forms[69]. The most common form in most living cells is B-DNA. To the best of our knowledge, B- and Z-forms are the only conformations directly found in functional living systems. Increasing evidence suggest that non-B conformations result in a number of diseases[70]. The changes in conformation (e.g. from B- to non-B) are induced by a variety of conditions (i.e. hydration level, chemical modifications of bases, presence of metal ions, and polyamine interactions)[71]. Polyamines like spermine and spermidine can cause a B- to Z-DNA transition in the presence of low ionic strength buffers[72]. Moreover, eDNA within the biofilms may also undergo change in structural conformations[73], suggesting that biofilms are dynamic worlds that continue to respond to their environments.

Changes in chemical and structural conformations are important to understand because they dictate the interactions between eDNA and biofilm constituents. As far as we know, conformational changes of eDNA within the biofilms have not been directly observed. However, it is very possible since the behaviors of eDNA are dynamic within the biofilm; for example, eDNA can chemically modulate its interactions to regulate its contribution to the overall viscoelastic relaxation of the biofilm[74]. It was also observed that the composition of eDNA was altered when Cu^{2+} stress was applied. Using RAPD analysis, Lin et al. observed smaller- and medium- sized fragments of eDNA compared to gDNA; the smaller sizes are possibly due to eDNA fragmentation or nucleotide deletion in the biofilm matrix. In addition, they also found some banding patterns specific to the eDNA samples subjected to Cu^{2+} stress[54]. These new bands suggest possible nucleotide additions, deletions, or modifications when eDNA is exposed to Cu^{2+}. This observation

shows how eDNA aids in biofilm response and adaptation. These interactions are crucial when considering anti-biofilm therapies.

While DNase treatments are widely used for anti-biofilm therapies, this approach still faces limitations. For example, DNase will not likely work for DNA conformations other than B-DNA. DNase treatments also are not likely to work against DNA in the Z-form[75]. However, some groups still suggest that any type of DNase can disperse biofilms[22]. Although DNase may not likely work with Z-form DNA, it is possible that eDNA can flip between Z-, B- and other forms. The eDNA digestion via DNase may also affect the conformation of the remaining Z-DNA rendering the Z-DNA susceptible to enzymatic degradation. Nevertheless, DNase is still currently expensive so translating this treatment into large-scale settings will be costly. Furthermore, rising cases of biofilm resistance against DNase are already being reported [76].

eDNA interactions with Biofilm components

The biofilm matrix is composed of various components that can interact with eDNA. It may be helpful to distinguish such interactions into: specific and non-specific. Specific interactions include molecules and macromolecules with high affinity to particular sites or sequences of DNA. Examples of these are various DNA-specific-binding proteins. In contrast, non-specific DNA interactions involve lower affinity, for example, positively-charged molecules that electrostatically interact with the negative phosphate-backbone of DNA.

eDNA interactions with proteins

Proteins are complex molecules that serve many cellular purposes; they may function as part of the immune system, catalyze reactions as enzymes, transmit signals as messengers, provide support as structural components, or help supply the cell with molecules required for survival as transporters and storage units[77]. In addition to these cellular purposes, proteins also have further functions within biofilms. Cellular proteins (e.g., virulence factors and ribosomal proteins) released into the extracellular environment seem to promote biofilm formation by also binding to eDNA[78]. Many cellular proteins naturally interact with genomic DNA; for example condensins and cohesins are protein complexes that tether DNA to produce DNA loops for chromosome assembly[79]. In the biofilms, eDNA-protein interaction can promote bacterial aggregation by stabilizing anionic eDNA through electrostatic forces and creating a favorable network for biofilm stability[80]. When proteins bind eDNA via charge-charge interactions, eDNA can function as an adhesive between the bacteria[81-82].

Proteins are also important for intracellular bacterial nucleoid structure and function. The DNABII family of proteins bind and pack DNA; these proteins are usually located within the cell, but they also occur in the extracellular matrix of the biofilm. Within this protein family are Integration Host Factor (IHF) and Histone-like protein (HU), that bind DNA with high-affinity[83]. Targeting DNABII proteins in biofilms using monoclonal antibodies (MAbs) disrupted diverse bacterial biofilms *in vitro* and *in vivo*[84]. The two *in vivo* models used for this finding are Nontypeable *Haemophilus influenza* infection on chinchilla ear and *P. aeruginosa* infection of murine lung. DNABII proteins and eDNA are both observed to be universal biofilm components (i.e. found across multiple species) and are not only crucial to the biofilm structure but are also important in understanding the mechanisms of multispecies interactions in mixed microbial

biofilm populations[85]. Consequently, DNABII proteins can serve as anti-biofilm targets. However, little is known about the extracellular localization mechanism of the DNA-binding proteins, thereby demanding more research in this area[14]. Other than DNABII-type proteins, amyloid accumulation can also promote biofilm stability. Amyloids are aggregates of proteins usually associated with protein misfolding and many neurodegenerative disorders[86]. Amyloids can provide additional support to the biofilm matrix through their inherent resistance to protease degradation thereby protecting the matrix from destruction. In *S. aureus* biofilms grown in peptone media, amyloids comprise of small peptides called phenol soluble modulins (PSMs)[87]. These cationic PSMs interact with eDNA resulting in polymerization and increased amyloid aggregation. Furthermore, biofilms that have PSMs but lack eDNA, fail to assemble PSM amyloids[88]. Collectively, these studies suggest that protein-eDNA interactions can serve as worthy therapeutic targets to disrupt biofilms.

eDNA interactions with exopolysaccharides

Exopolysaccharides are high-molecular weight (10 to 1000 kDa) carbohydrate polymers secreted by microorganisms in the biofilms. Functions of exopolysaccharides in biofilms include cellular adhesion, stress protection, water retention, and absorption of excess energy[89]. In a recent study, the interaction between the exopolysaccharide, Psl, and eDNA was observed in *P. aeruginosa* biofilms; the two components crosslink to form a skeleton that allows bacteria to adhere and grow[90]. Using molecular modeling, the authors were able to mimic the physical interaction between Psl and DNA. Psl was able to fit into the minor groove of DNA double helix forming hydrogen bonds with an estimated -2.18 kcal mol^{-1} interaction energy. Additionally, in *C. crescentus* biofilms, eDNA can bind to polar polysaccharide "hold-fast" regions of cells, which are necessary for surface adhesion, thereby promoting biofilm dispersion[63]. It is critical to note

here that controlled biofilm dispersion is an essential stage in the biofilm life cycle since it contributes to bacterial dispersal and disease transmission[91]. In summary, eDNA-interactions with biofilm exopolysaccharides appear essential to bacterial aggregation, adhesion, dispersion and vary in detail from species to species.

eDNA interactions with other biofilm components

Within the biofilms, interacting with eDNA, are various metabolites and cations crucial for bacterial survival and biofilm development[92]. For example, pyocyanin (PYO) is a redox-active metabolite that provides *P. aeruginosa* a blue-green color. PYO is a phenazine that has a number of significant roles in cell-signaling, biofilm development, iron-acquisition, cell metabolism and antibiotic tolerance[93-94]. In *P. aeruginosa* biofilms, PYO interacts with eDNA resulting in: enhanced electron transfer within the biofilm components, better eDNA binding to *P. aeruginosa* cell surface, and increased DNA and sputum viscosity[20, 95]. Since PYO-eDNA interactions are vital to the biofilm development, the disruption of such interactions can present a favorable target for biofilm biomass reduction and decreased biofilm exudates in infections. Das et al. therefore suggested the potential of elevating antioxidant levels (e.g. glutathione and ascorbic acid) to disrupt PYO-eDNA intercalation in *P. aeruginosa* biofilms[95].

Besides metabolites, cations in the biofilms also interact with eDNA. Extracellular DNA can sequester divalent cations and trigger resistance mechanisms that increase the pathogen's virulence[65-66]. Cation limitation destabilizes the negative charges of the lipopolysaccharides on the outer membrane of Gram-negative bacteria, which can cause cell lysis. Consequently, this event triggers a virulence response. Therefore, sub-inhibitory concentrations of eDNA can induce increased antibiotic resistance. Additionally, in a study investigating heavy metal stress and eDNA formation, it was identified that extracellular nucleic acids in the EPS of unsaturated *Pseudomonas*

putida CZ1 biofilm also bind Cu^{2+}. The phosphate groups of DNA have a cation-binding ability that allows biofilms to store cation and nutrient reservoirs for the cells. The increase of eDNA contents under Cu^{2+} stress may also be attributed to expression of resistance mechanisms[54]. Using a different approach, external addition of metal chelators (e.g. EDTA) was used to disperse PAO1 biofilms [96]. Exposing *P. aeruginosa* biofilms to EDTA induced bacterial cell detachment from biofilms likely caused by chelation of several divalent ions required to stabilize the biofilm matrix. It is, however, important to note that high concentrations of chelators are needed for treatments to be effective; sub-inhibitory concentrations can only trigger resistance mechanisms. Hence, cytotoxicity becomes a challenge for this approach.

Extracellular DNA as anti-biofilm target

Extracellular DNA may serve as an effective anti-biofilm target. Research has focused on DNase treatments ever since DNase was used to degrade eDNA and disrupt biofilms[22, 37, 97]. By applying nucleases directly into biofilms, eDNA is degraded and the biofilm matrix is weakened. Likewise, disturbing eDNA interactions can threaten the matrix. It is important to realize that even if the biofilm is not completely disrupted, access points for other treatments can still be created. Access points and disturbances in the biofilm matrix can ultimately increase antibiotic susceptibility of the pathogens living within.

Nuclease treatments

Nucleases are enzymes that degrade nucleic acids. The most common anti-biofilm treatment *in vitro* that uses nucleases is DNase I, a DNA specific endonuclease[98]. DNase I cleaves single- and double-stranded DNA into oligonucleotides with 5′-phosphorylated and 3′-hydroxylated ends[99]. Okshevsky et al. reported a comprehensive study of various bacterial species where DNase treatments were implemented for biofilm control [22]. Overall, it is noted that DNase treatments may prevent biofilm formation, but they do not always disrupt pre-formed biofilms. The growth phase of the biofilm dictates the effectiveness of this therapy; only younger *S. epidermidis* biofilms (6-hr old or less) are disrupted. This therapeutic approach is also applied in clinical settings; cystic fibrosis (CF) patients are commonly treated with Dornase alfa (Pulmozyme, recombinant human DNAse I, rhDNAse) [100]. CF patients accumulate sputum in their lungs, thereby reducing pulmonary function. The accumulated sputum for these patients is rich with actin and eDNA; hence, treatment with dornase alfa results to degradation of eDNA and reduced sputum viscosity[100]. This therapeutic strategy can also be applied in bacterial infections by cleaving eDNA in the biofilms and creating access points for co-administered antibiotic treatments.

Pathogens like *S. aureus* can also produce extracellular nucleases. They release nucleases to signal controlled biofilm dispersion and also to defend themselves from neutrophil extracellular traps (NETs). These NETs are composed of the host's nuclear DNA associated with antimicrobial peptides, histones and proteases[101]; they are released by the host's neutrophils to kill bacteria. Furthermore, as pathogens fight for survival, surface colonization and nutrient availability become very important. Some bacteria, therefore, release nucleases to prevent biofilm formation of other pathogens. For example, nucleases released by *Bacillus licheniformis* have anti-biofilm

properties[102]. Hence, identifying more extracellular nucleases secreted by biofilm-forming pathogens may have future therapeutic use.

Alternatively, Okshevsky et al. suggested the upregulation of the nuclease production of a singular species in a multi-colony biofilm for biofilm control. However, since nucleases serve a variety of purposes (e.g. transformation, bacterial dispersal, protection against NETs) that can increase biofilm production, this approach still needs to be investigated[22]. We still do not know if upregulating nucleases would be beneficial or destructive to the overall biofilm life cycle. Furthermore, few studies so far have used nuclease treatments to target biofilms *in vivo*[9].

eDNA and eDNA-interactions as targets for anti-biofilm therapy

We have detailed various eDNA interactions within the biofilm matrix in this review (e.g. proteins, exopolysaccharides, metabolites, etc.) but it is essential to find and investigate more. Targeting eDNA interactions can cause biofilm matrix disturbances that can lead to eradication of a bacterial colony. However, many of these interactions still need to be investigated as anti-biofilm targets. For example, although eDNA-protein complexes are found in *B. licheniformis* biofilms, only the DNase treatment increased biofilm permeability; the proteinase treatment (Proteinase K) did not[33]. In this case, the proteinaceous components of the biofilm were digested by Proteinase K but the overall permeability of the biofilm matrix was largely unaffected. It could be that targeting eDNA alone increases permeability of the matrix and targeting the matrix proteins structurally weakens the framework. This explanation support findings that report DNABII targeting can collapse diverse bacterial biofilms both *in vitro* and *in vivo* [84]. Here, highly-specific MAbs against protective epitopes of a DNABII protein disrupted pre-formed biofilms and released the encapsulated bacterial population, rendering them less resistant. It is also important to note that

DNABII proteins are positioned at the vertices of strands of eDNA within the biofilm so targeting them induced a collapse of the whole matrix[84]. By applying this strategy, both proteins and eDNA (and their interactions) are compromised, disrupting the overall structural integrity of the biofilm. This approach can be very effective in disrupting and even preventing biofilm formation. With this strategy in mind, there may possibly be more lynchpin proteins like DNABII that contribute significantly to the biofilm matrix. Therefore, we need to identify more eDNA-interacting proteins that can be targeted.

Similarly, exopolysaccharides and metabolites may serve as anti-biofilm targets. The Psl polysaccharide interacts with eDNA to benefit the biofilm in many ways: to form a backbone skeleton support for the matrix, to encourage bacteria to produce more EPS, and to inhibit over-cation chelation that can lyse the cells within the biofilm[90]. Like the strategy for eDNA-DNABII proteins, targeting eDNA-exopolysaccharide interactions may also collapse the biofilm structure. However, since polysaccharides are also ubiquitous in the biofilms of various species, targeting them directly has been the goal of different studies[103-104]. Most research would rather focus on direct polysaccharide-degradation than identifying interactions, which work as indirect anti-biofilm targets. In addition, metabolites and cations in the biofilm can dynamically affect the biofilm matrix. For example, extracellular DNA can increase antibiotic resistance by sequestering Mg^{2+} ions and decreasing the pH of the biofilm. For *P. aeruginosa*, biofilms pH values range from pH 5.5-6.6[105]. Such acidic conditions can upregulate two-component systems, which are related to antibiotic resistance. Identifying more metabolites and cations may introduce more anti-biofilm targets.

Biofilms create a barrier that is very difficult for antibiotics to pass through and access the bacterial cells. Antibiotic-conjugated molecules that inhibit the eDNA-biofilm component

interactions may be utilized for anti-biofilm therapies. By attaching inhibitors to antibiotics, the biofilm can be disrupted, and antibiotic delivery becomes more efficient. Conjugating antibiotics to polymers, proteins, antibodies, and other molecules with high affinity to eDNA can directly interrupt and disturb the biofilm matrix. Hence, understanding the structural differences that occur with gDNA once secreted and becomes eDNA is vital. Once the matrix is dissolved, antibiotics delivered nearby can attack the pathogens.

The concept of antibiotic-conjugation has already been previously reported. For example, antibody-antibiotic conjugates are being used against *S. aureus*. Human MAbs designed to bind on the surface of *S. aureus* bacteria are conjugated with an antibiotic (dmDNA31), thereby directing the drug closer to the target pathogen[106]. In another study, chitosan, a derivative of the polysaccharide chitin, was linked to an aminoglycoside antibiotic (streptomycin)[107]. This chitosan-antibiotic conjugate reduced biofilm mass and suppressed biofilm formation of Gram-positive bacteria but not Gram-negative bacteria. Chitosan allowed streptomycin access into the biofilms secreted by *Listeria monocytogenes*[107].

Major Conclusions

Biofilms create barriers that challenge our current therapeutic approaches. Extracellular DNA may function as a worthwhile anti-biofilm target. In this review, we highlighted recent developments defining the importance, production mechanisms and possible conformations of eDNA in biofilms. We described components in the matrix that interact with eDNA noting their potential as anti-biofilm targets. Overall, these various interactions, whether known or unknown, are very important in biofilm regulation. Therefore, we need to continue pursuing creative approaches in eradicating biofilms.

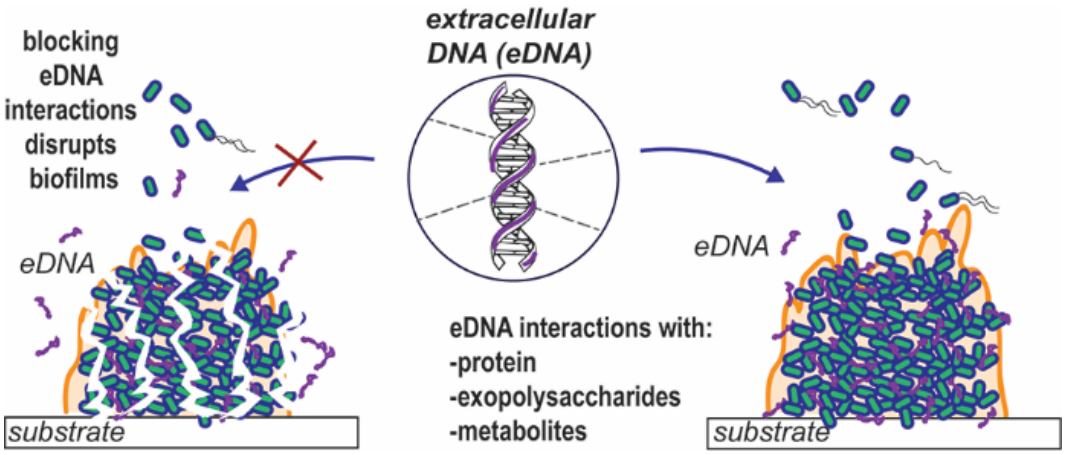

Figure 4. Summary of eDNA review. Figure shows eDNA interactions with molecules within biofilms; blocking eDNA-interactions may disrupt biofilm architecture and reduce resistance

Chapter 2: Gram-negative bacteria: *Pseudomonas aeruginosa, Escherichia coli* and *Klebsiella pneumoniae* and technology to counteract them

Background and Significance of Research

Microorganisms are ubiquitous in nature. Among the organisms of the microscopic world are bacteria—single-celled organisms found almost everywhere on Earth. To differentiate bacteria, scientists use the Gram staining classification. Through this method, most bacteria are categorized into two fundamental groups classifying the nature of their cell wall. Pathogens that retain the crystal violet stain are called "Gram-positive" and those that do not are called "Gram-negative" bacteria[108]. Gram-negative tend to decolorize and stain red with safranin. Within Gram-negative pathogens, there are two large groups that make up most of the clinical isolates currently identified—the *Enterobacteriaceae* and the non-fermenters[109]. Some of the *Enterobacteriaceae* genera include *Escherichia*, *Proteus*, *Enterobacter*, *Klebsiella*, *Citrobacter*, *Yersinia*, *Shigella*, and *Salmonella*. Examples of non-fermenters are *Pseudomonas aeruginosa*, *Acinetobacter baumannii*, and *Burkholderia cepacian*. In this doctoral work, *Escherichia coli, Klebsiella pneumonia* and *Pseudomonas aeruginosa* were used as model organisms.

Gram-negative bacterial pathogens can cause significant public health problems. Infections caused by these pathogens can quickly become problematic. However, it was reported that, before the 1920s, infections caused by Gram-negative pathogens were rare[110]. It was not until antibiotics were extensively used that these pathogens became a healthcare issue. One of the factors attributed to the rise of Gram-negative bacteremia is the selectivity of antibiotics used at the time (e.g., penicillin)[110]. Antibiotics like penicillin are ineffective against Gram-negative pathogens because of their outer membrane (OM) that prevents penicillin from getting to the peptidoglycan. In

addition to the OM, various resistance mechanisms also take place to evade treatments (i.e., antibiotic modification/degradation, upregulation of efflux pumps, antibiotic sequestration, target modification, and biofilm production).

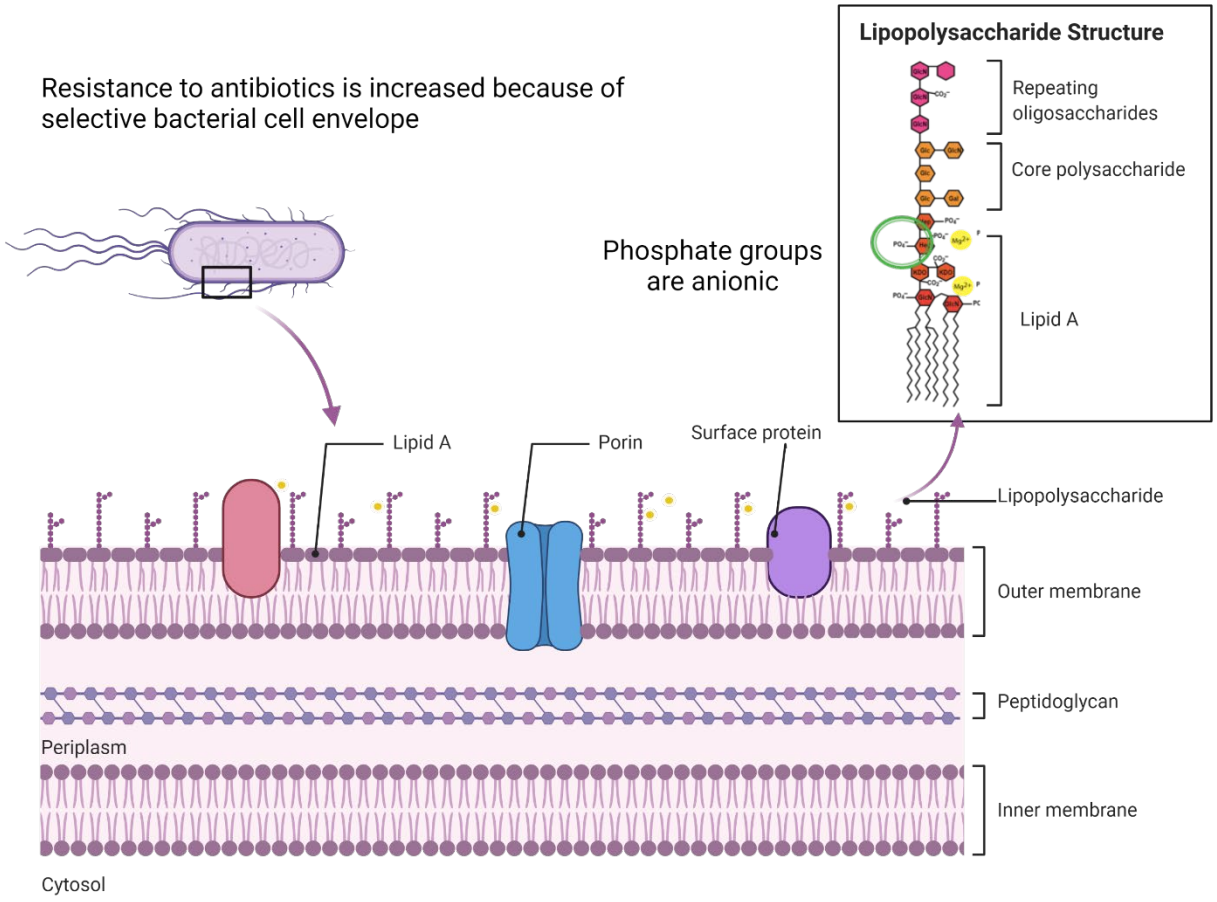

Figure 5. Illustration of Gram-negative bacteria. Gram-negative bacterial cell envelope components consist of the outer membrane, peptidoglycan, and the inner membrane. The cell envelope selectively allows molecules to cross in and out of the cell.

Bacterial cells evolved a sophisticated cell envelope facilitating selective entry (of nutrients) and exit (of waste)[111]. The cell envelope protects bacteria from the outside environment (Figure 5). It is composed of the cell membrane(s) and other structures that surround the cytoplasm. As

mentioned previously, Gram staining classification divides bacteria into two categories: Gram-positive and Gram-negative. The foundation of Gram-staining relies in the structural difference in the cell envelope composition of bacteria[108]. The cell envelope of Gram-negative bacteria consists of the outer membrane (OM), the peptidoglycan cell wall, and the cytoplasmic or inner membrane (IM) (Figure 5). On the other hand, the cell envelope of Gram-positive bacteria lacks the OM[109]. In Gram-negative bacteria, the outer leaflet of the OM consists mainly of lipopolysaccharides (LPS). These LPS contribute significantly to the structural integrity of the membrane and are comprised of three parts—O-antigen, core, and Lipid A, which cumulatively give the OM an overall negative charge. These negative charges on the membrane are stabilized by divalent cations (Mg^{2+} and Ca^{2+}) creating a rigid membrane that is difficult to penetrate, especially for hydrophobic molecules[112]. Hydrophilic molecules are also filtered in the OM and can only be transported via membrane-bound porins. The Peptidoglycan cell wall is comprised of N-acetyl glucosamine-N-actyl muramic acid, which are cross-linked by penicillin binding proteins (PBPs)[113-114]. Between the OM and the IM is an aqueous cellular space called the periplasm. This compartment can house various enzymes able to degrade harmful threats (i.e. antibiotics). The IM, like the OM, is a phospholipid bilayer. In Gram-positive cells, the IM is simply referred to as plasma membrane. This membrane is the site of active transport, respiratory chain components, the H^{+}-ATPase proton pumps, and some of the steps in peptidoglycan biosynthesis[115]. Overall, the cell envelopes of bacteria are complex structures vital for survival. Current and developing therapies focus on selectively disrupting bacterial cell envelopes with antimicrobials[114, 116-117].

Antibiotic Resistance

This doctoral project aims to develop a drug potentiator to fight against antibiotic-resistant-Gram-negative pathogens. Antibiotic resistance is a rapidly-growing crisis as effective antibiotics run out. Antibiotics were first prescribed to treat severe infections and over time, antibiotics that target different bacterial machineries were introduced to the market. As antibiotics help patients overcome infections, infectious pathogens also started responding to treatments by developing various "evading" mechanisms. Furthermore, the rate of discovery and introduction of new antibiotic classes has recently stagnated[118]. Antibiotic resistance arises when pathogens evolve to survive current treatments[2, 119]. The World Health Organization (WHO) surveys the current trends in antibiotic resistance using the Global Antimicrobial Resistance and Use Surveillance System (GLASS)[120]. Launched in 2015, the GLASS is the first system that collects and compares national antimicrobial resistance and antimicrobial consumption data. In their 2021 report, 109 countries or territories participated. Their report highlights increased rates of resistance in bloodstream, urinary, and gastroenteric infections in most countries that participated. Furthermore, increased resistance to last resort antibiotics (e.g., carbapenems) and first-line drugs (e.g., co-trimoxazole)[120] was widespread in many countries.

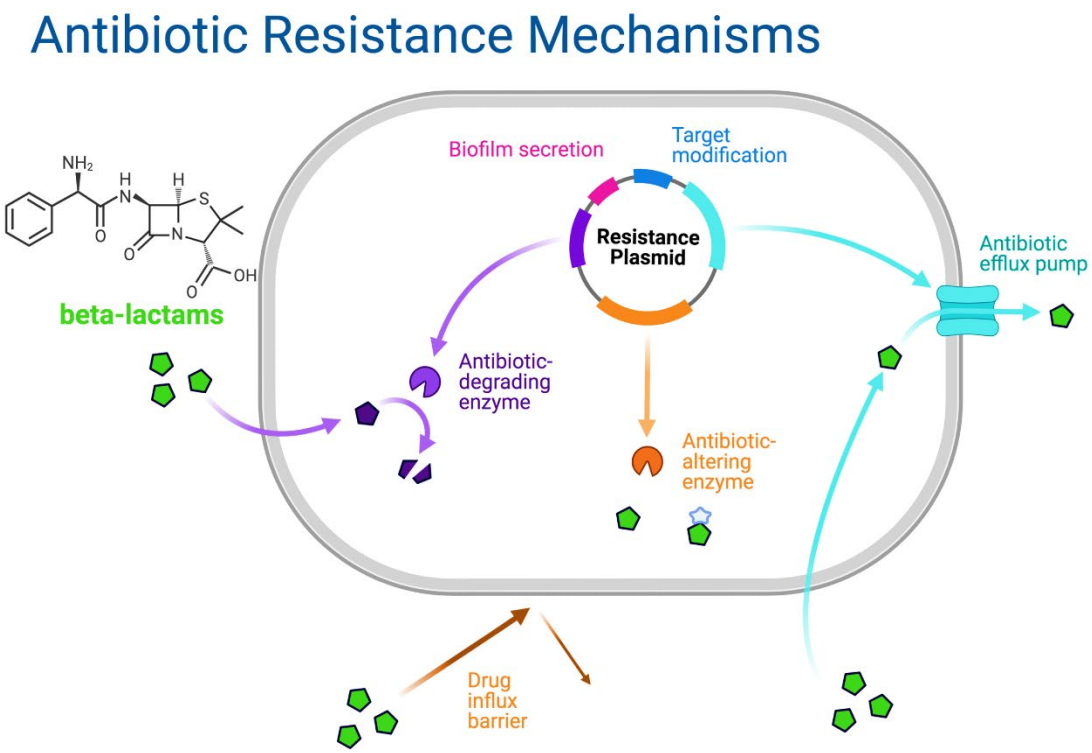

Figure 6. Simplified illustration of antibiotic resistance mechanisms. Pathogens can evade beta-lactam antibiotics via applying multiple mechanisms: employing enzymes, increasing its barriers, pumping out the antibiotic and secreting biofilms.

Beta-lactam (β-lactam) antibiotics are one of the most commonly prescribed drugs to treat infections. Approximately 65% of current antibiotics fall under this class[121]. Hence, overuse and misuse of these antibiotics over the years resulted to β-lactam-resistant pathogens. It is generally agreed that such acquired resistance evolve by implementing Darwinian selection (i.e. mutations in preexisting genes in the bacterial chromosome positively selected for survival)[122-123]. Some resistance mechanisms can also be caused by over-expression of naturally-occurring processes when pathogens are faced with high concentrations of antimicrobials (e.g. beta-lactamases)[124]. The β-lactam class are unified by a common feature: a 3-carbon and 1-nitrogen ring (beta-lactam ring),

which is highly reactive. β-lactams are bactericidal by targeting penicillin-binding proteins (PBPs) and ultimately disabling peptidoglycan synthesis[114]. Penicillins, cephalosporins, carbapenems, and monobactams fall under the β-lactam class[121]. Bacterial cells employ multiple mechanisms to resist β-lactams, some mechanisms include inactivation via β-lactamase enzymes, decreased penetration of the cell membrane, modification of PBPs and efflux from the periplasmic space via pumps[121]. Furthermore, as discussed in Chapter 1, bacteria also cluster and form biofilms to collectively evade antibiotics.

Model Gram-negative Pathogens*: Escherichia coli, Klebsiella pneumoniae, and Pseudomonas aeruginosa*

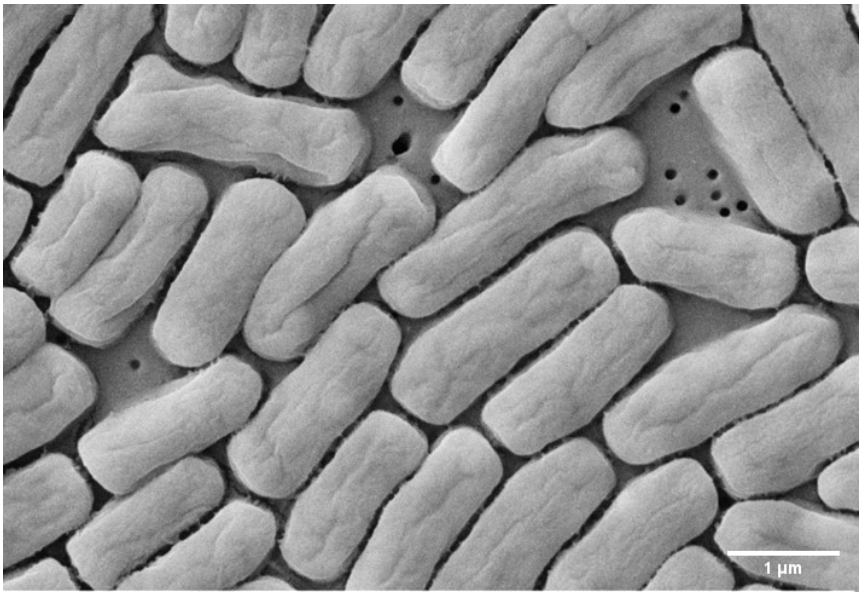

Figure 7. *Escherichia coli* cells image via Scanning Electron Microscope. Cells are resting on a porous substrate grown for 24 hrs on an agar plate

Escherichia coli (E. coli)

E. coli is a model organism widely-used in research (Figure 7) [125]. Its hardiness and versatility allow scientists to intensively study its biological systems. *E. coli* is a rod-shaped bacteria that rapidly grows in growing medium (doubling time of ~20 min)[126]. This pathogen was discovered by a microbiologist and pediatrician Theodor Escherich in 1884 while he was studying infant gut microbes[127]. This bacterium usually harmlessly dwells in the lower intestinal track of warm-blooded animals and then discharged into the environment. However, certain strains of *E. coli* can cause illnesses. In humans, two types of infections are usually caused by *E. coli*: gastrointestinal and extraintestinal infections (i.e. urinary tract infections, bloodstream infections).

As *E. coli* fights for its survival, it acquires antibiotic resistance genes. Some of these genes code for extended-spectrum β-lactamases and carbapenemases (resistance to a myriad of beta-lactam antibiotics), 16S rRNA methylases (resistance to aminoglycoside), and mcr genes (resistance to polymyxins)[128]. Hence, this pathogen remains to be among the most pervasive clinical challenge among clinicians.

Klebsiella pneumoniae (K. pneumoniae)

K. pneumoniae was first isolated in the late 19th century by Carl Friedlander from the lungs of people who had died from pneumonia[129]. It is an encapsulated, non-motile pathogen that naturally colonizes human mucosal surfaces (e.g. human intestines)[130]. Infections occur when pathogens enter an immunocompromised system. Means of exposure include entry of contaminated medical devices (e.g., ventilators) into patients and these lung infections can carry a mortality rate of 30-50%[129]. Classically, when infections occur among the hospitalized, patients are routinely treated with β-lactams effective against *Enterobacteriaceae*[131].

Over time, *K. pneumoniae* acquired multiple "survival" genes. As a result, antibiotic resistance for these pathogens also developed. Two major types of resistance are commonly observed in *K. pneumoniae*: a. expression of extended-spectrum β-lactamases and b. expression of carbapenemases[130]. According to the CDC, carbapenems often are the last line of defense against multidrug resistant pathogens; this means that resistant *K. pneumoniae* can now evade almost all β-lactams—including the drugs of last resort. Today, *K. pneumoniae* causes the most hospital-acquired cases of pneumonia in the United States. Therefore, identifying treatment options for these resistant strains is urgent.

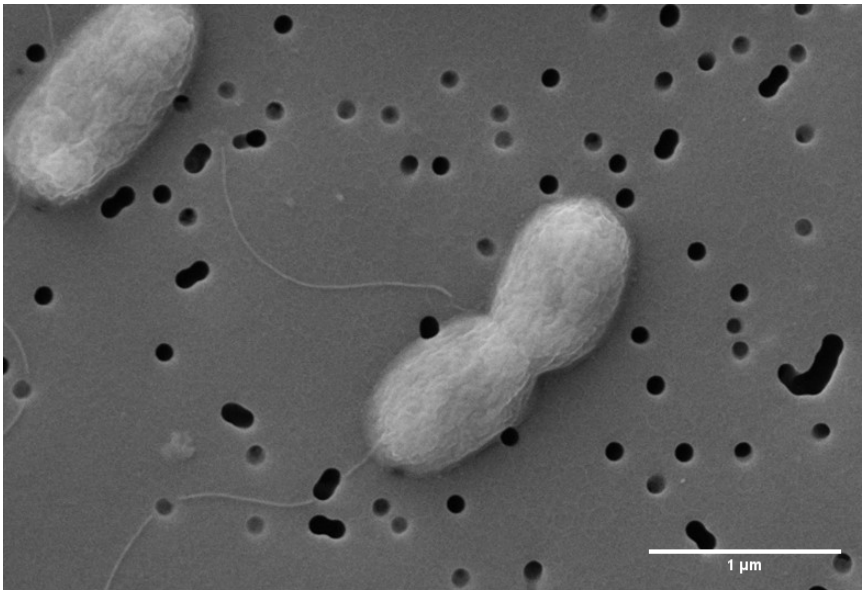

Figure 8. *Pseudomonas aeruginosa* cells with intact flagella imaged via Scanning Electron Microscope. Cells are resting on a porous substrate grown for 24 hrs on an agar plate.

Pseudomonas aeruginosa (P. aeruginosa)

P. aeruginosa (Figure 8) is an opportunistic pathogen that cause about 33,000 hospital-acquired infections annually and about 3,000 deaths in the United States alone in 2017[2]. *P. aeruginosa* is

ubiquitous in the environment, particularly in fresh water. This pathogen was first successfully isolated in 1882 by Carle Gessar and documented his work, which he titled, "On the blue and green coloration that appears on bandages[132]." Despite the widespread distribution of *P. aeruginosa* in nature, it is rarely found in the normal microbial flora of humans[133]. Predominant infections are usually hospital-acquired; and like *K. pneumoniae,* this pathogen is also an important cause of ventilator-associated pneumonia[134]. Additionally, *P. aeruginosa* infections are common to patients with cystic fibrosis, burns/chronic wounds, cancer, AIDS, organ transplant, and uncontrolled diabetes mellitus[134]. Furthermore, WHO officially listed *P. aeruginosa* as one of the "critical priority pathogens" in 2019.

P. aeruginosa exhibit antibiotic resistance mechanisms to evade a wide-range of antibiotics, including aminoglycosides, quinolones and β-lactams[135]. These pathogens employ efflux pumps and β-lactamases to "pump out" and/or degrade antibiotics[135]. In addition, *P. aeruginosa* form biofilms that serve as a physical layer of protection. The combination of developing biofilms and antibiotic resistance create substantial technological hurdles to patient treatment[136]. Therefore, there is a critical need for new therapeutic approaches to combat these pathogens.

Current Therapies

To combat resistant pathogens, much focus is directed toward the discovery of new antibiotic classes and the modification of known antibiotic scaffolds through high throughput screenings and synthesis[137]. However, these efforts are still moving very slowly. Therefore, there is a crucial need for developing new strategies in combating these life-threatening infections. One way to address

this issue is by implementing a co-treatment approach where an anti-resistant potentiator compound is co-administered with existing drugs.

Some groups have already taken the combination approach and had been successful in their research efforts[138-139]. For example, SPR741, a polymxin class analogue, was recently identified to be an antibiotic potentiator that acts as a membrane perturber[139]. As a result, SPR741 increases the passage rate of molecules (i.e. antibiotics) into the bacterial cell. Other than polymyxin analogues, Oligo-acyl-lysyls (OAKs) also showed the ability to overcome the outer membrane barrier facilitating the passage of antibiotics—more specifically rifampin, into the cell[140]. In addition to planktonic effects of potentiators, a polyamine compound, norspermidine, has shown an ability to disrupt and eradicate pre-formed *P. aeruginosa* biofilms by, among other ways, interrupting cell-surface attachment.

Innovation: Branched Polyethylenimine (BPEI)

Even with current research endeavors, we need more potentiators. We, here in the Rice Lab, have identified low-molecular weight branched polyethylenimine (BPEI) and its derivatives as broad-spectrum potentiators of beta-lactams against both Gram-positive and Gram-negative pathogens. In Gram-positive resistant bacteria (e.g. Methicillin Resistant *Staphylococcus aureus* and Methicillin Resistant *Staphylococcus epidermidis*), we showed that BPEI re-activate beta-lactams by disabling bacterial cell wall synthesis components[114]. In this work, we have also seen a synergistic relationship between BPEI and beta-lactams against the Gram-negative bacteria. Overall, we propose that BPEI is a multi-functional adjuvant that can resensitize bacteria to existing antibiotics as it interacts with LPS of the bacteria and also with eDNA of the biofilms.

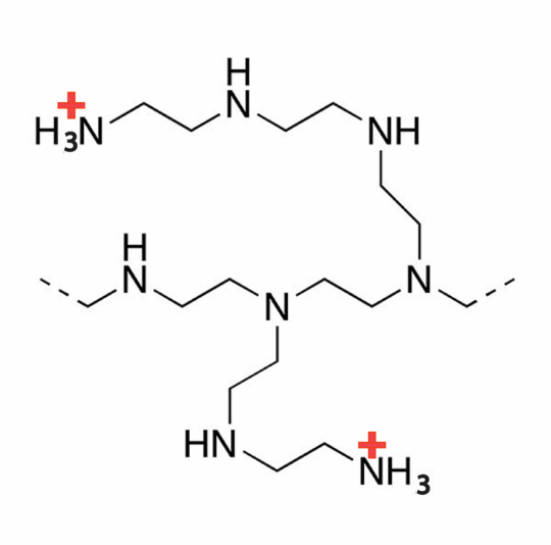

Figure 9. An illustration of a single molecules of highly branched polyethylenimine. This 600 Da BPEI has 25/50/25 ratio of primary, secondary, and tertiary amine groups.

Chemistry and Applications of BPEI

600-Da Branched polyethylenimine is a highly branched cationic polyamine (Figure 9). Polyethylenimines (PEIs) are polymers of repeating amine groups separated by ethyl groups. PEIs are commercially available polymers; the companies Badische Anilin-und Soda-Fabrik AG. (Germany) and Chemirad Corporation (USA) introduced the industrial manufacturing of PEIs in 1938.[141] Commercial synthesis of PEIs involve polymerization of aziridines or thermal decomposition of 2-oxooxazolidine.[141] Synthesized PEIs can either be linear or branched. Linear polyethylenimines (LPEIs) are long polymers of secondary amines while branched polyethylenimines (BPEIs) contain primary, secondary, and tertiary amine groups.[141] Although branched PEIs can get up to 50 kDa in size, we used 600 Da (Polysciences Inc.) in our assays to mitigate cytotoxicity concerns. In addition, we worked with the branched version since it displays a higher density of primary groups than the linear PEIs. Primary amines protonate at a lower pH

compared to the secondary and tertiary amines, which results to a higher cationic charge. Branched PEIs protonate in three steps: first the primary amines are protonated at pH = ~8, then the second protonation occurs at pH near 5, and finally the remaining tertiary groups protonate in a last protonation step at a very low pH.[142] Unfortunately, the last protonation step has not been well observed in many studies since it occurs at pH range of -1 and 0.5.

PEIs are used in a variety of ways: industrial, cosmetics, pharmaceutical, and environmental. At first, PEIs were heavily used in manufacturing: as a textile additive, finishing for paper and textiles and component in resins.[141] As years passed, researchers discovered more uses for these polymers. PEIs—especially the larger molecular weight forms—are now applied in gene delivery, water treatments and antimicrobial therapies[143-147]. One of the most common applications of BPEI is gene therapy. Cationic polymers, like BPEI, have great potential as gene carriers because of their cationic charge that electrostatically interact with nucleic acids. Cationic polymers can condense DNA and RNA as they interact with the phosphodiester backbones and allow them to be delivered into mammalian cells.[148-149]

History of BPEI as Co-administered Molecule

BPEI was first used in the Rice lab to study metal-binding in bacteria. Metals, such as magnesium and calcium, are necessary for bacterial survival. However, metal transport into the cytoplasm was not completely understood. Hence, Gram-positive *Bacillus subtilis* 1A578 was used as the model organism in the Rice lab to investigate this phenomenon. In the dissertation work of Keith Thomas Ph.D., a former member of the Rice lab, BPEI was used to displace metals in the cells. In Keith's experiments, he observed that BPEI also somehow caused phenotypic changes to the bacterial cells. Furthermore, BPEI resensitized *B. subtillis* to chloramphenicol (an antibiotic that inhibits

bacterial protein synthesis)[150]. These findings laid foundation for the antibacterial research that followed.

The first application of BPEI against pathogenic bacteria was performed by Melissa Hill Ph.D., another former member of the Rice lab. Melissa used BPEI as a potentiator of penicillin against Methicillin-Resistant *Staphylococcus aureus* (MRSA). She also investigated how BPEI disables resistance mechanisms of MRSA. In her dissertation work, she discovered that BPEI interacts with the wall teichoic acids (WTA) of the peptidoglycan, which results to the delocalization of penicillin binding proteins (PBP4) in MRSA strains. With BPEI co-administered, penicillin antibiotics can then disrupt the cell wall synthesis and ultimately kill the MRSA cells. Continuing Melissa's work, Anh Lam Ph.D. investigated the ability of BPEI to restore activity of beta-lactams against Methicillin-Resistant *Staphylococcus epidermidis* (MRSE). Similar to MRSA, BPEI also interacts with the WTA of MRSE strains, thus disabling their resistance. Since BPEI is a highly cationic molecule, the lab then started exploring further uses of cationic 600-Da BPEI. Anh explored whether 600-Da BPEI can neutralize any other Gram-positive cell envelope components (i.e. released peptidoglycan). When *Staphylococci* cells die, they release their peptidoglycan into the host's system. The release of peptidoglycan can cause a complex series of events that triggers the release of inflammatory cytokines[151]. Over production of cytokines can overwhelm the host's immune system and can be life threatening[151]. However, Anh found that 600-Da BPEI binds to the anionic sites of the peptidoglycan, therefore neutralizing it. Consequently, 600-Da BPEI reduces the concentration of cytokines produced when *S. aureus* peptidoglycan are added to HEKa cells. This lays an important groundwork in developing 600-Da BPEI as a wound healing agent.

Another foundational piece that Anh discovered is the ability of BPEI to disrupt biofilms of MRSE. Anh used a microtiter biofilm model (MBEC) to test synergistic effects of BPEI and β-lactam

antibiotics against preformed biofilms on surfaces. Since MRSE and MRSA are both Gram-positive bacteria, we started investigating if we can extend the use of 600 Da BPEI against Gram-negative pathogens as well. To study Gram-negative pathogens, *Pseudomonas aeruginosa* was first used as a model pathogen. This investigation is detailed in the third chapter of this dissertation. The study on planktonic *P. aeruginosa* was performed by Anh Lam Ph.D., Hannah Panlilio and Jennifer Pusavat with equal contributions. The findings from that study supported the hypotheses designed in the generation of this dissertation work.

Characterization of BPEI and its PEGylated Derivative: PEG-BPEI

The 600 Da BPEI utilized in this work was bought from Polysciences Inc. In order to validate the structure, Anh Lam Ph.D. used high-performance liquid chromatography, mass spectrometry, and fourier-transform infrared spectroscopy. In her dissertation work, she reported that the BPEI stocks purchased from Polysciences Inc. are highly pure and very hydrophilic. Furthermore, her work confirmed the identity and purity of 600 Da BPEI utilized in this work. While low molecular weight BPEIs were already reported to have high biocompatibility[152], we wanted to ensure increased safety of this therapy. Hence, we modified 600 Da BPEI with polyethylene glycol (PEG) in a straightforward one-step reaction. After synthesis, nuclear magnetic resonance (NMR) was used to characterize 600 Da BPEI and its PEGylated derivative, PEG350 BPEI. When applied *in vitro,* the PEGylated BPEI also disabled β-lactam resistance in MRSA, MRSE, and *P. aeruginosa*. This work was published in 2020.[116]

Future Experiments and Perspectives

Studies conducted subsequently are reported in the next chapters of this dissertation. In these chapters, it is evident that the potential therapeutic uses of BPEI keep increasing. The central hypothesis of this doctoral work investigates 600 Da BPEI and derivative as broad-spectrum therapeutic agents against Gram-negative bacteria. We have already shown that BPEI can also disable resistance mechanisms of Gram-positive pathogens. As a broad-spectrum agent, we envision BPEI to be developed into a topical agent for chronic wounds. We aim to advance this molecule as a safe and effective agent that disables resistance. Future studies will include resistance (against BPEI) studies, quorum sensing and immune response. This simple molecule that was first used in materials/manufacturing now may have drug applications.

Chapter 3: Overcoming Multidrug Resistance and Biofilms of *Pseudomonas aeruginosa* with a Single Dual-Function Potentiator of β-Lactams

Background and Significance

Pseudomonas aeruginosa (P. aeruginosa) is an infectious pathogen that causes severe pneumonia, bloodstream infections, respiratory tract infections (RTIs), urinary tract infections (UTIs), skin infections, and eye infections. Prominent in burn units, *P. aeruginosa* is of particular concern in wound healing[153-154] because it produces biofilms that are impenetrable to antibiotics, leading to chronic infections [155-156].

P. aeruginosa is a Gram-negative bacterium for which antibiotic therapy is useful, but resistant strains often result in severe chronic infections. Targeting Gram-negative bacterium like *P. aeruginosa* continues to be a challenge because of the presence of an outer membrane (OM) and other resistance mechanisms like developing biofilms. The outer leaflet of the OM of Gram-negative bacteria consists mainly of lipopolysaccharides (LPS). These LPS contribute significantly to the structural integrity of the membrane and are comprised of three parts—O-antigen, core, and Lipid A, which cumulatively give the OM an overall negative charge. These negative charges on the membrane are stabilized by divalent cations (Mg^{2+} and Ca^{2+}) creating a rigid membrane that is difficult to penetrate[112] In addition, biofilms sequester bacterial pathogens and protect them from antimicrobial attack. *P. aeruginosa* infections and their biofilms create serious health issues, and the threat to patient survival increases when the bacterium is multidrug-resistant *P. aeruginosa* (MDR-PA).[157-158]

Biofilms and antibiotic resistance create substantial technological hurdles to patient treatment.[136] This presents a significant and critical need for a way to counteract them. Existing

drugs and regimens are coupled with potentiators that overcome antibiotic resistance or biofilms.[159] However, it is possible to develop a single compound that disables biofilms and combats antibiotic resistance.

Purpose of Experiment

We have shown previously that 600 Da BPEI has synergy with existing antibiotics (i.e. beta-lactams) against Gram-positive pathogens like Methicillin Resistant *Staphylococcus aureus* (MRSA)[114] and Methicillin Resistant *Staphylococcus epidermidis* (MRSE).[113] The combination of antibiotics and 600 Da BPEI can resensitize multidrug resistant Gram-positive pathogens. The purpose of this experiment is to investigate the relationship of beta-lactams and 600 Da BPEI against Gram-negative bacterium—more specifically against *P. aeruginosa*. In this study, we also examined the mechanism(s) of action that 600 Da BPEI employs against *P. aeruginosa* planktonic bacteria and biofilms.

Principle of Techniques

In the *in vitro* stage of drug testing, the relationship between 600 Da BPEI and beta lactams can be identified via checkerboard assays. This assay is a conventional technique that tests different drug combinations across a well plate with a consistent bacterial inoculum size. This technique is applied over other methods of antibiotic susceptibility testing because of the quantitative information (i.e. MICs, FICIs) that can be obtained from it. For each antibiotic, the minimum inhibitory concentration (MIC) can be identified, which is the minimum amount of antibiotic needed to stop bacterial growth. A Fractional inhibitory concentration index (FICI) can also be determined using the MICs of different compounds. An FICI can be calculated using Equation 1.

An FICI less than 0.5 indicates synergy, greater than 1 indicates antagony and a value between 0.5 and 1 indicates additivity.[160]

$$FICI = \frac{Concentration_{a}\ combination}{MIC_{a}\ alone} + \frac{Concentration_{b}\ combination}{MIC_{b}\ alone} \quad \text{(Equation 1)}$$

The minimum biofilm eradication concentration (MBEC) assay is also applied in this study to study the anti-biofilm properties of 600 Da BPEI. MBEC assay is a technique developed for testing biofilm elimination efficacy. MBEC assay will identify the minimum concentration of drug needed for the biofilm to be suppressed in a high-throughput manner.[161] FICI values were also calculated for this assay using Equation 1. The MBEC assay is the first step in testing for the anti-biofilm ability of 600 Da BPEI. Other biofilm models will be applied in future studies.

Besides culture-based assays, techniques involving calorimetry, fluorescence and imaging were also performed in this study. Isothermal titration calorimetry (ITC) was utilized to investigate the mechanism of action of 600 Da BPEI with respect to the bacterial cell envelope. ITC is useful in identifying the thermodynamic properties of a system consisting of at least two molecules. Through observing the changes in enthalpy when titrating one molecule into the other, one can characterize interactions within the system and the molar ratios of binding. ITC directly measures the heat released or absorbed during this binding event. In this study, we hypothesized that the anionic LPS molecules of the outer membrane of the Gram-negative bacteria electrostatically interacted with the cationic amines of the 600 Da BPEI. Accumulation assays (NPN and H33342 Bisbenzimide) were also employed here to continue investigating the mechanism of action of 600 Da BPEI. After identifying the binding interaction between LPS and 600 Da BPEI, the effects of such interactions were explored. We hypothesized that the aforementioned interactions create

access points for beta lactams to cross the outer membrane into the periplasm and gain access to the peptidoglycan (Figure 22). The accumulation assays used in this study utilized fluorescent probes that can be directly measured after entering the bacterial cell. The fluorescent probes fluoresce when bound to specific substrates found inside the cell. H33342 Bisbenzimide probe fluoresces when bound to DNA. Finally, scanning electron Microscopy (SEM) was used to visualize any morphological changes in the cells when treatments were applied. SEM uses beams of electrons that hit the surface of a sample to generate detectable signals. This imaging technique is optimal for imaging bacteria because it has better resolution capability than traditional light microscope. The resolution of SEM can range from 3-6 nm, which is almost 100 times better than light microscope[162].

Methods

Materials

In this study, *Pseudomonas aeruginosa* bacteria were purchased from the American Type Culture Collection (ATCC BAA-47 and 27853). Additional MDR-PA strains were obtained from clinical isolates from the University of Oklahoma Health Sciences Center using appropriate IRB protocols and procedures. Wild-type *P. aeruginosa* PAO1 and its efflux pump deficient mutant, PaΔ3, were kindly provided by Prof. Helen Zgurskaya, University of Oklahoma. Chemicals were purchased from Sigma-Aldrich (DMSO, growth media, and electron microscopy fixatives). Antibiotics were purchased from Gold Biotechnology. 600 Da BPEI was purchased from Polysciences, Inc. MBEC Biofilm Inoculator with 96-well base plates was purchased from Innovotech, Inc.

Checkerboard Assays and Growth Curves

Checkerboard assays followed the methods of Lam et al.[117] to determine the synergistic effect between 600 Da BPEI and antibiotics against the *P. aeruginosa* strains growing in cation-adjusted Mueller-Hinton broth (CAMHB). Bacterial growth curves were obtained using CAMHB media augmented with various amounts of 600 Da BPEI and/or piperacillin inoculated with *P. aeruginosa* BAA-47 cells from an overnight culture (5×10^5 CFU/mL). Cells were grown at 35 °C with shaking. The OD600 (optical density at 600 nm) was monitored and recorded for each sample over 24 h. Each checkerboard trial was done in triplicate using sterile Greiner CellStar flat bottom polystyrene plates, catalog #655180. Each growth curve was done in duplicate.

MBEC Assay

The MBEC assay is adapted from previous literature reports. [113, 163]

MBEC Inoculation and Biofilm Formation

A subculture of *P. aeruginosa* BAA-47 was grown from the cryogenic stock on an agar plate overnight at 35 °C. The MBEC plate was inoculated with 150 µL of CAMHB/well plus 1 µL of a stock culture made from 1 colony/mL *P. aeruginosa* BAA-47 in CAMHB (~5×10^5 CFU/mL). The MBEC inoculator plate was sealed with Parafilm and incubated for 24 h at 35 °C with 100 rpm shaking to facilitate biofilm formation on the prongs. Following biofilm formation, the lid of the MBEC inoculator was removed and placed in a rinse plate containing 200 µL of sterile PBS for 10 s.

MBEC Antimicrobial Challenge

A challenge plate was made in a new presterilized 96-well plate in a checkerboard-assay pattern to test the synergistic activity of 600 Da BPEI + antibiotic combinations. Antimicrobial solutions

were serial-diluted and added to the 96-well plate, which contained 200 μL of CAMHB per well. After the rinsing step, the preformed biofilm prong lid was immediately transferred into the prepared antimicrobial challenge plate and incubated at 35 °C for 20–24 h.

MBEC Recovery and Quantitative MBEC

After the challenge period, the MBEC inoculator lid was washed and transferred into a recovery plate containing 200 μL of CAMHB per well, sonicated on high (Branson B-220, frequency of 40 kHz) for 30 min to dislodge the biofilm, and then incubated at 35 °C for 20–24 h to allow the surviving bacterial cells to grow. After incubation, the OD600 of the recovery plate was measured using a Tecan Infinite M20 plate reader to determine the MBEC of the antimicrobial compounds tested. A change in OD600 greater than 0.05 indicated growth. Likewise, the OD600 for the base of the challenge plate was measured to determine the MICs of the antimicrobial compounds. The fractional inhibitory concentration index (FICI) calculated on the basis of the established equation[160] was used to determine synergy (FICI $\leq$ 0.5), additivity (0.5 < FICI < 1), and no synergy (FICI $\geq$ 1).

Scanning Electron Microscopy

P. aeruginosa BAA-47 cells were inoculated from an overnight culture (5×10^5 CFU/mL) and grown at 35 °C with shaking. The bacteria were grown in four separate sublethal treatments: 600 Da BPEI (4 μg/mL), piperacillin (1 μg/mL), combination (4 μg/mL 600 Da BPEI + 1 μg/mL piperacillin), and untreated control. Growth was stopped at late-lag phase. Samples were collected by centrifugation and fixed with Karnovsky fixative (2% glutaraldehyde and 2% paraformaldehyde in 0.1 M cacodylate buffer) for 30 min. The cells were then fixed with 1% OsO4 for 30 min in the dark. The cells were washed with water three times. A couple drops of each

sample were placed on clean, poly-l-lysine coated coverslips and air-dried for 30 min. The samples were dehydrated by going through a series of ethanol solutions (20%, 35%, 50%, 70%, and 95%), spending 15 min in each solution. Afterward, the samples were dried with hexamethyldisilazane (HMDS). They were then mounted on aluminum stubs with carbon tape and sputter coated with AuPd. A Zeiss NEON SEM was used to image the samples at 5 kV accelerating voltage.

Isothermal Titration Calorimetry (ITC)

An isothermal titration calorimeter (MicroCal PEAQ-ITC, Malvern Inc., Malvern, U.K.) was used to assess *P. aeruginosa* lipopolysaccharide (LPS) binding with 600 Da BPEI. Solutions of BPEI (0.64 mg/mL) and L8643 *P. aeruginosa* LPS (5 mg/mL) were prepared in 50 mM Tris-HCl (pH 7) buffer at 25 °C. Titrations were carried out at 25 °C using injections of 2 μL that lasted 4 s and were separated by 150 s time intervals. For each experimental setup, controls were performed in which the titrant was injected into pure buffer, buffer was injected into the cell, and buffer was injected into pure buffer. The experiment was done in duplicate.

H33342 Bisbenzimide and NPN Accumulation Assays

An overnight culture of *P. aeruginosa* BAA-47 was used to inoculate fresh CAMHB media for another 5 h at 35 °C with shaking. Bacterial cells were collected by centrifugation at 6000 rpm for 40 min and resuspended in PBS. The OD600 of the cell suspension was adjusted to ∼1.0 and kept at room temperature during the experiment. Aliquots (180 μL/well) of the cell suspension were transferred to a 96-well flat-bottom black plate in the format of column 1, PBS blank; column 2, untreated control cells BAA-47; column 3, cells BAA-47 + BPEI (sublethal concentration). Five technical replicates of each group were conducted. Fluorescent probes(40−42) Hoechst 33342 bisbenzimide (H33342) or 1-N-phenylnaphthylamine (NPN) were added (20 μL) to each well with a final concentration of 5 μM. Fluorescence was read immediately after the addition of H33342 or

NPN by a Tecan Infinite M20 plate reader with the excitation and emission filters of 355 and 460 nm for H33342 or 350 and 420 nm for NPN, respectively. Fluorescence data were normalized to the emission before cells were added in the PBS control, and they were plotted against time to show the cellular uptake of H33342 or NPN over 10 min. Fluorescence emission values obtained from the control experiments of dye + 600 Da BPEI were the same as those of dye only.

Results and Discussion

Checkerboard assay reveals synergistic relationship between 600 Da BPEI and β-lactam antibiotics

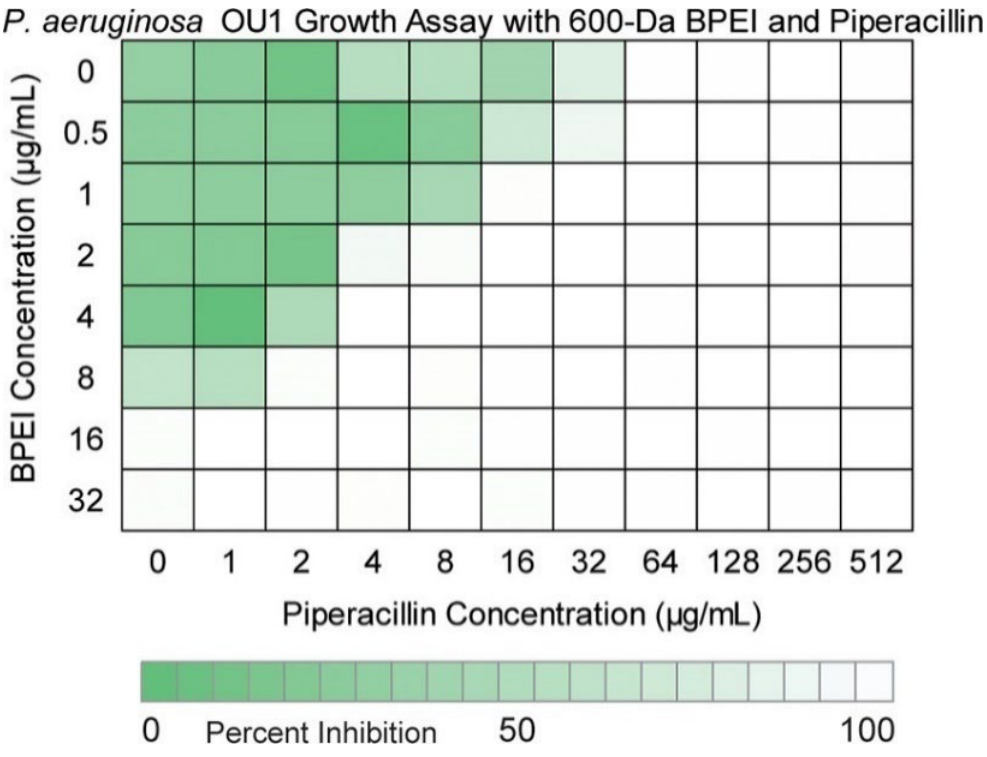

Figure 10. Representative checkerboard assay demonstrating that sublethal amounts of 600 Da BPEI lower that piperacillin MIC against a multidrug resistant *P. aeruginosa* clinical isolate. The MIC of piperacillin (64 µg/mL = resistant) is reduced when combined with 2 µg/mL

In this study, checkerboard assays exhibited synergistic effects between 600 Da BPEI and β-lactam antibiotics against two laboratory strains of *P. aeruginosa*, ATCC 27853 and ATCC BAA-47,[164] and several multidrug-resistant (MDR) clinical isolates from patients at the University of Oklahoma College of Medicine. Additional information regarding resistance and antibiotic susceptibility profiles of clinical isolates can be found in Supplemental information (See Appendix). The minimum inhibitory concentrations (MICs) of 600 Da BPEI and piperacillin against these strains were determined and used to calculate the fractional inhibitory concentration index (FICI).[113, 165] An FICI lower than 0.5 indicates synergy, while an FICI between 0.5 and 1 represents additivity. The 600 Da BPEI MICs against *P. aeruginosa* ATCC 27853 and ATCC BAA-47 and 5 clinical isolates varied from 8 to 64 μg mL^{-1} (Table 1 and Figure 11). For the β-lactam antibiotic piperacillin, resistance in *P. aeruginosa* is defined by USCAST as a minimum inhibitory concentration (MIC) ≥ 8 μg/mL.[160] As shown in Table 1, the ATCC strains were susceptible to piperacillin, yet the clinical isolates exhibited strong piperacillin resistance. Using checkerboard assays (Figure 11), the presence of 600 Da BPEI lowered the MIC of piperacillin against MDR-PA isolate OU1 and the other tested strains shown in the Supplemental information (See Appendix).[166] The clinical isolates are multidrug-resistant, and all were rendered susceptible to piperacillin with the exception of OU15. Fortunately, we were able to restore susceptibility of OU15 to cefepime, whose 32 μg/mL MIC (resistant) is lowered to 0.5 μg/mL with 16 μg/mL 600 Da BPEI (see Supplemental information in Appendix). Cefepime resistance in OU19 and OU22 (MIC = 64 and 128 μg/mL, respectively) is also eliminated with 16 μg/mL 600 Da BPEI (MIC lowered to 8 μg/mL for both strains (see Supplemental information in Appendix).

Table 1. MIC and calculated FICI values for *P. aeruginosa* treated with 600 Da BPEI and/or Piperacillin

Strain	MIC [µg/mL]						FICI	Outcome
	600-Da BPEI	PIP/TAZO[1,2]	PIP[1,3]	PIP[1,3]	+	600-Da BPEI		
PA 27853	16	-	4	0.25	+	4 µg/mL	0.31	Synergy
PA BAA-47	32	-	4	1	+	8 µg/mL	0.50	Additivity
PA OU1	16	64	64	4	+	2 µg/mL	0.31	Synergy
PA OU12	8	128	128	8	+	4 µg/mL	0.31	Synergy
PA OU15	32	n.d.	128	32	+	8 µg/mL	0.50	Synergy
PA OU19	64	n.d.	> 256	1	+	16 µg/mL	0.31	Synergy
PA OU22	64	n.d.	> 256	4	+	16 µg/mL	0.37	Synergy

[1]Piperacillin (PIP) susceptibility breakpoints are resistance ≥ 8 µg/mL; susceptible < 8 µg/mL
[2]Determined by the OUHSC Clinical Microbiology laboratory; TAZO = tazobactam
[3]Determined in this work; piperacillin only, no tazobactam added
n.d. = not determined

The data in Table 1 were collected without tazobactam, a β-lactamase inhibitor, suggesting that β-lactamases of the listed strains can be overcome by 600 Da BPEI. Perhaps the intracellular piperacillin concentration is sufficient to overcome losses from β-lactamase hydrolysis. Sublethal concentrations of piperacillin become bacteriostatic when combined with sublethal concentrations of 600 Da BPEI (Figure 12). Within 24 h, the untreated control group grew to an OD_{600} of 2, as did the individual treatment of either 600 Da BPEI or piperacillin alone, indicating that these concentrations are insufficient to kill the bacteria. Only the combination 600 Da BPEI + piperacillin treatment could effectively stop its growth, highlighting the restorative value of 600 Da BPEI on β-lactam antibiotic efficacy.

Growth Curve shows that sublethal amounts of 600 Da BPEI and piperacillin slow bacterial growth

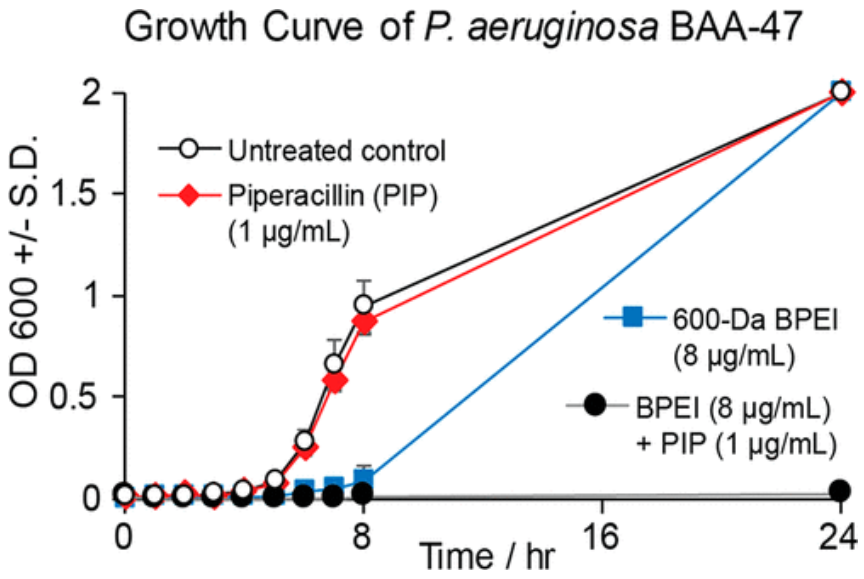

Figure 11. Growth curves of P. aeruginosa BAA-47 showing that sublethal amounts of 600 Da BPEI and piperacillin are bacteriostatic. However, treating the culture with the combination of 600 Da BPEI and piperacillin, each at sublethal concentrations, stops growth.

There are concentration dependent effects of 600 Da BPEI, which has antibiotic properties at high concentrations. At lower concentrations used for β-lactam potentiation, the mechanism of action likely involves creating new avenues of access through the LPS layer to increase intracellular antibiotic concentrations and overcome β-lactamase enzymes and efflux pumps. At slightly higher concentrations needed to potentiate erythromycin, 600 Da BPEI causes slight perturbations to the outer membrane. However, previous data collected with fluorescence microscopy show that sub-MIC concentrations of 600 Da BPEI do not accumulate within *E. coli* cells.[165]

The ability to improve β-lactam efficacy at low concentration occurs because the cross-linked network of LPS presents a barrier to free-diffusion of antibiotics. The outer membrane of *P. aeruginosa* contains numerous beta barrel proteins amongst the alkyl chains of the phospholipid and LPS leaflets. These porins allow for the diffusion of β-lactam antibiotics[167] between the extracellular milieu and the periplasmic space.[168] However, the inner-core, outer-core, and O-antigen regions of LPS slow the uptake of β-lactams.[169] Ca^{2+} and Mg^{2+} ions stabilize these anionic

regions and we posit that 600-Da BPEI also binds to these sites to cause localized reduction in the diffusion barrier. This was evaluated by determining if 600-Da BPEI binds to LPS and by performing permeation assays that monitor the intracellular concentration of probe molecules.

Mechanism of Action: 600 Da BPEI interacts with *P. aeruginosa* LPS

To directly measure any interactions between 600 Da BPEI and LPS, Isothermal Titration Calorimetry (ITC) was utilized. Here, it was used to confirm interactions between 600-Da BPEI and *P. aeruginosa* LPS. The raw thermogram data obtained when 600-Da BPEI was titrated into LPS show exothermic peaks resulting from each injection. Signals also gradually became smaller suggesting that the LPS became increasingly saturated with 600-Da BPEI. These titration data are converted to an isotherm (Figure 14). The negative ΔH values indicate exothermic binding. This binding profile indicates that there was an interaction between 600-Da BPEI and LPS which is likely through electrostatic interactions between cationic amines of 600-Da BPEI and anionic phosphates and carboxylate groups of LPS molecules. The x-axis of the thermogram is used to reveal the molar ratio of each species if their respective molecular weights are known. Using an LPS molecular weight of 20 kDa,[170] the molar ratio of ~2.5 indicates the several molecules of 600-Da BPEI can bind to a single LPS molecule. In the bacterial outer membrane environment, this would allow for multiple 600-Da BPEI binding events with the inner-core, outer-core, O-antigen, and lipid A regions. This scenario would alter the localized LPS packing scheme and open new pathways for the passive diffusion of antibiotics to the membrane and its porin transporters.

The inner-core and outer-core polysaccharides of LPS contain phosphate and carboxylate groups that attract metal ions. These binding sites, and the corresponding metal ions, are located 1-2 nm away from the membrane.[169, 171-172]. Likewise, the LPS O-antigen region contains carboxylates that bind metal ions.[173-174] The metal ions form bridges between adjacent LPS molecules and this

network presents a barrier to the passive diffusion of hydrophilic compounds, including β-lactam antibiotics. However, the ITC data show that cationic 600-Da BPEI binds with these anionic sites of LPS. This would cause localized disruption of the LPS-metals network and creates new avenues of access for β-lactams to reach porin transporters imbedded in the membrane lipid tails. In this manner, 600-Da BPEI increases intracellular concentration of β-lactam antibiotics but does not need to cross the membrane itself to be effective (Figure 15).

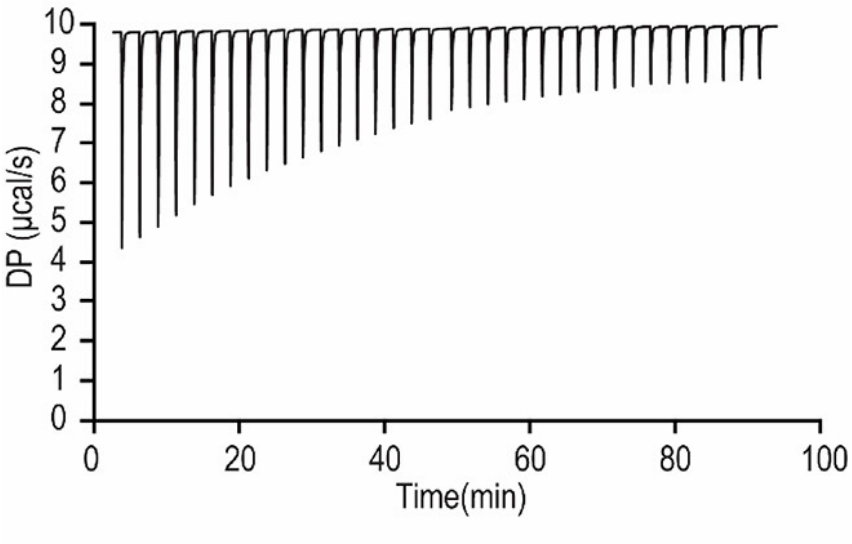

Figure 12. Raw ITC thermogram of 600 Da BPEI interacting with *P. aeruginosa* LPS. 600 Da BPEI was titrated into LPS via 2 µL injections in 50 mM Tris-HCl buffer at 25 °C. Raw data show exothermic binding event.

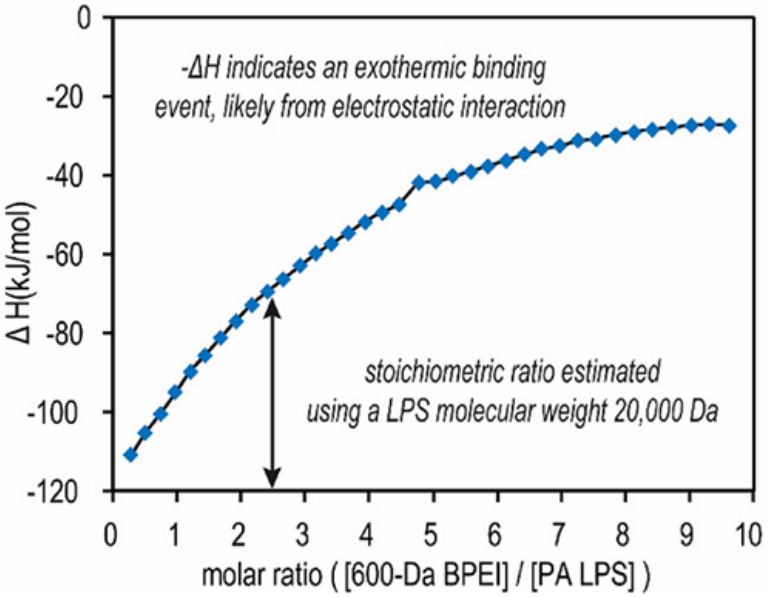

Figure 13. Thermogram abscissa generated from the molar ratio of each species. Here, the molecular mass of LPS was estimated to be 20 kDa in accordance with literature reports.

Mechanism of Action: 600 Da BPEI increases Passive Influx

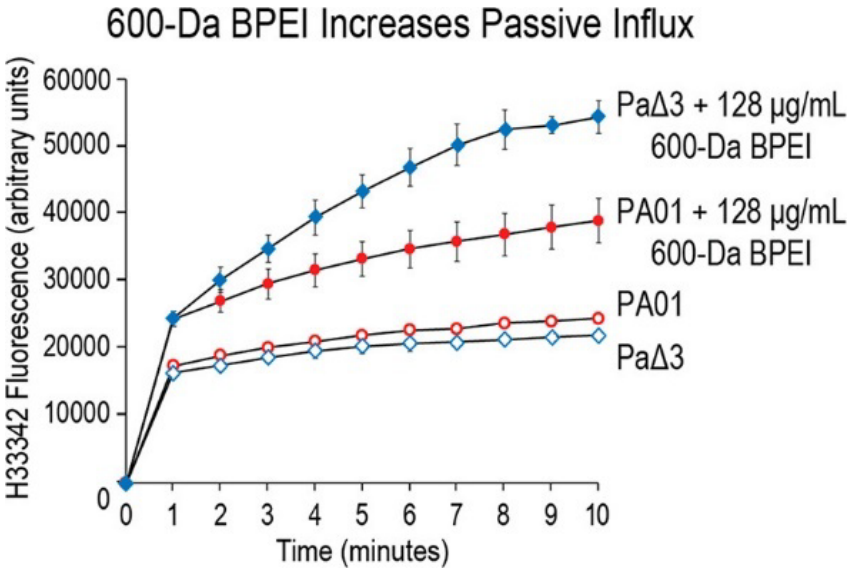

Figure 14. Fluorescence profile of H33342 dye accumulation assay shows the effect of 600 Da BPEI on the intracellular accumulation of the dye.

Although 600-Da BPEI may be increasing antibiotic influx, it may also be hindering efflux pumps. This can be tested with a fluorescence assay. Using *P. aeruginosa* PA01 that is multi-drug resistant,[175] bacterial cells were exposed to the fluorescent probe H33342 that is also a substrate for efflux pumps. Fluorescence spectroscopy data measure its accumulation within the cells (Figure 15). The fluorescence intensity of H33342 is significantly enhanced when bound to the cell membranes and bacterial DNA, leveling off at the maximum intracellular cellular concentration of H33342. The addition of 600-Da BPEI increased its fluorescence intensity four-fold. The increase of H33342 intracellular concentration suggests that 600-Da BPEI either enhanced the passive diffusion or inactivated the active efflux system. Using PA01's efflux-deficient mutant, PaΔ3,[175] the fluorescence intensity increases further. This shows that 600-Da BPEI is not blocking efflux processes. If BPEI was blocking efflux, the intensities would be same because the efflux pump target is absent in PaΔ3 cells and 600-Da BPEI would not influence the intracellular concentration in this mutant strain. However, the probe concentration does increase in the presence of 600-Da BPEI and thus the effect is attributed to increased drug influx that allows *Pseudomonas* cells take up more of the fluorescent molecule.

A noteworthy consideration is that the concentration of BPEI (128 μg/mL) used in fluorescence assays is higher than that needed for potentiation or MICs because the cell density needed for a detectable fluorescence signal was much higher. All fluorescence studies used a cell density of ~6 × 10^9 CFU/mL, while checkerboard assays only inoculated a cell density of 5 × 10^5 CFU/mL. Therefore, an amount of 128 μg/mL BPEI for fluorescence assays is considered sublethal, which is tested and confirmed by resazurin assays (Figure S6; see Supplemental information in Appendix). The reduction of resazurin to resorufin occurs via cellular metabolism and thus is an excellent reporter of cell viability.[176] As shown in Figure S6, 128 μg/mL 600 Da BPEI for this

large cell density (~6×10^9 CFU/mL) is not lethal but causes a 12.5% reduction in cell viability. However, resazurin fluorescence values for cells treated with polymyxin B are near background levels, indicating that these cells are dead. These results have several important impacts. First, the cells in the fluorescence assays are viable, and thus, drug influx and efflux processes control the intracellular concentration rather than widespread disruption of the outer membrane that leads to cell lysis. Second, 600 Da BPEI is less toxic to *P. aeruginosa* BAA-47 cells than polymyxin B, which is also toxic toward eukaryotic cells. The biocompatibility of 600 Da BPEI has been demonstrated against mouse fibroblast cells, ,[165] immortal human cell lines,[177] and primary human kidney epithelial cells.[177] Finally, at sublethal concentrations, 600 Da BPEI is not disrupting cellular energy metabolism because resazurin reduction occurs via the conversion of NADH/H+ to NAD+, and thus, outer membrane energetics are also likely to be unaffected.

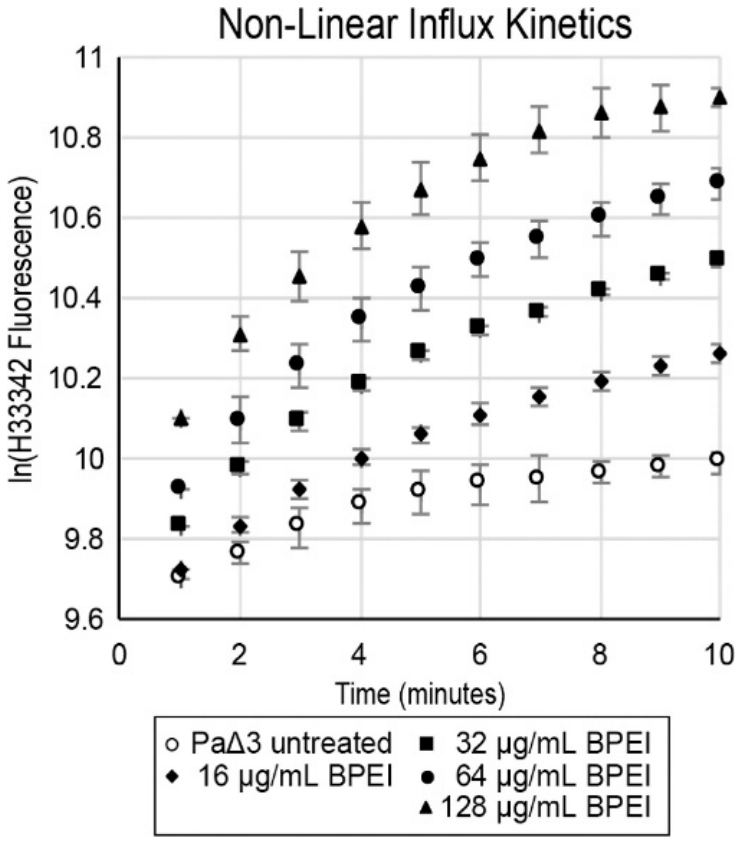

Figure 15. Uptake of H33342 is a multistep process with exponential kinetics. This phenomenon can be identified by plotting the natural logarithm of dye concentration versus time.

The ability of 600 Da BPEI to increase H33342 influx is concentration dependent. In the PAO1 cells, the competition between influx and efflux results in a gradual increase in H33342 concentration over time. The data points for H33342 concentration in cells treated with 16 and 32 µg/mL 600 Da BPEI overlap, whereas the data for 64 µg/mL 600 Da BPEI is slightly higher and 128 µg/mL 600 Da BPEI gives the highest reading (Figure 13). As shown in Figure S6, these concentrations are not lethal toward a high density of *P. aeruginosa* cells. However, the presence of efflux creates a multifactor condition that complicates the interpretation of biochemical mechanisms.[178] Thus, this experiment was repeated with the efflux-deficient mutant PaΔ3. Inspection of the data reveal that the increase in H33342 concentration over time is not linear but rather exponential in nature, in agreement with a recent kinetic analysis.[178] By plotting the

ln[H33342] versus time, it is apparent that the rate of influx is slowest with the lowest concentration of 600 Da BPEI (Figure 16). Thus, a faster rate of influx at a higher concentration of 600 Da BPEI is due to binding with additional anionic sites of the O-antigen, outer-core, and inner-core regions. As illustrated in Figure S7 (see Supplemental information in Appendix), low concentrations of 600 Da BPEI limit binding to the outermost regions of LPS. As the BPEI concentration is increased, additional binding sites are occupied until, at levels approaching the MIC, 600 Da BPEI binds to lipid A. This scenario allows sub-MIC concentrations of 600 Da BPEI to open the LPS network and facilitate diffusion of the H33342 dye. This model also explains the high MIC of 600 Da BPEI (16–64 μg/mL), whereas only a fraction of this amount is required for β-lactam potentiation (Table 1). The increased piperacillin MIC in the clinical isolates may be due to overexpression and/or novel β-lactamases, deletion, or reduced expression of specific porins, mutations within the porin channel that hinder β-lactam transport, or efflux pumps that are overexpressed. Regardless, 600 Da BPEI can restore piperacillin susceptibility in the clinical isolates, causing a considerable reduction of piperacillin MICs.

With regards to other antibiotics, such as Meropenem and erythromycin, the situation is more complicated. For the clinical isolates OU15, OU19, and OU22, the Meropenem MIC was 16–64 μg/mL, but there was no synergy with 600 Da BPEI, only additivity that caused a modest reduction in MIC values (Figure S4; see Supplemental information in Appendix). Likewise, the erythromycin MICs were 256 μg/mL for these 3 isolates, and 600 Da BPEI exhibited synergy but only reduced the erythromycin MIC by a factor of 4 (Figure S5; see Supplemental information in Appendix). Recognizing that 600 Da BPEI increases the influx of H33342 in a concentration dependent manner and that the rate of influx also increases with concentration, it is possible to understand the antibiotic potentiation data. When 600 Da BPEI at 1/4th of its MIC value is added,

the diffusion barrier of LPS is reduced. This reduces the piperacillin MIC from over 256 to 1–4 μg/mL. The potentiation effect on Meropenem is lower, which may be due to hindered porin transport. For erythromycin, reducing the MIC from 256 to 64 μg/mL occurs in the presence of 16 μg/mL 600 Da BPEI. As with H33342, erythromycin crosses membranes by passive diffusion, and thus, at 16 μg/mL, 600 Da BPEI is reducing diffusion barriers from LPS rather than disrupting the membrane itself. Membrane disruption occurs at the MIC of BPEI, 64 μg/mL.

Magnesium Cations can restore LPS

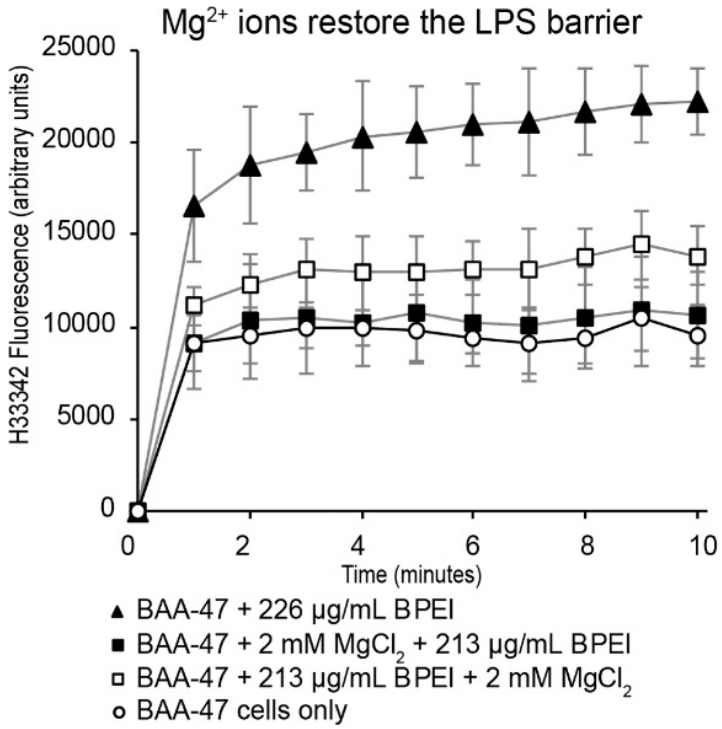

Figure 16. 600 Da BPEI binds to LPS through anionic sites on the inner-core, outer-core, and O-antigen regions. These sites also bind divalent metal ions.

The ability of 600 Da BPEI to potentiate β-lactams occurs through electrostatic interactions with LPS anionic sites that also attract metal ions. In the absence of metal ions, the anionic LPS molecules would repel each other and disperse into the extracellular milieu. Instead, Mg^{2+} ions allow the formation of a stable membrane layer by binding to phosphate groups of the lipid A moiety and forming electrostatic bridges between adjacent LPS molecules. Additional phosphate and carboxylate groups are found on heptose and ketodeoxyoctulosonate units of the core oligosaccharides.[168-169, 171, 173] The O-antigen groups are decorated with hydroxyls and the occasional carboxylate group that can attract metal ions. [173] These anionic LPS sites are critical resistance mechanisms. [179] As Hancock and co-workers found, various compounds (including

cationic species) disrupt the LPS's Mg^{2+} chelation and increase *P. aeruginosa*'s susceptibility to antibacterial agents.[180-182] The primary amines on 600 Da BPEI enable it to bind with phosphate and carboxylate groups, and its flexible branches facilitate structural reorganization to reach multiple binding sites within the inner- and outer-core regions of LPS and span adjacent LPS molecules. The ability of 600 Da BPEI to influence membrane permeability, such as the influx of H33342 (Figure 15), readily occurs at sublethal concentrations (Figure S8; see Supplemental information in Appendix). However, there is a dependence on divalent metal ions. 600 Da BPEI weakens the LPS network that otherwise hinders drug uptake. Conversely, adding Mg^{2+} and Ca^{2+} ions stabilize the LPS to strengthen the barrier. This competition is demonstrated in Figure 17. Here, 2 mM Mg^{2+} ions were exposed to BAA-47 cells that were treated with 600 Da BPEI. The lower fluorescence of H33342 indicates that its influx has been slowed by metal ions that reverse the weakening of the LPS diffusion barrier, but this process is insufficient to completely dislodge 600 Da BPEI from the phosphate/carboxylate binding sites and restore the LPS barrier to its full strength. Similar effects are observed for Ca^{2+} ions (Figure S8; see Supplemental information in Appendix)[116]. For both metal ions, the order of addition affects the data. When the cells are treated with 600 Da BPEI first and metal ions second, the H33342 intensity reaches a magnitude lower than the BPEI-only data but greater than that for cells only (open squares, Figure 17). However, if the metal ions are added first, the addition of 600 Da BPEI does not affect the H33342 intensity (closed squares, Figure 17). One possible explanation is that the anionic sites of LPS are fully occupied by divalent metal ions, and thus, 600 Da BPEI cannot bind and promote the diffusion of the fluorescent dye (Figure S9; see Supplemental information in Appendix). The mechanism for 600 Da BPEI is different from other agents that weaken the LPS barrier by chelating metal ions, such as ethylenediamine tetraacetic acid (EDTA). Using data collected with ITC, 600 Da BPEI

will chelate Cu^{2+} ions (Figure S10; see Supplemental information in Appendix), but there is no interaction with Mg^{2+} or Ca^{2+} ions (Figure S10B,C; see Supplemental information in Appendix).

The importance of metal ions in the antibiotic mechanism is well established, and thus, the Clinical and Laboratory Standards Institute (CLSI) guidelines for MIC testing specify the use of cation-adjusted MHB (CAMHB).[183] These protocols were followed for the growth assay experiments, and thus, under standard conditions, metal ions in CAMHB do not interfere with potentiation by 600 Da BPEI. These data suggest that, when cells are grown in CAMHB, the array of metal binding sites within the outer membrane LPS are not fully occupied. This provides an opportunity for 600 Da BPEI to establish its own electrostatic interactions with the LPS and create new avenues of access for drugs to reach the membrane. This effect is concentration dependent. Lower amounts of 600 Da BPEI facilitate the uptake of piperacillin, a 517 g/mol β-lactam antibiotic that is readily transported to the cytoplasm by transmembrane porins. However, larger amounts of 600 Da BPEI are needed to create the larger avenues of access for erythromycin, a 734 g/mol macrolide that reaches the cytoplasm via passive diffusion.

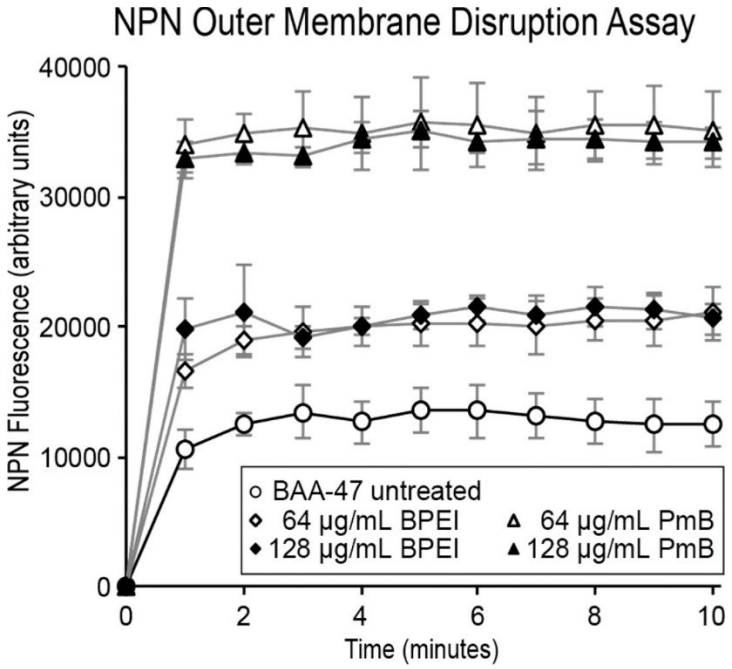

Figure 17.Dye 1-N-phenylnaphthylamine (NPN) accumulates in hydrophobic regions and fluoresces when bound to phosphate groups. Polymyxin B (PmB) allows greater uptake of NPN than 600 Da BPEI.

In addition to weakening the LPS barrier to diffusion, 600 Da BPEI could be increasing drug influx by changing the permeation properties of the outer membrane and perhaps even disrupting the outer membrane lipid bilayer itself. The phenomenon can be tested with the fluorescence probe molecule 1-N-phenylnaphthylamine (NPN) that localizes to the lipid membrane and fluoresces when bound to phospholipids.[184-186] In the absence of agents that disrupt the cell membrane, fluorescence is weak from barriers to passive diffusion. However, when the outer membrane is breached, NPN can easily reach phospholipids of the inner leaflet and fluorescence intensity increases. As shown in Figure 18, NPN fluorescence reaches value of about 13 000 units in a sample of ~6×10^9 CFU/mL *P. aeruginosa* BAA-47 cells. The treatment of a similar sample with 64 µg/mL polymyxin B causes a 2.7-fold increase in fluorescence intensity, which occurs via insertion of polymyxin B into the membrane via self-promoted uptake.[180] However, 64 and 128

μg/mL 600 Da BPEI cause a 1.5-fold increase in NPN fluorescence, and we know that these concentrations of 600 Da BPEI are nonlethal (Figure S6; see Supplemental information in Appendix). Thus, we suggest that 600 Da BPEI is weakening the LPS diffusion barrier, but it is not intercalating into the membrane bilayer that otherwise would lead to a higher increase in NPN fluorescence intensity.

Mechanism of action: 600 Da BPEI causes morphological changes in *P. aeruginosa* cells

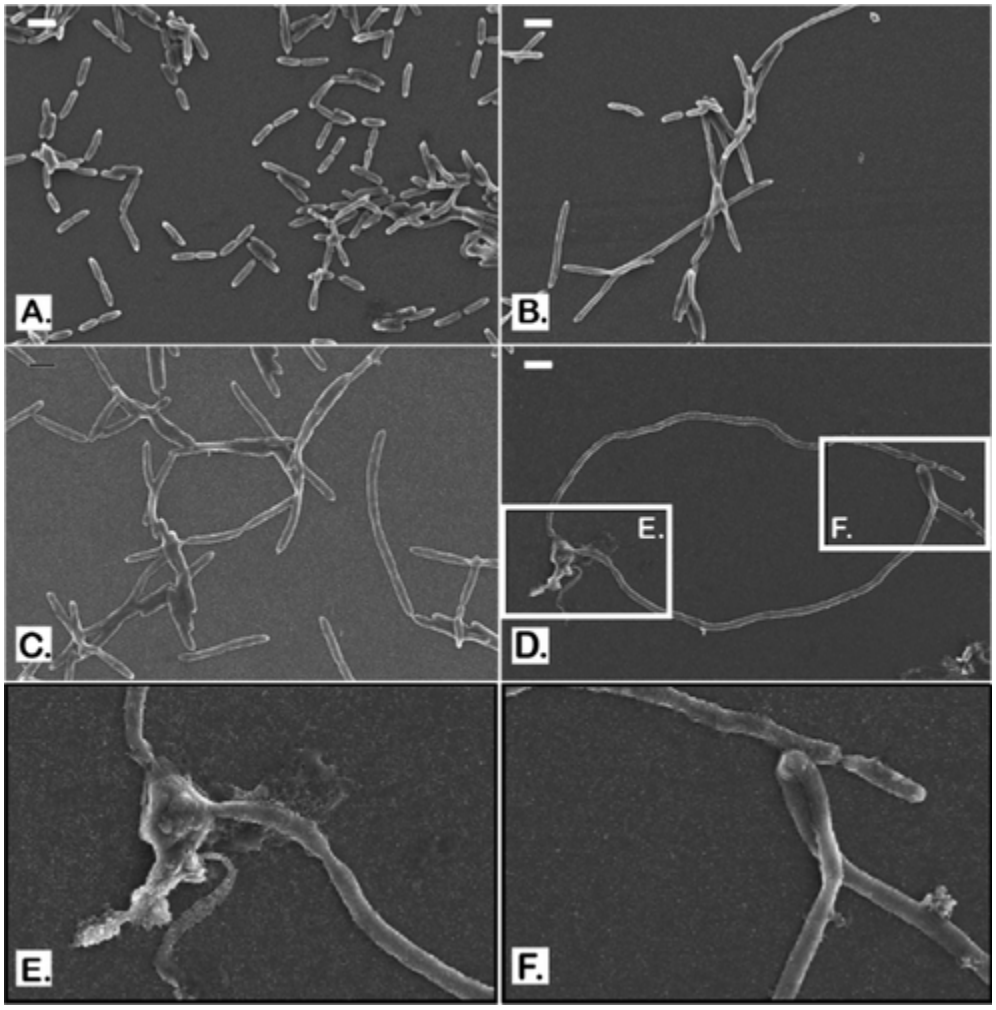

Figure 18. SEM of PA BAA-47. Untreated control (A), 600 Da BPEI treated cells (4 μg/mL) (B) and piperacillin treated cells (1 μg/mL) (C). The combination of 4 μg/mL 600 Da BPEI + 1 μg/mL piperacillin treated cells (D) with insets (E) and (F) with higher magnification.

The ability of 600 Da BPEI to weaken the LPS diffusion barrier without causing widespread membrane disruption and cell lysis is shown with scanning electron microscopy (SEM). SEM was conducted to examine the morphology and the possible effects of 600 Da BPEI on bacterial cell division. *P. aeruginosa* BAA-47 cells were grown to mid-log phase and subjected to four separate treatments: untreated control, sublethal 600 Da BPEI, sublethal piperacillin, and a combination of 600 Da BPEI and piperacillin, each at sublethal combinations. SEM images of the untreated control sample (Figure 19A) show that all the cells have a regular rod shape with a normal size distribution and division septa are clear. BPEI treated cells (Figure 19B) are longer, and cell-divided septa show a gradual narrowing rather than a sharper interface. The piperacillin treated cells (Figure 19C) are longer, have signs of a well-formed division septum, and exhibit signs of cell wall weakening without bursting. The combination of BPEI + piperacillin caused the treated cells (Figure 19D) to rupture (Figure 19E), and they show extreme distortions in shape (Figure 19F). The extreme distortions in both size (~20 times longer than untreated control cells) and shape without obvious division septa suggests that the recruiting, activity, and/or competence of bacterial divisome [187-188] components is hindered. These cellular morphological changes aid in explaining the killing properties of the BPEI + piperacillin combination, although the concentration of each compound is sublethal on their own.

600 Da BPEI has *P. aeruginosa* antibiofilm activity

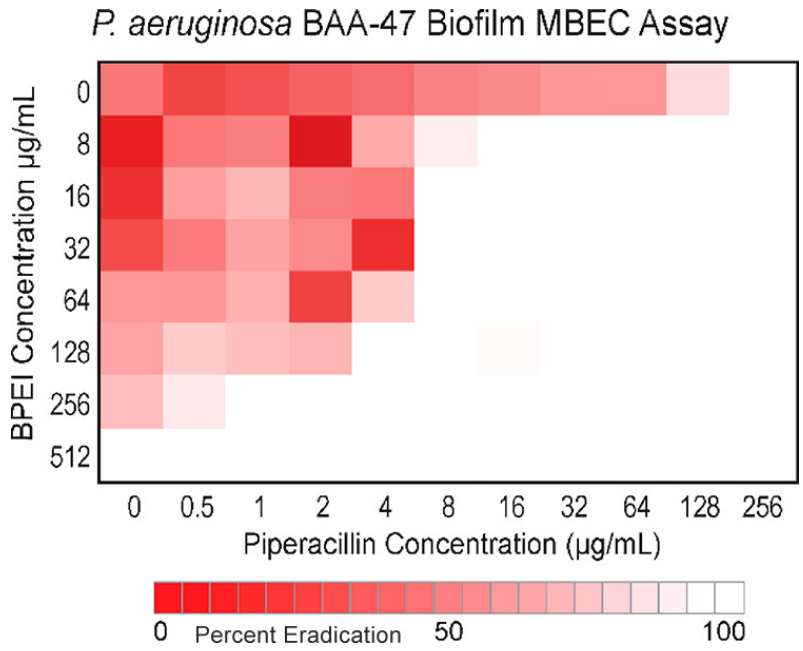

Figure 19. Biofilm eradication assay data collected with the MBEC assay. EPS creates additional barriers to piperacillin efficacy, and thus, 256 µg/mL is required to kill the bacteria.

Biofilms are accumulations of microorganisms embedded in a polysaccharide matrix known as extracellular polymeric substance (EPS), which protects the bacteria from antimicrobial agents.[189-190] Current in-patient treatments include cleansing the wound, debridement, maintaining a moist tissue environment, and when possible, eliminating the underlying factors that contributed to poor wound healing.[191] BPEI confronts the biofilm directly by disrupting the protective EPS. As shown in Figure 20, biofilms of *P. aeruginosa* BAA-47 create additional barriers that require 256 µg/mL piperacillin to kill the bacteria. This minimum biofilm eradication concentration (MBEC) is significantly higher than the MIC of 4 µg/mL. Likewise, the MBEC of 600 Da BPEI is 512 µg/mL, compared to its MIC of 32 µg/mL. A combination treatment results in biofilm eradication with 16 µg/mL BPEI and 8 µg/mL piperacillin. As with the planktonic checkerboard assays, this data was collected without a β-lactamase inhibitor. The mechanism of action for disrupting the biofilm relies

on the ability of cationic 600 Da BPEI to interact with anionic targets. Instead of binding with LPS in the planktonic cells, the biofilm targets are extracellular DNA, anionic polysaccharide Psl, and anionic polysaccharide alginic acid. [192-202]

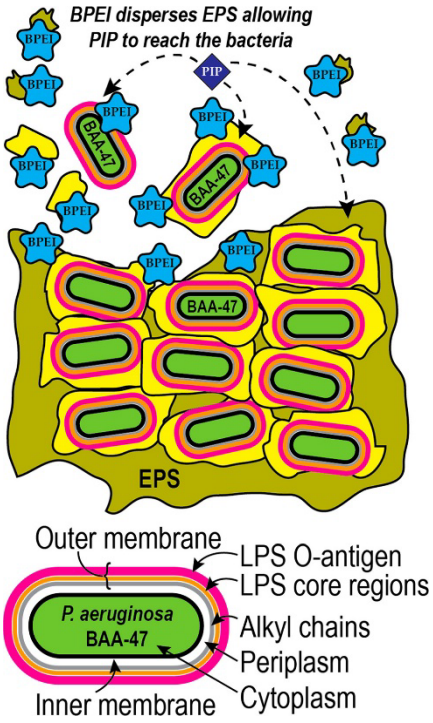

Figure 20. Illustration shows ability of BPEI to disperse *P. aeruginosa* biofilm and reach the planktonic populations.

The presence of the cationic polysaccharide Pel in P. *aeruginosa* biofilms would repel BPEI, but this effect does not prevent 600 Da BPEI from disrupting the biofilm matrix; thus, piperacillin can access the underlying cells (Figure 21). The data in Figure 20 also confirms the paradigm that antibiotics effective against planktonic *P. aeruginosa* are nearly inert against biofilms and resistant strains. When 600 Da BPEI binds to EPS, the biofilm disperses because the intermolecular network of exopolymers, protein, and metals ions is disrupted. [117] As a result, quiescent bacteria are released

into solution where they become metabolically active, and thus, the antibiotic can kill the bacteria after additional BPEI molecules reduce LPS barriers to drug influx.

Antimicrobial polyamines

The antimicrobial properties of cationic compounds are well-documented, including polyethylenimines (PEIs). An important caveat in considering this previous work is that PEIs, whether linear or branched, are available in a wide range of sizes, from 600 to 1 000 000 Da. The MW range correlates with the ability to disrupt membranes and cause toxicity toward eukaryotic cells. Fortunately, 600 Da BPEI has low toxicity, is nonmutagenic, has high biocompatibility,[152] and the low likelihood of causing red blood cell hemolysis has been demonstrated.[203] Khalil et al. reported the synergy of PEI with various antibiotics.[204] However, this work used 10 kDa PEI, which has a high toxicity, at a concentration of 250 μg/mL, which is 25 μM rather than the reported concentration of 250 nM. Nevertheless, the potentiation of antibiotics varied across different classes, with modest potentiation of β-lactams and no potentiation of erythromycin. Helander et al. reported that 50 kDa PEI causes catastrophic damage to the outer membrane of *Salmonella typhimurium* cells at 10 μg/mL.[184] This work was followed by a study of increased NPN uptake in *Escherichia coli*, *S. typhimurium*, and *P. aeruginosa* from citrate that chelates metal ions and the restoration of the diffusion barrier by excess Mg^{2+} ions.[205] Hancock and co-workers published an elegant summary of ways to overcome resistance mechanisms.[181] The strategy described by Hancock and Wong involves disrupting Mg^{2+} chelation by LPS in the outer envelope.[186] Cationic oligo-acyl-lysyls have 3 primary amines that potentiate rifampicin against *K. pneumoniae*, but this approach did not lower the MIC of penicillin G.[140] Recently, Fleeman et al. reported that small polyamines with benzene functional groups were found to be efflux-pump inhibitors,[206] but using

the efflux deficient mutant PaΔ3, our data show that 600 Da BPEI does not inhibit efflux pumps but instead functions by increasing antibiotic permeation. Synthetic diamines are reported to have antibacterial and antibiofilm properties against *P. aeruginosa* PAO1 via membrane depolarization and disruption.[207] Kwon and Lu found that spermine exhibited synergy with antibiotics against *Staphylococcus aureus* and *P. aeruginosa* PAO1.[208] Although spermine increased the MICs of cationic peptides, aminoglycosides, and quinolone antibiotics, there was a decrease in the MICs of β-lactams, chloramphenicol, and polymyxin B after the addition of 1 mM spermine. In contrast, 600 Da BPEI produces superior results where the piperacillin MIC is lowered to 1 μg/mL with only 13.5 μM (8 μg/mL) 600 Da BPEI.

Conclusion

We envision 600 Da BPEI as a topical agent applied to acute and chronic wounds. Instead of taking 3–6 weeks to heal, chronic wounds persist for 3–6 months,[190] in large part due to infections with bacteria exhibiting antimicrobial resistance (AMR) and their associated biofilms.[155, 209] Each year, chronic wounds arise from the hundreds of millions of acute skin and soft-tissue infections (SSTIs)[210] because anti-infective therapeutics work against many but not all SSTIs. The estimated 4.5 million chronic wound infections[211-214] increase the risk of recurrent infection and tissue necrosis[215-216] and are a major problem in healthcare and community settings.[215-217] Because 600 Da BPEI + antibiotic combinations can kill susceptible and resistant bacteria in their biofilm and planktonic environments, this strategy can reduce the bacterial burden in wound infections and speed healing before acute SSTIs become chronic, complicated infections.[210] Topical use reduces problems of matching pharmacokinetics (PK) and pharmacodynamics (PD) with those of antibiotics. There is a strong likelihood of developing a topical agent for wound treatment because

the water-soluble hydrophilic properties of 600 Da BPEI enable easy drug delivery to directly attack AMR and biofilms in the wound environment. There are minimal protein binding effects that would prevent activity in the wound environment, demonstrated with antibiotic potentiation assays using fetal bovine serum (FBS).[177] Growth media were prepared with 50% FBS, which did not change the oxacillin MIC. [177] Likewise, when 600 Da BPEI was subsequently added, serum proteins did not hinder potentiation. This is not surprising as 600 Da BPEI is very hydrophilic and would only bind with protein anionic groups that are accessible and not chelated with a metal or other protein residues. We reported minimal in vitro cytotoxicity[177] in studies that were serum-free in order to obtain a more accurate evaluation of toxicity without serum proteins preventing contact with the eukaryotic cells. The low cytotoxicity differentiates 600 Da BPEI from polymyxins.[182] *in vivo* toxicity issues are paramount, which will be the subject of future research investigations.

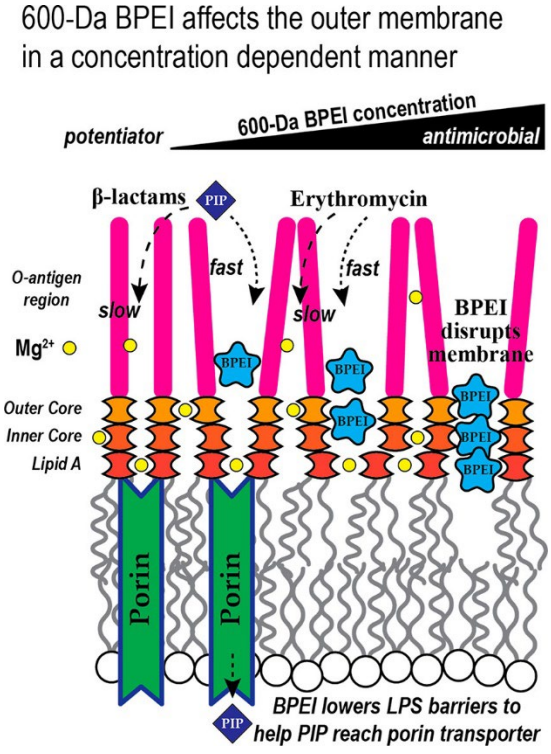

Figure 21. Summary image illustrating 600-Da BPEI as a potentiator of antibiotics and its proposed mechanisms of action.

Chapter 4: Biofilm disruption activity of PEGylated branched polyethylenimine

Background

Chronic wound infections present a significant burden to patients, clinicians, and the entire health care system. In the US, total Medicare spending on chronic wound care is estimated to be around $32 billion annually[218] stifling and complicating healing processes. *Pseudomonas aeruginosa* (*P. aeruginosa*) is a dangerous pathogen commonly found in wound infections. Wound infections aggravate the spread of pathogens and antimicrobial resistance genes because patients reside in, and are transported among, out-patient clinical facilities, in-patient hospitals, long-term care facilities, long-term acute care facilities, and skilled nursing home facilities.[219-222] Ineffective treatment of infected wounds can lead to tissue necrosis, bacteremia, and septicemia, allowing the spread of *P. aeruginosa* infections to major organs and the central nervous system.[223]

The danger to human health increases with multidrug resistant (MDR) *P. aeruginosa* infections, which are listed as a serious threat by the Centers for Disease Control and Prevention (CDC) 2019 Annual Report.[2] The threat is heightened by the ability of *P. aeruginosa* to aggregate and form biofilms. Microbial biofilms are communities of microorganisms enclosed in a protective extracellular polymeric substance (EPS) matrix.[6] Biofilm formation is an adaptive survival mechanism that pathogens activate as a physical protection from external stresses (i.e. antibiotics and antimicrobials, nutrient deprivation, sheer forces). Bacteria within biofilms have stronger resilience compared to free-floating planktonic bacteria and thus are harder to eradicate.[224] Biofilm formation by MDR strains of *P. aeruginosa* continue to pose a threat to human health and hence new antimicrobial and antibiofilm agents are required.

We have previously identified low molecular weight 600 Da branched polyethylenimine (600 Da BPEI) as a broad-spectrum antibiotic potentiator that can overcome antibiotic resistance and restore the susceptibility of MDR strains of Gram-positive and Gram-negative bacteria to existing antibiotics.[114, 166, 225-227] We have also reported its anti-biofilm properties and suggested that the cationic nature of BPEI enables electrostatic interactions with anionic targets in biofilms. However, the primary amines of 600 Da BPEI create cytotoxicity concerns that cannot be overlooked. As a result, modification by covalent attachment of a low-molecular-weight (350 MW) polyethylene glycol (PEG) group to 600 Da BPEI (PEG350-BPEI) led to a reduction in acute toxicity in a mouse model.[228] Additionally, PEGylation of BPEI improved the dispersal of methicillin-resistant *Staphylococcus epidermidis* (MRSE) biofilms while retaining β-lactam potentiation activity.[228]

Purpose of Experiment

In the previous chapter, we investigated the mechanism(s) of action that 600 Da BPEI employs against *P. aeruginosa* planktonic bacteria. In the same study, we also explored the effects of 600 Da BPEI on biofilms of *P. aeruginosa* using a Minimum Biofilm Eradication Concentration (MBEC) assay. In this work, we investigate both 600 Da BPEI and its less toxic derivative, PEG350-BPEI, in the eradication of *P. aeruginosa* biofilms, including biofilms of a MDR clinical isolate. The colony biofilm model was used to produce static biofilms and this model was a particularly useful method to observe the effect(s) of antimicrobials on static biofilms that known to form in wound infections.[229] This model produces more robust biofilms compared to a MBEC assay.[166] Treatments with 600 Da BPEI and PEG350-BPEI resulted in a reduction of bacterial colony forming units (CFU).

Principle of Techniques

In this study, we demonstrate the colony biofilm model as a useful method to test antimicrobial solutions. Figure 21 shows an overview of the growth and treatment conditions employed in our study. Biofilms grown via the biofilm colony model for 24 h show visible biomass deposited on the surface on the polycarbonate membrane resting on an agar plate. The polycarbonate membrane is a porous membrane that allows nutrients to pass through and feed the bacterial population. This model is adapted from a study conducted by Stoffel et al. where the authors compared various biofilm models while testing antibiofilm topical solutions[230]. After growing the *P. aeruginosa* biofilms using the modified colony biofilm model, we subjected the biofilms into biofilm killing assays. We used immersion and "drop" techniques to evaluate the antibiofilm capability of our molecules. The models were evaluated using a standard cell counting technique. We also observed the reduction in biofilm biomass through a modified crystal violet assay. Crystal violet is widely used for biofilm research. When biofilms are formed on the surface of a growth medium (e.g., 96-well plate, MBEC pegs), the adherent cells and biomass can be stained. Cells that die lose their adherence, which results to a lower crystal violet color intensity[231].

Fluorescence microscopy was used to study the anti-biofilm mode of action by which the bioactive moiety, 600 Da BPEI, disrupts pseudomonal biofilms. Light microscopy suffers from resolution limitation because of the "diffraction barrier"[162, 232]. This restricts to the ability of an optical system to resolve two objects, which means that the system has lower resolution. Laser scanning confocal microscopy (LSCM) was then developed to be a powerful imaging tool that can reach diffraction-limited resolution. In LSCM, a laser is scanned onto a sample and when the sample is excited, it can emit lower energy photons[232]. These photons are collected by a detector and an image can be

reconstructed. In this study, we utilized autofluorescence of *P. aeruginosa*. These pathogens secret a siderophore called, pyoverdine, which can be excited and give emission at specific wavelengths. Biofilms were imaged using autofluorescence (as opposed to staining) to minimize the variables applied to the biofilm before imaging it. Such variables may affect the sample conditions and can skew the imaging data. Thermodynamic interactions between 600 Da BPEI with DNA, a major stabilizing component of the biofilm architecture, were measured via ITC. Additional insights regarding the action of biofilm disruption were provided through scanning electron microscopy imaging (SEM). The principles of ITC and SEM are detailed in Chapter 3.

Methods

Materials

Pseudomonas aeruginosa bacterial stocks were purchased from American Type Culture Collection (ATCC BAA-47, a PAO1 strain, and ATCC 27853) and the multidrug-resistant strain (OU1) was obtained from the University of Oklahoma Health Sciences Center using appropriate Institutional Review Boards (IRB) protocols and procedures. Chemicals were purchased from Sigma-Aldrich (growth media and microscopy fixatives). 600 Da BPEI was purchased from Polysciences, Inc. and PEG350-BPEI is synthesized as previously described.[228]

Biofilm Biomass Disruption Assay

This assay is as adapted from a protocol previously described by Lam *et al*[225] with slight modification. A subculture of *P. aeruginosa* cells was grown from a cryogenic stock overnight at 37 °C. A presterilized 96-well polystyrene plate was inoculated with 100 µL of M63 media/well

(22 mM KH_2PO_4, 40 mM K_2HPO_4, 15 mM $(NH_4)_2SO_4$, 1mM $MgSO_4$, 0.4% arginine)[229] and 1 µL of 1 colony/mL in M63 media. The plate was incubated for 24 h at 37 °C to form established biofilms. After incubation, the planktonic bacteria were carefully removed by turning the plate over and removing excess liquid with gentle shaking. The plate was then washed by gently submerging in a small tub of water with shaking. To stain the biomass, 125 µL of 0.1% crystal violet was added to each well and incubated at room temperature for 10-15 minutes. After incubation, the crystal violet was removed, and the excess dye was washed 3-4 times. After washing, the plate was allowed to dry for 1 h.

To treat the biofilms, different treatment concentrations were added to the biofilm plate for a total volume of 100 µL (in Tris-HCl 0.05 M pH=7). The negative control was treated with Tris buffer alone. The positive control was treated with 100 µL of 30% acetic acid for 2 minutes. After 3 h of incubation at 37 °C, the dissolved solutions were carefully transferred into a separate flat-bottom 96-well plate for OD_{550} measurements. Statistical analysis among treated samples was preformed using t-test, $p<0.01$.

Biofilm Killing Assay

Biofilm Growth

A subculture of *P. aeruginosa* cells was grown from a cryogenic stock overnight at 37 °C. To grow biofilms, sterilized 13-mm polycarbonate membranes with 0.1µm pore size (Isopore™, Merck Millipore Ltd.) were placed on TSA plates and inoculated with 1 µL of cell culture from 1 colony/mL in TSB. One colony/mL of *P. aeruginosa* is approximately 5 x 10^5 CFU/mL[166] thus, a 1 µL inoculation is about 5 x 10^2 CFU. The plates were incubated at 37 °C for 24 h. After

incubation, the biofilms were subjected to immersion treatment or cellulose filtration disc treatment.

Immersion Treatment

The membranes with mature biofilms were transferred into solutions of 500 μL of Tris buffer with or without anti-biofilm agents. The samples were incubated in the treatment solutions overnight at 37 °C. After incubation, the membranes, along with the treatment culture, were transferred into vials and were subjected to sonication for 10 minutes. Cell viability was identified via agar plating with enumeration of colony formation units, or by measuring solution turbidity via optical density with visible light spectroscopy at 600 nm (OD_{600})..

Cellulose Filtration Disc Treatment

Membranes with mature biofilms were transferred to a fresh TSA plate and sterilized 7-mm cellulose filtration discs were carefully placed on top of the biofilm. A micropipette was used to deliver 40 μL of treatment (600 Da BPEI or PEG350-BPEI in Tris buffer) or control (Tris buffer only) to the disc. The biofilms were incubated at 37 °C for 8 h. After treatment, the membranes and cellulose filtration discs were transferred into vials with 10 mL of Tris buffer and subjected to sonication for 15 minutes to detach biofilms. After vortex mixing to create homogenous solutions, the amount of viable bacterial cells was determined via enumeration of colonies on agar plates using a spot plate technique.[233] Spot plating is an alternative to the more common method of spreading bacterial suspensions onto agar. Briefly, homogenous cell suspensions in 10 mL Tris buffer were serially diluted up to nine times. Then, 10 μL aliquots of each dilution were placed onto TSA plates and incubated overnight at 37 °C. Mean viable cell counts were converted to $\log_{10}$ units and standard deviations were calculated (n = 5 per treatment condition).

Scanning electron Microscopy

P. aeruginosa ATCC BAA-47 (PAO1) biofilms grown on sterilized polycarbonate membranes for 24 h were submerged in primary fixative (5% glutaraldehyde in 0.1 M cacodylate buffer) and incubated at 4 °C for 2 days. The membranes were removed from fixing solution and air-dried for at least 72 h at 25 °C. After drying, the membranes were mounted on aluminum stubs with carbon tape and sputter-coated with AuPd. Scanning electron microscopy images were taken using a Zeiss NEON at 5 kV accelerating voltage. For the treated samples, 24 h biofilms were treated with hydrated 7-mm cellulose filtration discs. The biofilms were treated with 40 µL of Tris buffer or 1024 µg/mL of 600 Da BPEI at time = 0, followed by a second dose/rehydration at time = 4 hours. After a total of 8 h incubation at 37 °C, the 7 mm cellulose filtration discs were carefully removed and the biomass remaining on the polycarbonate membrane was fixed and imaged as described above.

Isothermal Titration Calorimetry (ITC)

To identify any binding interactions between 600 Da BPEI and DNA, isothermal titration calorimetry (MicroCal PEAQ-ITC, Malvern Inc., Malvern, U.K.) was used. Briefly, 600 Da BPEI (3.2 mg/mL in Tris-HCl buffer) was titrated into a DNA solution (DNA Sodium Salt, Fish Sperm Ampresco®; 1.0 mg/mL in Tris-HCl buffer) in 2 µL lasting 4 s and separated by 150 s time intervals at 25 °C. Controls were performed and the experiment was done in duplicate.

Fluorescent Dye Diffusion Experiment

A subculture of the MDR clinical isolate, *P. aeruginosa* OU1, was grown from a cryogenic stock overnight at 37 °C as described above. To produce biofilms, sterilized 13-mm polycarbonate membranes (Isopore™, Merck Millipore Ltd.) were placed on TSA plates and inoculated with 5

μL of cell culture (1 colony/mL in TSB) and incubated for 48 h at 37 °C. After incubation, 5 μL of treatment solutions (0.5% 600 Da BPEI or Tris buffer only) were carefully applied with micropipette directly to the top of the biomass and incubated again at 37 °C for 3 hrs. Afterwards, samples were fixed with 4% paraformaldehyde for 16 hours at 4 °C before fluorescent imaging.

Confocal Laser Scanning Microscopy (CLSM)

CLSM experiments were performed using Leica SP8 confocal laser scanning microscope. Images were collected using a HCPL FLUOTAR 5x / 0.15 Dry objective lens. All images were 1024 pixels x 1024 pixels in size (3,100 μm x 3,100 μm). Biofilm samples (treated with Tris buffer or 0.5% 600 Da BPEI) were mounted on the microscope stage. Prior to scanning, 3 μL of rhodamine B dye (50 μg/mL) was carefully applied via micropipette directly to the top of the biofilm. Immediately after adding the dye, fluorescence microscopy images of the dye were collected. Representative images for biofilms treated with Tris buffer only and 0.5% 600 Da BPEI were collected. The autofluorescence of the biofilm was excited with a 405 nm GaN laser and was detected by a HyD detector at the emission window between 415 nm and 550 nm. The rhodamine B dye was excited with a 561 nm DPSS laser and the fluorescent emission image was collected between 571 nm and 650 nm using a PMT detector. Z-series of images were acquired depending on the height of each sample. The Z step size was set equal to the pixel size in X and Y at 3.03 μm. Image analysis was performed using Microscopy Image Analysis Software – Imaris (Oxford Instruments).

Results and Discussion

The pseudomonal biofilm matrix is composed of bacterial cells, extracellular polysaccharides, rhamnolipids, biofilm matrix-related proteins, nucleic acids, secondary metabolites, and water.[234]

These components can assemble into a matrix that protects the bacterial population within the biofilm. Some interactions between the biofilm components also play a significant role in maintaining the structural integrity of the biofilm matrix. For example, extracellular DNA (eDNA) can interact with proteins and exopolysaccharides via charge-charge interactions.[224] Hence, cationic compounds, like 600 Da BPEI and its PEGylated derivatives, can bind to the biofilm matrix and interfere with inter- and intramolecular interactions that stabilize the matrix, creating an environment that increases bacterial susceptibility to external agents, such as antimicrobial compounds. We have previously shown the ability of 600 Da BPEI to disrupt bacterial EPS of Gram-positive staphylococcal biofilms and Gram-negative *Pseudomonas aeruginosa* using the MBEC model.[113, 166, 228, 235]

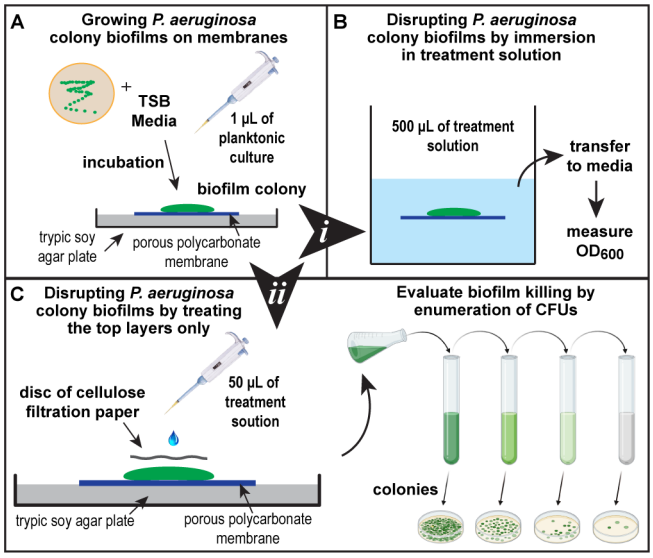

Figure 22. Illustration of the modified Colony Biofilm Model (A). (B) Treatment option (i) in a bulk solution of treatment agent, (C) Treatment option (ii) and evaluation method via CFU counting.

The colony biofilm model is a useful method to test antimicrobial solutions. Figure 23 shows an overview of the growth and treatment conditions employed in our study. Biofilms grown via the biofilm colony model for 24 h show visible biomass deposited on the surface on the polycarbonate

membrane. To confirm the presence of bacteria and EPS after 24-h incubation, scanning electron microscopy (SEM) was utilized to visualize the bacteria ((Figure 24A,B). The biofilm matrix of *P. aeruginosa* is composed of three major exopolysaccharides: alginate, *Psl* (polysaccharide synthesis locus) and *Pel* (short for pellicle). Alginate is a polymer of (1,4)-linked β-D-mannuronate and α-L-guluronate, *Psl* is repeating pentamer consisting of D-mannose, L-rhamnose, and D-glucose residues, and *Pel* is a N-acetyl glucosamine (GlcNAc)- and N-acetyl galactosamine (GalNAc)-rich polysaccharide.[17, 236] These exopolysaccharides are not only crucial in maintaining the biofilm matrix structure but also play a role in increasing antimicrobial resistance of *P. aeruginosa* cells within the biofilms.[237-238] These exopolysaccharides, along with other biofilm components (i.e proteins and eDNA), create a three-dimensional matrix.

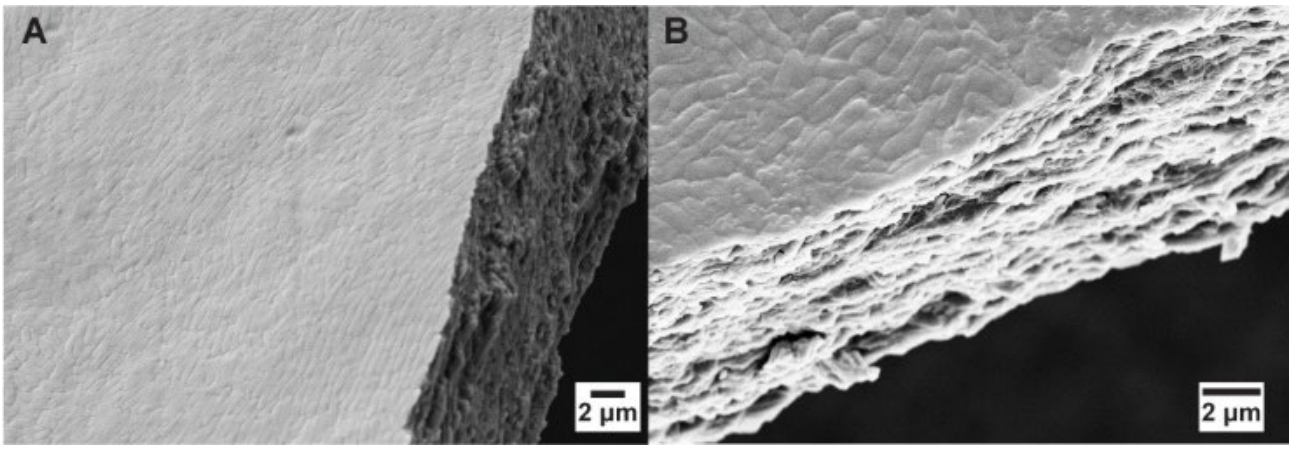

Figure 23. Scanning electron micrographs of ATCC BAA-47 (PAO1*) P. aeruginosa* grown via colony biofilm model. Thick layers of biofilms are visualized in perspective (A) and (B).

Treatment solutions were applied via immersion (method *i* in Figure 23) and cellulose filtration discs (method *ii* in Figure 23). Starting from a 5 x 10^2 CFU inoculation, 24 hours of growth increases the biomass to: 5 x 10^9 CFU/mL for ATCC BAA-47 (PAO1), 10 x 10^6 CFU/mL for ATCC 27853, and 2 x 10^7 CFU/mL for the MDR strain OU1. *P. aeruginosa* BAA-47 is a PAO1

strain isolated from a wound in 1954 [164, 239-240] and ATCC 27853 was isolated from a hospital blood specimen in 1971.[241] The MDR clinical isolate OU1 exhibits resistance against aztreonam, ceftazidime, ciprofloxacin, meropenem, and piperacillin/tazobactam.[166] We have previously identified the ability of 600 Da BPEI to re-sensitize β-lactams against multidrug-resistant (MDR) *P. aeruginosa* using checkerboard and MBEC assays.[166]

After growing the *P. aeruginosa* biofilms using the modified colony biofilm model (Figure 23A), we subjected the biofilms into biofilm killing assays. We first implemented a biofilm killing treatment model where the whole membrane is immersed into a treatment solution. A volume of 500 μL Tris buffer was prepared with varying concentrations of 600 Da BPEI. Then, the established biofilms were exposed to treatments overnight. Using this treatment model, complete bacterial eradication (CFU/mL = 0) was observed when 512 μg/mL 600 Da BPEI was applied to BAA-47 (PAO1) biofilms (~5 x 10^9 CFU/mL). This treatment delivery provides about 420 nmoles of 600 Da BPEI. However, with this treatment model, we observed a passive dispersal (i.e. erosion) of the biofilm when the membrane is immersed into a liquid solution. This could be caused by "environmentally induced dispersion" because of the shift from solid agar interface to liquid treatments.[242] Dispersion of the biofilm may turn sessile biofilm bacteria into planktonic cells, which are more susceptible to antimicrobials, including 600 Da BPEI and PEG350-BPEI.[117, 243-245] Although we observed efficacy using the immersion treatment model, it is also possible that the 600 Da BPEI molecules accessed the biofilm via the pores in the polycarbonate membrane. Hence, 600 Da BPEI could have bypassed the biofilm outer layers and attack the biofilm at a weaker location. Thus, a follow-up study was designed to treat the top layers of the biofilm only. A sterile cellulose filtration paper disc was applied to the biofilm surface and then treatments were applied to the paper disc (Figure 23C). This ensures the treatment solutions stay on top of the

biofilm, reduces evaporation, and resembles clinical wound treatments.[246] The application of the 600 Da BPEI and PEG350-BPEI kills *P. aeruginosa* cells within the biofilm. This activity is quantified by measuring the viable cell concentration in colony forming units (CFU/mL) after treatment with Tris buffer only, 600 Da BPEI, or PEG350-BPEI. The difference in CFU/mL between Tris and 600 Da BPEI (or PEG350-BPEI) treated samples are used to calculate log reduction values (LRVs). Dose dependent LRVs are shown in Figure 25.

To deliver effective quantities of 600 Da BPEI or PEG350-BPEI while also keeping the liquid on the biofilm surface, low volumes of high concentration solutions were used. The 40 μL volume of a 1024 μg/mL solution of 600 Da BPEI delivers 68 nmoles to the biofilm surface. This results in a LRV less than one (Figure 25A). However, 40 μL of a 1024 μg/mL solution of PEG350-BPEI delivers 43 nmoles and produces a LRV close to 1 for *P. aeruginosa* 27853 (Figure 25B). For *P. aeruginosa* BAA-47 (PAO1) and MDR-PA OU1, LRVs show that PEG350-BPEI is less effective than 600 Da BPEI. However, higher amounts of 600 Da BPEI or PEG350-BPEI produce larger LRVs for all strains (Figure 25). Both 600 Da BPEI and PEG350-BPEI were effective at killing *P. aeruginosa* biofilms, including biofilms of MDR-PA OU1. It appears that PEGylation may reduce the eradication activity of 600 Da BPEI, but this effect is strain dependent. For *P. aeruginosa* ATCC 27853, the LRVs for PEG350-BPEI are higher than 600 Da BPEI even though less of the compound was used (~2/3rd the 600 Da BPEI amount). In a comparative genomic study between *P. aeruginosa* ATCC 27853 and PAO1, results suggest that ATCC 27853 expresses *Psl* genes at a much higher rate compared to PAO1 in the development of colony biofilms.[241] The *Psl* locus contains the *PslA-O* gene that encodes for the mannose and galactose components of the matrix. In the same comparative study, it was reported that both PAO1 and ATCC 27853 expressed low *pel* and alginate biosynthesis genes.[241] High levels of the polysaccharides mannose and

galactose in ATCC 27853 biofilms, and low levels of the anionic *pel* and alginate components, may leave the bacterial cells more susceptible to the action of 600 Da BPEI and PEG350-BPEI compared to the BAA-47 (PAO1) and MDR strains. High amounts ion anionic EPS components would attract and bind greater fractions of the 600 Da BPEI or PEG350-BPEI dose. This action would leave a smaller fraction of BPEI remaining to kill the bacteria via attack on its outer membrane. Finally, the data in Figure 25 demonstrate that PEG350-BPEI can be used to kill *P. aeruginosa* biofilms. These data do not demonstrate the amount required for *in vivo* studies, where it is not our intention to eradicate *P. aeruginosa* biofilms with a single high concentration dose. Instead, we envision that low-concentration doses of PEG350-BPEI will be applied to wounds as a topical agent administered as a monotherapy or in combination with IV/oral antibiotics. Topical use lowers toxicity concerns whereas the risk is greater if PEG-BPEI were intended for internal use. PEG-BPEI may be a useful therapeutic against wound infections by simultaneously providing anti-inflammation and infection prevention, in addition to anti-biofilm properties that assist with localized wound decolonization. This will reduce inflammation and tissue damage and accordingly will shorten the inflammatory phase of wound healing, lowering the chance that wound infections lead to bacteremia, sepsis, and death. PEG-BPEI will complement other wound treatment interventions, such as treatment with antibiotics and wound debridement.

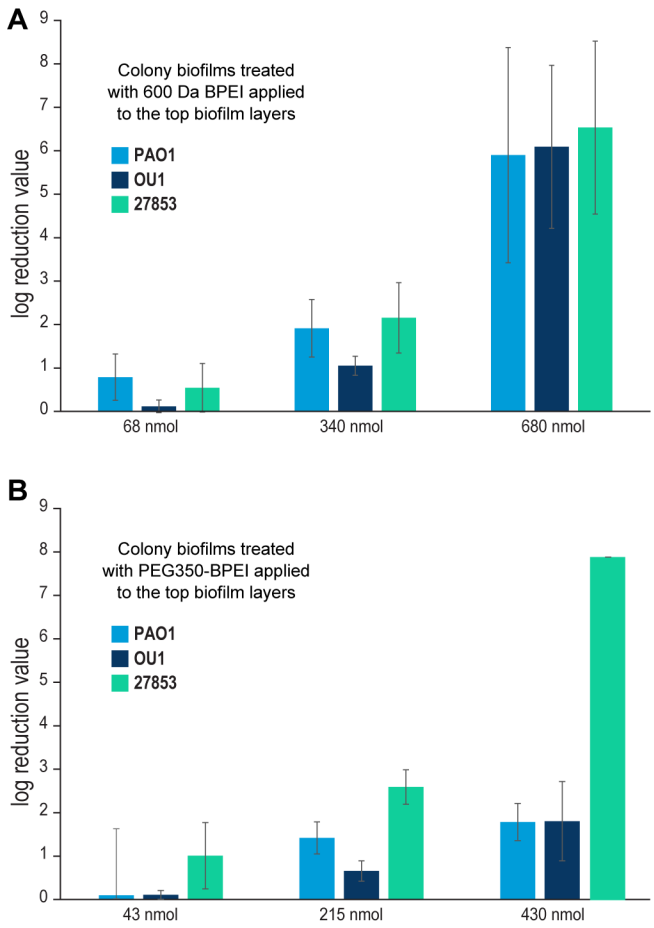

Figure 24. Log reduction values (LRV) of 600 Da BPEI (A) and PEG350-BPEI (B). Error bars denote standard deviation (n = 5).

After identifying the ability of 600 Da BPEI and PEG350-BPEI to reduce bacterial biofilm bioburden, we sought to clarify the mode through which these compounds attack biofilms. In our previous study on Methicillin-Resistant *Staphylococcus epidermidis* (MRSE) and Methicillin-resistant *Staphylococcus aureus* (MRSA) biofilms, we implemented a biofilm disruption assay via crystal violet staining.[226, 235] Here, we also applied a similar biofilm disruption assay. Growing *P. aeruginosa* biofilms on microtiter plates presents a technical challenge because growth in TSB media results in poor biofilm adhesion. The biofilms were observed slide off the microtiter plates during washing. However, for *P. aeruginosa*, it is known that an inverse relationship exists between biofilm formation (attachment) and swarming motility (movement)[247-248], and by

modulating the amino acid concentrations in the growth media, biofilm formation and attachment can be enhanced. Hence, we inoculated a minimal salts media supplemented with 0.4% arginine as described by Bernier et al.[247] With this new procedure, biofilm formation is more uniform and robust for ATCC BAA-47 (PAO1) and ATCC 27853 in microtiter plates. This media, however, did not produce quantifiable biofilm biomass for the MDR clinical isolate OU1 (data not shown). Biofilms of laboratory reference strain ATCC BAA-47 (PAO1) *P. aeruginosa* were stained with crystal violet and treated with increasing concentrations of 600 Da BPEI and PEG350-BPEI (2-64 μg/mL). The positive control was 30% acetic acid, and the negative control was Tris buffer. The stained biomass samples were incubated with the treatment solutions for 3 h and then dissolved stained biomass was carefully transferred into new 96-well plates for OD_{550} measurement. The amount of dissolved biomass was directly correlated to the intensity of OD_{550} values. Measured values were compared to the negative control using Student's t-test. Statistical analysis shows that both 600 Da BPEI and PEG350-BPEI dissolved the biomass in 3 h ($n = 12$, p-value < 0.01), and minimal biomass remained in the original biofilm plate (Figure 26A). Increasing the concentration of 600 Da BPEI increases the amount of biofilm biomass dissolved (Figure 26B). A similar trend is observed with PEG350-BPEI (Figure 26C).

Crystal violet assay data for the anti-biofilm action of 600 Da BPEI and PEG350-BPEI against *P. aeruginosa* BAA-47 (PAO1) and 27853 are shown in Figure 27. These results show that the amount of crystal violet dissolved and quantified for the two treatments are indistinguishable ($n = 10$, p-value > 0.01) for these two bacterial strains. Hence, it seems that the apparent ability of 600 Da BPEI to dissolve biomass is unaffected by PEGylation and thus the differences observed in the LRVs (Figure 25) may be due to differences in bacterial susceptibility to 600 Da BPEI and PEG350-BPEI. Growth inhibition assays of these two compounds, using MDR-PA OU1 and

ATCC 27853 strains, show that the minimum inhibitory concentration (MIC) of 600 Da BPEI is 67 µM for both strains. However, the MIC values of PEG350-BPEI are 268 µM and 67 µM against these two strains, respectively.[228] This indicates higher bacterial susceptibility of ATCC 27853 to PEG350-BPEI compared to MDR OU1.

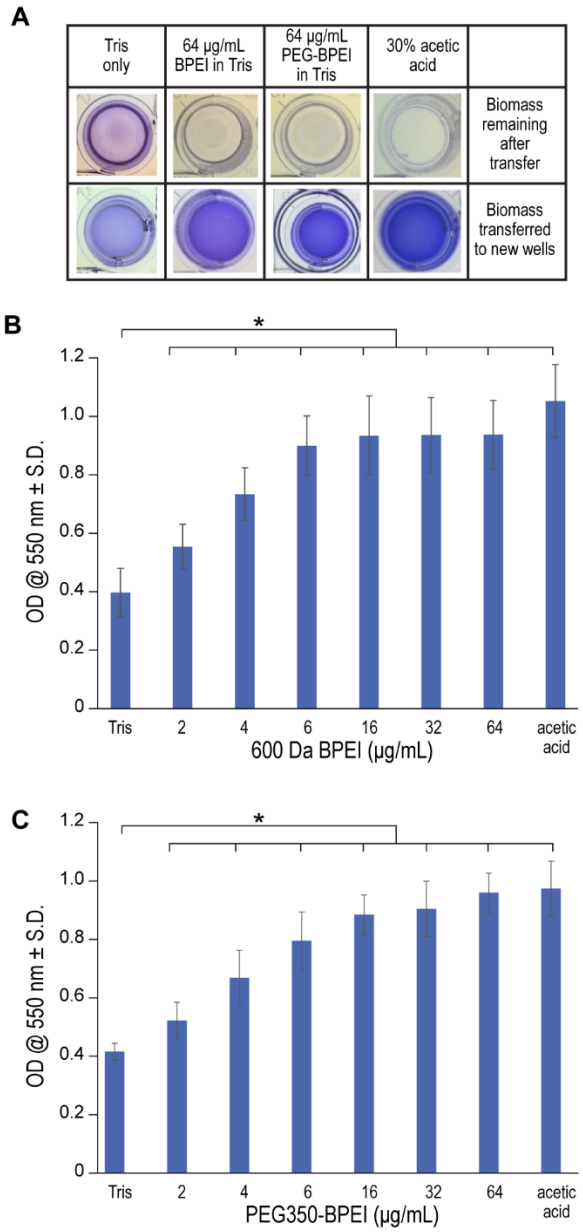

Figure 25. Crystal violet staining assay (A). Biofilms of *P. aeruginosa* ATCC BAA-47 (PAO1) stained with crystal violet were treated with increasing concentrations of 600 Da BPEI (B) and PEG350-BPEI (C) for 3 h, in addition to negative and positive controls. Error bars denote standard deviation (n = 12). OD_{550} nm readings show significant difference between buffer-treated (Tris) control and treatments indicated with an asterisk (*t* test, *p*-value < 0.01).

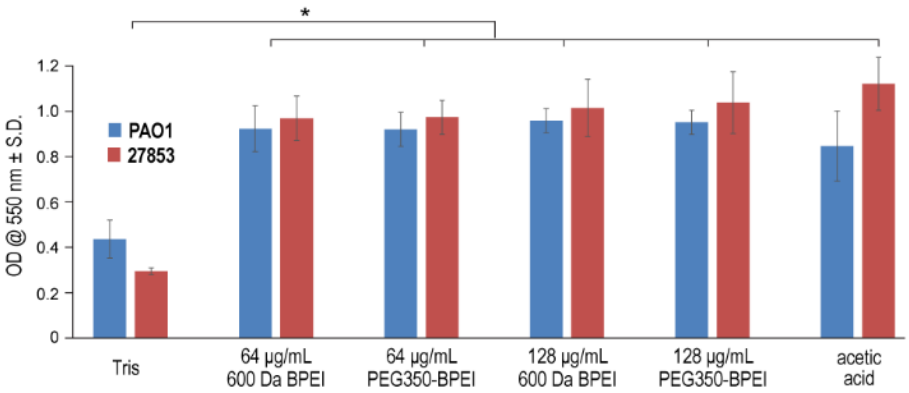

Figure 26. Biofilm disruption assay via crystal violet staining for *P. aeruginosa* BAA-47 (PAO1) and 27853 treated with 600 Da BPEI and PEG350-BPEI. OD_{550} nm values indicate that PEGylated BPEI can disrupt *P. aeruginosa* with an activity similar to that of 600 Da BPEI (*t* test, *p*-value > 0.01, denoted by not significant, n.s.). OD_{550} nm readings show significant difference between buffer-treated (Tris) control and treatments indicated with an asterisk (*t* test, *p*-value < 0.01).

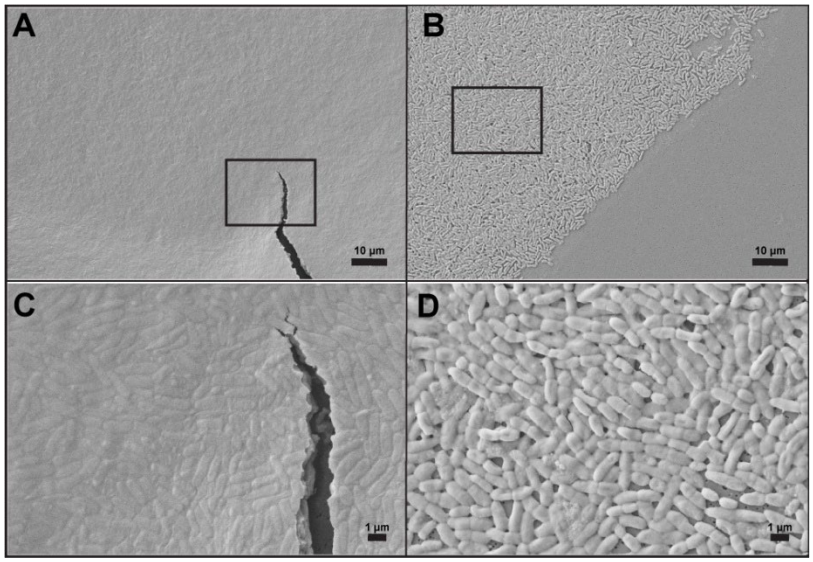

Figure 27. Scanning electron micrographs of ATCC BAA-47 (PAO1) *P. aeruginosa* biofilms after treatment via colony biofilm model. Buffer-treated (Tris) biofilms (panels A,C) are observed to have a film-like layer whereas the 600 Da BPEI-treated biofilms lack this film-like layer coating the cells.

To further understand the action of 600 Da BPEI against *P. aeruginosa* biofilms, SEM images were taken to discern any topographical changes within the biofilm environment. Biofilms were grown on polycarbonate membranes and treated with 130 nmoles of 600 Da BPEI, or Tris buffer

only, using the modified colony biofilm model (Figure 23C). In this method, sterile cellulose filtration paper discs are used to keep the BPEI (or Tris) solution on the biofilm surface. The cellulose paper was carefully removed prior to SEM imaging. A comparison between a buffer-treated control and BPEI-treated biofilm shows that buffer-treated biofilms have a layer of *P. aeruginosa* cells covered in a layer of EPS (Figures 26A and 26C). The noticeable fracture in the biofilm is likely the result of sample drying under the vacuum conditions required for SEM imaging. The SEM images of BPEI-treated biofilms (Figure 26B and 26D) show a considerable reduction of EPS coating surrounding the bacterial cells. It appears that 600 Da BPEI causes dissolution of the EPS. This observation is consistent with the results in the biofilm disruption (crystal violet) assay (Figures 24 and 25). This observation may also be caused by delamination of the biofilm architecture when the cellulose filter paper is removed. Buffer-treated biofilms were handled in a similar manner. Thus, changes in the biofilm EPS are caused by 600 Da BPEI. It is likely that 600 Da BPEI treatment creates several effects, such as disruption and dissolution of the biofilm EPS, a weakening of the biofilm architecture, and delamination of the biofilm when the cellulose paper is removed. Regardless, the net effect is a reduction in bacterial bioburden on the polycarbonate membrane and it is conceivable that a similar action would occur in the treatment of wound infections when wound coverings are removed and changed during treatment. Reducing the EPS layer in the biofilms may leave the cells more susceptible to antimicrobial agents. Here, EPS reduction allows 600 BPEI greater access to the underlying cells. We previously discussed the mechanism of action of BPEI against *P. aeruginosa* planktonic cells.[166] Those data were interpreted as 600 Da BPEI reducing the diffusion barriers caused by LPS biomolecules in the outer membrane, and, at higher concentrations, 600 Da BPEI causing disruption of the outer

membrane itself.[166] Hence, the dual-effect of dissolving EPS barriers and antimicrobial action at high concentration is a possible explanation for the dose dependent LRVs shown in Figure 23.

To dissolve the biofilm matrix, 600 Da BPEI needs to interact with biofilm components, which can destabilize the EPS matrix. One important biofilm component is extracellular DNA (eDNA). Biofilm nucleic acids are important in biofilm formation, cell-to-cell adhesion, cell signaling and maintaining the structural integrity of the biofilm matrix.[224] This importance of eDNA allows it to be a possible drug target candidate for anti-biofilm treatments. Furthermore, polyethylenimines (PEIs) are widely used transfection agents, hence their interaction with DNA is well-recognized.[249-250] To confirm this interaction, isothermal titration calorimetry (ITC) data were collected. The thermodynamic profile for titration of 600 Da BPEI into DNA solutions is shown in Figure 29. The binding isotherm illustrates a biphasic response to the increasing concentration of 600 Da BPEI. This response may indicate two binding sites for 600 Da BPEI in the DNA molecules. In a thermodynamic analysis between 600 Da BPEI and DNA, these two types of binding modes were described as: (a) binding of the PEI to the DNA groove and (b) external binding of PEI to the phosphate backbone of DNA.[250] These possible interactions of the PEI molecules with the eDNA in the matrix can further disorganize its structural integrity rendering the bacterial cells within the biofilm more susceptible to treatments. In addition, the PEI-DNA interaction may dislocate some of the pre-existing eDNA interactions (i.e., with proteins, exopolysaccharides, metabolites) and inhibit some of its signaling and modulating functions. For example, as the phenazine pyocyanin (PYO) interacts with eDNA, enhanced electron shuttling within the biofilm is observed, as well as increased sputum viscosity.[20, 95] Inhibiting these interactions may leave the biofilm structure less fit and more vulnerable.

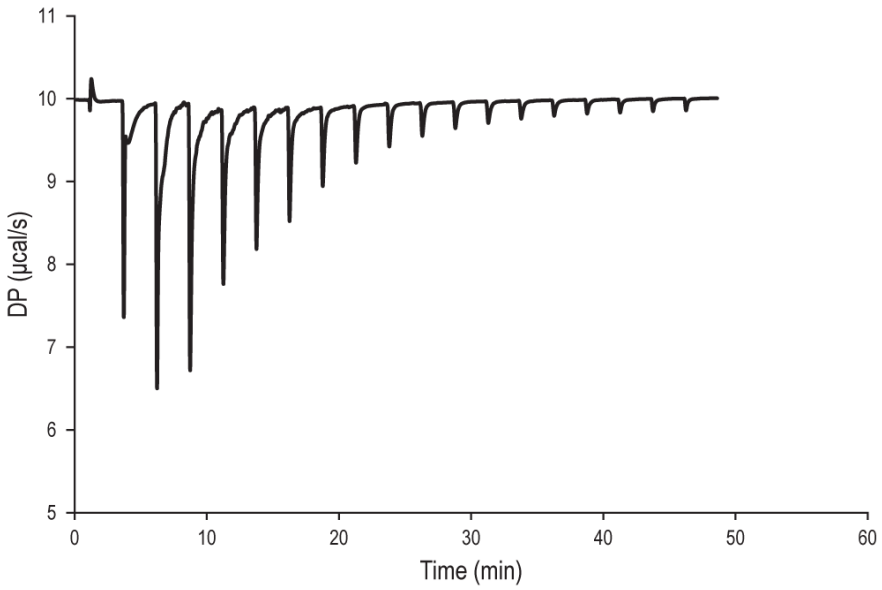

Figure 28. Isothermal titration calorimetry binding isotherm shows that 600 Da BPEI interacts with DNA.

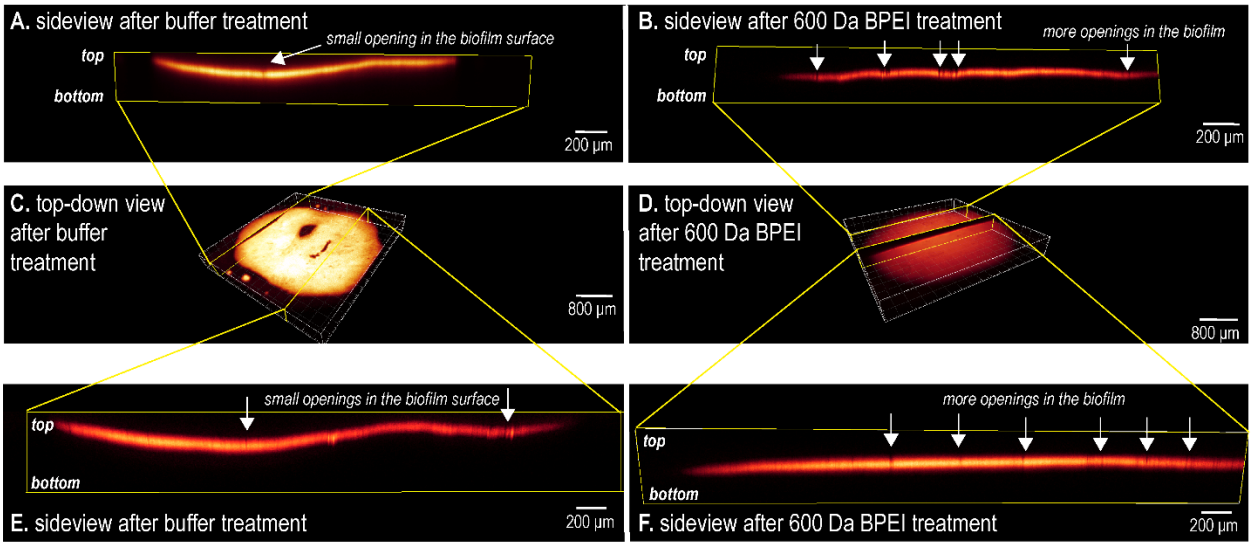

Figure 29. Confocal Laser Scanning Microscopy Imaging of *P. aeruginosa* biofilms. Colony biofilms were grown for 24 h and then 4 µL of Tris buffer (A, C, E) or 42.5 nmoles of 600 Da BPEI (B, D, E) were carefully added to the biofilm surface and incubated for 3 h.

After considering the interactions of 600 Da BPEI with the biofilm and the ability to dissolve EPS, it was desirable to examine biofilm disruption using microscopy without the need for vacuum drying. Thus, the anti-biofilm mode-of-action was studied with fluorescence microscopy. A key factor to success is using a sufficient amount of 600 Da BPEI to attack the biofilm without

dissolving it. The ability to weaken EPS allows external agents to permeate the biofilm. Biofilms of the MDR strain OU1 were incubated with 42.5 nmoles 600 Da BPEI and buffer control. From the data in Figure 25A, these treatments should have a minimal biofilm killing effect. Without the addition of rhodamine B dye, it is possible to collect fluorescence images using the autofluorescence of *P. aeruginosa* from the fluorescent pigment, pyoverdine (405 nm excitation, 460 nm emission). This was used to confirm the biofilm size and topography. Next, rhodamine B dye was added as a probe molecule to visualize the ability of an external agent to penetrate the biofilm. A similar study was conducted by Rozenbaum et al., where they utilized fluorescent Rhodamine B dye to study penetration and accumulation of dendrons in *P. aeruginosa* biofilms.[251] In our study, we were motivated to examine disruption of the biofilm's outer layer(s). Thus, fluorescent images were collected immediately after dye addition and before the rhodamine B dye was able to completely penetrate through the biofilm, allowing for observation of the outer layers [251-252]. Focusing on the top layer permits visualization of any fractures/openings created on the biofilm surface due to treatments. After 3D rendering and sectioning, we identified the biofilm biomass and the distribution of the rhodamine B dye molecules. Selective excitation of rhodamine B permits visualization of biofilm fractures (Figure 30). The appearance of gaps in the 600 Da BPEI-treated samples suggests increased rhodamine B penetration into the biofilm (Figure 30B and 30F) compared to the buffer-treated biofilm (Figure 30A and 30E). Channels within the biofilm structure were recently observed using a high-resolution high-field-of-view optical system.[253] These channels provide networks for nutrients and waste to be transported and distributed within the biofilm system. In the same study, it was observed that such structures can reform even after a total mechanical disaggregation. Considering the fractures observed in this

work, 600 Da BPEI may be establishing more of these channels within biofilm. Studies to examine this effect are in the planning stages.

Conclusion

The anionic EPS matrix[192, 254-255] binds anti-biofilm agents, such as Ag^+ ions, cationic polyhexamethylene biguanide (PHMB), and cationic antibiotics, such as tobramycin.[256] These agents kill bacteria but do not disrupt the biofilm itself. In contrast, when EPS binds PEG-BPEI, the biofilm disperses.[245] Toxicity concerns of 600 Da BPEI can be mitigated by covalent linkage with low molecular weight PEG and, in this study, PEG350-BPEI was found exhibit superior antibiofilm activity against *P. aeruginosa*. The antibiofilm activity of both 600 Da BPEI and its PEG derivative was characterized with fluorescence studies and microscopy imaging.

PEG-BPEI can be formulated as a gel, cream, or foam for use as a stand-alone or adjunctive therapy that complements other wound treatment interventions. Billions of healthcare dollars are spent on therapeutic devices to alleviate diabetic wounds and pressure ulcers that cause physical pain, disabilities, and poor quality of life.[210, 257-258] Delayed healing is caused by bacterial pathogens and their biomolecules that form biofilms in the wound microenvironment. During the inflammation phase of wound healing, immune cells accumulate in response to biofilms and leads to dysregulation of the immune response and excessive inflammation that impairs wound healing, leading to recurrent infection and tissue necrosis.[259-260] Excessive inflammatory tissue microenvironments inhibit the migration of keratinocytes, fibroblasts, and the synthesis of new extracellular matrix in the granulation tissue.[260] Modulating the innate immune response with PEG-BPEI expands the possible utility of PEG-BPEI that counteract antibiotic resistance mechanisms.[245] This versatility of PEG-BPEI suggests that it may be a useful therapeutic agent by simultaneously

providing anti-inflammation and infection prevention with a new innovative product and decolonizing agent. This will speed wound healing while also slowing the emergence and spread of antibiotic resistance genes and antibiotic-resistant pathogens.

Chapter 5: Dual-Function Potentiation by PEG-BPEI Restores Activity of Carbapenems and Penicillins Against Carbapenem-Resistant *Enterobacteriaceae*

Background and Significance

The World Health Organization has developed the global priority pathogens list of antibiotic-resistant bacteria.[261] Included in the list of "Priority 1: Critical" pathogens are carbapenem-resistant *Enterobacteriaceae* (CRE). In this class are the dangerous *Escherichia coli* ATCC BAA-2452 and *Klebsiella pneumoniae* ATCC BAA-2146, which are resistant to nearly all available antibiotics. The lack of effective and timely treatments leads to severe illness and, in some cases, death. There is a high mortality rate and survivors can have severe morbidity from treatment with toxic last-resort antibiotics.[262-264] The danger from CRE arises because these bacteria produce enzymes that degrade a wide range of antibiotics, including carbapenems and β-lactams.[265] The predominate carbapenemases are the *Klebsiella pneumoniae* carbapenemases (KPCs).[266-268] Of greater concern are metallo-β-lactamases (MBLs) because they degrade more antibiotics than KPCs.[266-268]

In recent years, a variety of new compounds have emerged to combat CRE infections. CRE possess extended-spectrum β-lactamase enzymes, and recommended agents against CRE are combinations of an antibiotic and a β-lactamase inhibitor (such as ceftazidime-avibactam, meropenem-vaborbactam, imipenem-relebactam, or ceftaroline-avibactam), or a monotherapy of cefiderocol, tigecycline, eravacycline, plazomycin, or gentamycin.[269-270] Colistin and related polymyxins are recommended as last-resort antibiotics due to toxicity that can cause patient morbidity.[270-271] The presence of KPCs create complicated treatment decisions, as the agents listed above may have reduced or eliminated antibiotic efficacy.[270] There are even fewer effective agents

against the more dangerous CRE that express metallo-β-lactamases (MBL), such as the New-Delhi MBL (NDM-1).[270]

Although CRE are more commonly associated with urinary tract infections,[272-273] their presence in wound and skin and soft-tissue infections (SSTIs) cannot be overlooked. A 2018 study reported that 24% (2,521) of 10,698 non-susceptible isolates were from skin/wound infections,[274] and treatment options are similar to those listed above.[275] A 2017 analysis of the CRACKLE-1 surveillance data revealed the importance of wounds in CRE transmission.[221] The 4.5 million chronic wound infections[257, 276-277] increase the risk of CRE infection and transferring resistance genes to other species.[221, 266-268, 278-279] Treating chronic wounds requires repeated visits to, and stays in, healthcare facilities[276, 280] which increases the likelihood of spreading CRE.[219-221] Thus, more effective treatment of wound infections will reduce the danger from CRE. Cefiderocol is an alternative treatment option for CRE infections, regardless of the carbapenem resistance mechanism.[270, 281-282] But this agent, along with the other mono- and combination agents listed above, are unable to disable biofilms that perpetuate wound infections.

Purpose of Experiment

In this work, we demonstrate that 600 Da branched polyethylenimine (BPEI) and its less toxic PEGylated derivative (PEG-BPEI) restore meropenem (MER) and imipenem (IMI) susceptibility in a *K. pneumoniae* strain[283] harboring New-Delhi MBL (NDM-1) and an *E. coli* strain[284] with NDM-1. These effects do not require β-lactamase inhibitors (BLIs) and likely occur by sequestering Zn^{2+} ions essential for NDM-1. The importance of using low molecular weight BPEI potentiators against CRE *E. coli* and *K. pneumoniae* is magnified by the ability of 600 Da BPEI to disrupt biofilms and resistance in *P. aeruginosa* and staphylococci.[113-114, 116-117, 165, 177, 244, 285] We previously identified potentiation mechanisms across different antibiotic classes by

lowering LPS barriers, inhibiting cell wall synthesis, and disrupting biofilms.[114, 117, 285] The antibiofilm properties of 600 Da BPEI is associated with biofilm formation inhibition and an EPS-disruption mechanism.[117, 244] This current work expands not only the potential utility of these potentiators against infectious pathogens, but also our understanding of the multi-function nature of these compounds.

Principle of Techniques

As discussed previously, in *in vitro* stages of drug testing, the relationship between compounds and antibiotics can be identified via checkerboard assays. Similar to the methods described in Chapter 3, the interactions between 600 Da BPEI (or PEG350-BPEI) and antibiotics were characterized via calculations of MICs and FICIs. In some of the checkerboard assays described in this chapter, BLIs were added across the whole plate to assess the result of the difference in drug uptake between the *E. coli* and *K. pneumoniae* strains.

We hypothesized at least two possible mechanisms of action that 600 Da BPEI and PEG350-BPEI employ to potentiate carbapenems: (a) Zn^{2+} chelation from MBLs and (b) increasing drug uptake via creating slight membrane disturbances. Zn^{2+} and 600 Da BPEI (or PEG350-BPEI) interactions were measured using ITC. The principle of this technique is discussed more in depth in Chapter 3. Briefly, ITC directly measures heat released or absorbed during a molecular binding event. Thermogram profiles between 600 Da BPEI and PEG350-BPEI vs Zn^{2+} were compared. It is hypothesized that the available amines that can coordinate with Zn^{2+} for PEG350-BPEI will be less than that of 600 Da BPEI. Drug uptake was also measured via fluorescence accumulation assay, which is a method used to measure drug influx. This accumulation assay is also discussed in depth in Chapter 3.

Methods

Materials

In this study, carbapenem resistant *Enterobacteriaceae* expressing the metallo-β-lactamase NDM-1, *E. coli* BAA-2452™ and *K. pneumoniae* BAA-2146™ were purchased from the American Type Culture Collection. Chemicals were purchased from Sigma-Aldrich, Inc. and antibiotics obtained from GoldBio, Inc. Antibiotic purities are as follows: Imipenem 98.7%, Meropenem 98%, and Tazobactam Sodium 92.3%. For Piperacillin Sodium, the product lot fell within the specifications issued by the company. 600 Da BPEI was purchased from Polysciences, Inc. The synthesis and characterization of PEG350-BPEI has been described elsewhere.[286] Monofunctionalized PEG-epoxide was obtained from Nanocs, Inc. Briefly, approximately 600 Da BPEI was dried overnight with lyophilization and the final mass used to determine amount of mPEG-epoxide (350 MW) required to react with 600 Da BPEI in a 1-to-1 stoichiometric ratio. Both 600 Da BPEI and mPEG-epoxide are dispersed in anhydrous ethanol at 60 °C for 24 hours. The success of the epoxide ring-opening reactions was determined via ^{1}H NMR spectroscopy. Experiments to determine the acute toxicity of 600 Da BPEI and PEG350-BPEI were performed by a contract research organization (TransPharm Preclinical Solutions, Jackson, MI) and the data reported elsewhere.[286]

Checkerboard Assays

Checkerboard assays followed the methods of Lam *et al.*[20] to determine the synergistic effect between PEG350-BPEI or 600 Da BPEI and antibiotics against drug resistant strains growing in cation-adjusted Mueller-Hinton broth (CAMHB). CAMHB media augmented with various amounts of serially diluted potentiator and antibiotics (imipenem, piperacillin, and meropenem) was inoculated with bacterial cells from an overnight culture (5×10^5 CFU/mL). Cells were grown at 37 °C. The change in OD_{600} (optical density at 600nm) was measured and recorded after 24 hr of treatment. Each checkerboard trial was done in triplicate using sterile Greiner CellStar™ flat bottom polystyrene plates, catalog #655180.

Isothermal Titration Calorimetry (ITC)

Isothermal titration calorimetry (MicroCal PEAQ-ITC, Malvern Inc., Malvern, U.K.) was utilized to quantify the heat release upon mixing 600 Da BPEI with $ZnCl_2$ and PEG350-BPEI with $ZnCl_2$. Briefly, solutions of 600 Da BPEI or PEG350-BPEI (0.105 mM) and 1.8 mM $ZnCl_2$ were prepared in 50 mM Tris-HCl (pH 7) were titrated using injections of 2 µL lasting 4 s and separated by 150 s time intervals. Controls were performed and the experiment was done in duplicate.

H33342 Bisbenzimide Dye Uptake Assay

Overnight cultures of *E. coli* BAA-2452™ and *K. pneumoniae* BAA-2146™ were used to inoculate fresh CAMHB media for another 5 hr at 35 °C with shaking. Bacterial cells were collected by centrifugation at 6000 rpm for 40 min and resuspended in PBS. The OD_{600} of the cell suspension was adjusted to ~ 1.0 and kept at room temperature during the experiment. Aliquots (180 µL/well) of the cell suspension were transferred to a 96-well flat-bottom black plate in the format of column 1, PBS blank; column 2, untreated control cells; column 3, cells + potentiator

(sub-lethal concentration). Five technical replicates of each group were conducted. Fluorescent probes[40-42] Hoechst 33342 bisbenzimide (H33342) was added (20 μL) to each well with a final concentration of 5 μM. Fluorescence was read immediately after the addition of H33342 by a Tecan Infinite M20 plate reader with the excitation and emission filters of 355 and 460 nm for H33342. Fluorescence data were normalized to the emission before cells were added in the PBS control, and they were plotted against time to show the cellular uptake of H33342 over 10 min. Control experiments of dye + 600-Da BPEI were unchanged from fluorescence emission values obtained with dye only.

Results and Discussion

In our previous study, we observed a reduction of *in vivo* toxicity of 600 Da BPEI by modifying it with a single 350 MW chain of polyethylene glycol (PEG350) using a straightforward one-step reaction.[286] We also noted that the resulting compound, PEG350-BPEI, like its derivative, can disable β-lactam resistance in MRSA, MRSE, and MDR-PA.

Checkerboard assays reveal that 600 Da BPEI and PEG350-BPEI resensitize CRE strains to carbapenem antibiotics

Here, we also observe that both PEG350-BPEI, and its precursor, 600 Da BPEI, are able to render CRE strains expressing NDM-1, *K. pneumoniae* ATCC BAA-2146[283] and *E. coli* ATCC BAA-2452,[284] susceptible to the carbapenem antibiotics meropenem (MER) and imipenem (IMI). Without these potentiators, the NDM-1 strains are resistant to MER and IMI because their minimum inhibitory concentrations (MIC) are over the susceptibility breakpoints of 8 and 2 μg/mL,[287] respectively (Figure 31). Breakpoints are defined concentrations of antimicrobials set by The European Committee on Antimicrobial Susceptibility Testing (EUCAST) to characterize

susceptibility and resistance[287]. In this work, we found that 16 μg/mL (or greater) of either potentiator reduces the MIC to values below the resistance breakpoints. Restoring carbapenem susceptibility does not require the use of a β-lactamase inhibitor, such as vaborbactam or relebactam. Consequently, restoration can be attributed to the addition of polyethylenimine potentiators. Additionally, using polyethylene glycol (PEG) to lower toxicity does not prevent the ability to potentiate meropenem and imipenem against CRE *E. coli* and *K. pneumoniae*. The fractional inhibitory concentration index (FICI) is also calculated using the MIC of the antibiotics and potentiators. An FICI lower than 0.5 indicates synergy between the treatments, while an FICI between 0.5 and 1 represents additivity[288]. Based on these criteria, both potentiators have a synergistic relationship with MER and IMI. For example, using 16 μg/mL of 600 Da BPEI and 1 μg/mL of MER results to an FICI of 0.08 for *K. pneumoniae* ATCC BAA-2146, indicating synergy.

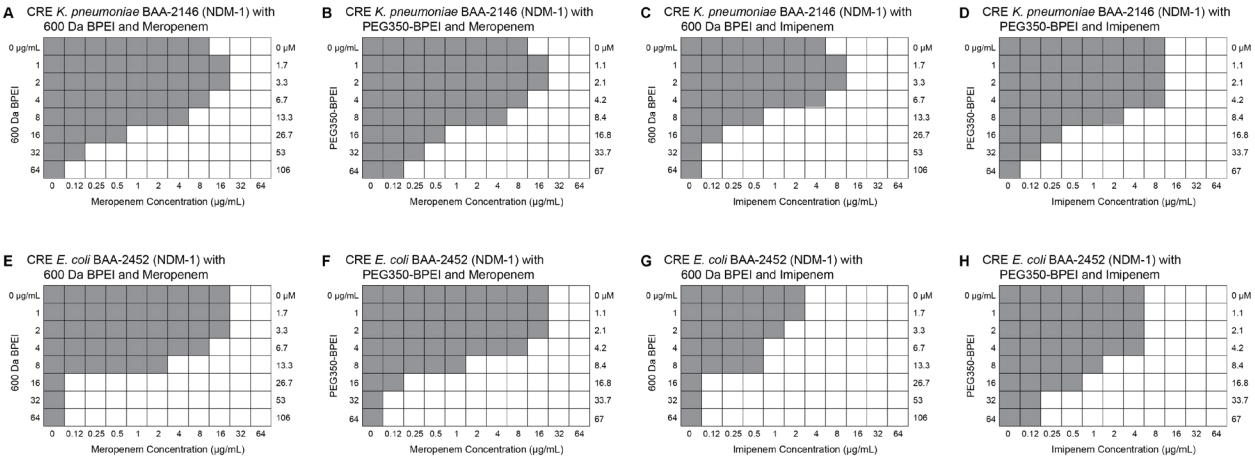

Figure 30. Checkerboard assay data for killing carbapenem-resistant Enterobacteriaceae (CRE) with meropenem (MER) and imipenem. Each panel shows a different combination of antibiotic + Potentiator with *E. coli* and *K. pneumoniae.*

Mechanism of action: 600 Da BPEi and PEG350-BPEI sequester Zinc ions

The NDM-1 enzyme requires Zn^{2+} ions for activity.[289-293] Overcoming carbapenem resistance by disabling MBLs with Zn^{2+} chelators is well-known.[289-290, 294-296] Other strategies overcome resistance by targeting MBLs with inhibitors.[292, 297-299] Compounds that bind to the LPS layer to facilitate the influx of antibacterial agents are often designed from peptide or peptidomimetic scaffolds,[182, 269-270, 300] although resistance has developed.[300] These well-founded and important developments highlight the utility of single-function compounds that inhibit carbapenemases, inhibit efflux pumps, increase the uptake of these inhibitors and various antibiotics, or chelate and sequester Zn^{2+} ions essential for MBLs. The amines of PEG-BPEI and 600 Da BPEI can chelate metals. We have reported that 600 Da BPEI binds Cu^{2+} but does not bind Ca^{2+} or Mg^{2+}.[116] The LPS layer of Gram-negative bacteria is stabilized by divalent metal ions like Ca^{2+} or Mg^{2+} [301], yet no interaction is observed between 600 Da BPEI and these two ions. Binding between Zn^{2+} and 600 Da BPEI is known[302] and we demonstrate this phenomenon using isothermal titration calorimetry (ITC). Metal chelation is an exothermic process and the release of heat for Zn^{2+} binding with PEG-BPEI and 600 Da BPEI is nearly identical (Figure 32). The difference in molar ratio (Zn:BPEI vs. Zn:PEG350-BPEI) may be attributed to the PEG group attached to the 600 Da BPEI, which hinders Zn^{2+} ions from some binding sites. Regardless, the ITC data shows that both PEG350-BPEI and 600 Da BPEI can chelate Zn^{2+} ions, which explains why they have similar MER and IMI potentiation effects against CRE expressing NDM-1.

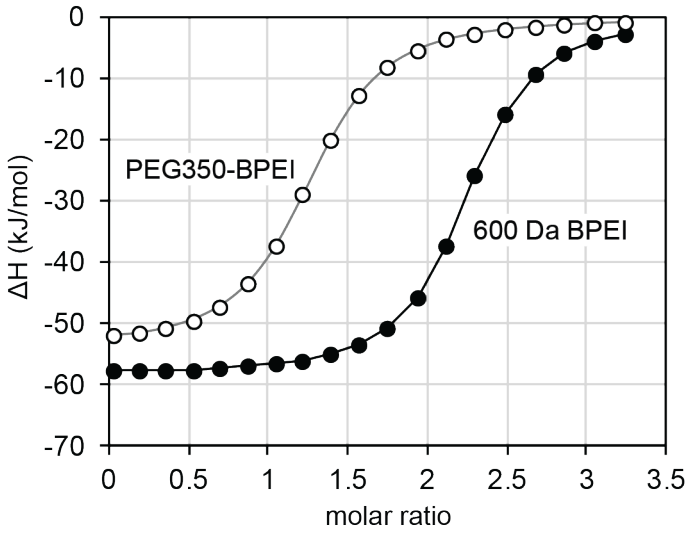

Figure 31. Isothermal titration calorimetry data demonstrate that 600 Da BPEI (closed circles) and PEG350- BPEI (open circles) bind Zn2+ ions.

Mechanism of action: 600 Da BPEI and PEG350-BPEI can increase drug influx

In addition to the chelation of essential Zn^{2+} ions, 600 Da BPEI and PEG-BPEI have other properties, such as disrupting biofilms[116-117, 244, 286] and increasing antibiotic influx without the need to disrupt the membrane.[116, 285] With regards to the latter effect, we investigated the ability of 600 Da BPEI and PEG-BPEI to increase drug uptake in *K. pneumoniae* ATCC BAA-2146 and *E. coli* ATCC BAA-2452. The fluorescent probe H33342 is a dye used to measure intracellular accumulation. Its fluorescence intensity increases when bound to cell membranes and bacterial DNA, which can be correlated to antibiotic uptake. As shown in Figure 33, the fluorescence of H33342 increases in the presence of 600 Da BPEI, PEG-BPEI, and polymyxin-B (PMB). The cells for this assay were harvested and studied at similar concentrations (OD_{600} values adjusted to 1.0) and the effect of enhanced influx is greatest with the NDM-1 *E. coli* strain BAA-2452. Pronounced differences are observed in the H33342 assay data for *K. pneumoniae* BAA-2146 and *E. coli*

NDM-1 strain (Figure 33). First, the corresponding fluorescence intensities are lower for *K. pneumoniae* than the *E. coli* strain, including the untreated cells. Secondly, 600 Da BPEI and PEG-BPEI have a smaller effect on H33342 influx of *K. pneumoniae* BAA-2146 and these effects are smaller than that of PMB. Here, the concentrations of 600 Da BPEI and PEG-BPEI are higher than PMB, and much higher than the amount required for potentiation (Figure 33). However, the cell density in the H33342 assay (7×10^8 CFU/mL) is also over 1000 times higher than that of the checkerboard assays (5×10^5 CFU/mL). Much higher concentrations were used for the fluorescent studies to achieve a detectable signal. Another important point to note here is that as we observed with H33342 influx against *P. aeruginosa*,[116, 285] it is possible that, at high concentrations, membrane disruption may be occurring—rather than merely reducing diffusion barriers. However, as previously stated, the cell density used in the fluorescent studies is very large, which makes the potentiator concentration sublethal. Considering the difference in drug uptake between *K. pneumoniae* BAA-2146 and *E. coli* NDM-1 strain, it would not be surprising if potentiation were better for *E. coli* NDM-1. However, we do not observe this trend in Figure 31. Thus, at a low concentration (16 μg/mL) that enables meropenem and imipenem potentiation, potentiation likely occurs by Zn^{2+} chelation.

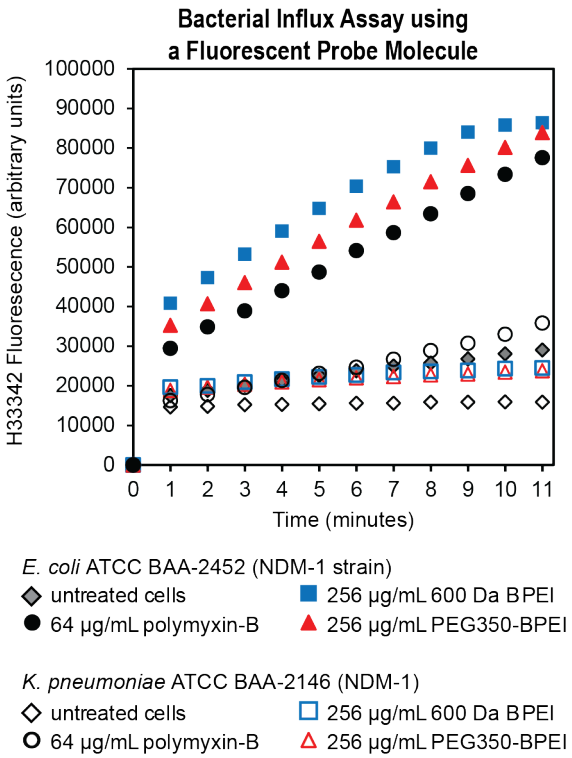

Figure 32. Fluorescence intensity data for the intracellular accumulation of the DNA-binding compound H33342. Both 600-Da BPEI (blue squares) and PEG350-BPEI (red triangles) increase the uptake of H33342 by *E. coli*, but the effect is lower with *K. pneumoniae*.

The smaller influence of 600 Da BPEI and PEG350-BPEI on H33342 uptake by *K. pneumoniae* NDM-1 should be reflected in the antibiotic potentiation of other agents, such as the β-lactam piperacillin. Indeed, 600 Da BPEI improves piperacillin efficacy against the *E. coli* NDM-1 strain (Figure 34D) but potentiation is not observed against *K. pneumoniae* BAA-2146 (Figure 34A). The paradigm increasing drug uptake applies equally to increasing the influx of β-lactamase inhibitors. Figures 34E and 34F show that 16 µg/mL of 600 Da BPEI and PEG350-BPEI lower the piperacillin MIC to a value below its susceptibility breakpoint in the presence of 4 µg/mL of tazobactam, a β-lactamase inhibitor. However, this effect is only observed with *E. coli* NDM-1 and not the *K. pneumoniae* NDM-1 strain (Figures 34B and C). This difference between the two strains may likely be caused by their difference in drug uptake (Figure 33). However, it is also

important to note here that there are other significant distinctions between the two strains to consider (i.e. presence of other beta-lactamases, efflux pumps, virulence factors) when making this assessment. These other factors may be explored in future work.

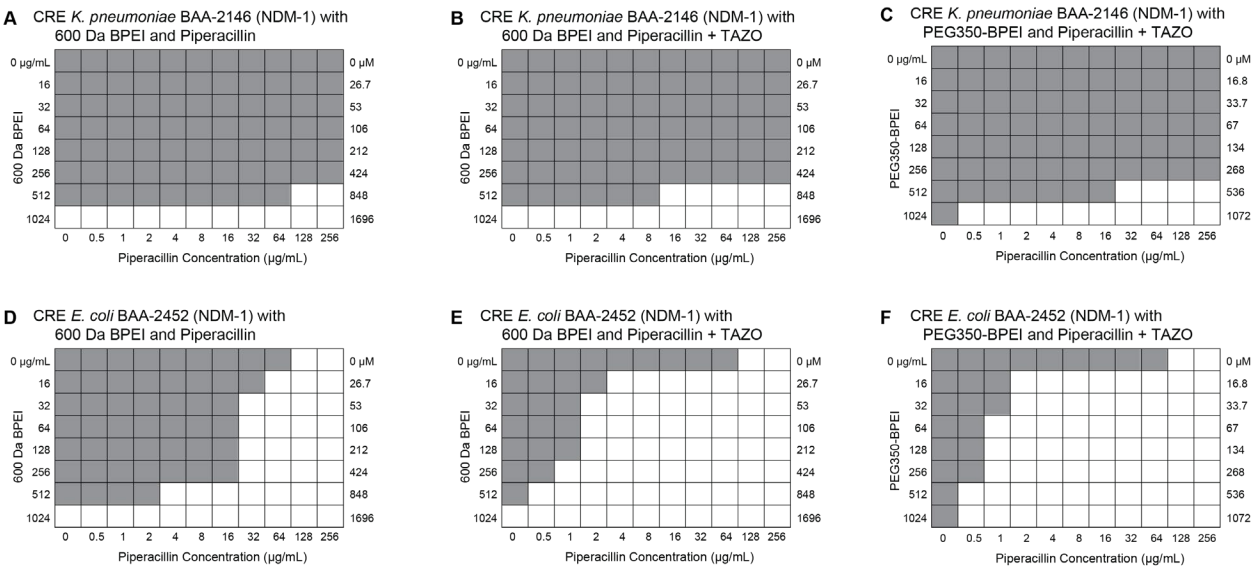

Figure 33. Checkerboard assay data for killing carbapenem-resistant *Enterobacteriaceae* (CRE) with piperacillin (PIP) and the β-lactamase inhibitor tazobactam (TAZO) antibiotics.

Conclusion

Although PEGylation of BPEI mitigates *in vivo* toxicity,[286] adverse events from systemic exposure remain a concern. Thus, we envision PEG-BPEIs as topical agents applied to acute and chronic wounds because PEG-BPEI + antibiotic combinations can kill susceptible and resistant bacteria in their biofilm and planktonic environments. Both 600 Da BPEI and PEG-BPEI disrupt biofilms[116-117, 244, 286] and disable resistance mechanisms of lab-strains and clinical isolates of multi-drug resistant *P. aeruginosa*,[116, 285-286] methicillin resistant *Staphylococcus aureus*,[114, 116, 165, 177, 286] and methicillin-resistant *S. epidermidis*.[113, 117, 286] The data presented here demonstrate that the possible utility of PEG-BPEI potentiators can be expanded to life-threatening carbapenem-

resistant *Enterobacteriaceae* (CRE) infections.[262, 265] Although we did not test antibiofilm activity against CRE bacteria in this study, we hypothesize that both potentiators can also disrupt biofilms CRE bacteria produce. This assumption might be addressed in future studies. CRE bacteria produce enzymes that degrade a wide range of antibiotics, including carbapenems and β-lactams.[265] There is a high mortality rate and survivors can have severe morbidity from treatment with toxic last-resort antibiotics.[262-263] CRE have mobile genetic elements that transfer resistance genes to other species.[266-268] These bacteria also circulate throughout the healthcare system.[266, 303-304] The mobility and spread of CRE needs to be curtailed, but these goals are impeded by wounds colonized and infected with CRE.[221, 274, 305] CRE wound infections are often polymicrobial, facilitating gene transfer.[221, 278-279] CRE wound infections also aggravate CRE spread because patients reside in, and are transported among, out-patient clinical facilities, in-patient hospitals, long-term care facilities, long-term acute care facilities, and skilled nursing home facilities.[219-221] Thus, improved therapeutic agents against CRE infected wounds may lead to better control of CRE exposure and spread. If possible, these compounds should have added benefits of mitigating wound biofilms and inflammatory cytokines that impair healing.[210] 600 Da BPEI provides these benefits, and modification with polyethylene glycol (PEG), forming PEG-BPEI, reduces *in vivo* toxicity. In a mouse model, the maximum tolerable dose, MTD, is 75 mg/kg for PEG350-BPEI whereas the MTD = 25 mg/kg for 600-Da BPEI.[286]

One of the potentiation mechanisms of action (MOA) here likely involve the chelation of Zn^{2+} ions essential for metallo-β-lactamases. Polyethylenimines have chelating properties with the ability to complex with some metal ions. Binding between Zn^{2+} and 600 Da BPEI is known[302] and is shown by ITC (Figure 32). 600 Da BPEI binds Cu^{2+} but does not bind Ca^{2+} or Mg^{2+}.[116] PEG-BPEI can also chelate Zn^{2+} ions. Additionally, PEG-BPEI can function as an influx potentiator. As shown in

Figure 33, PEG-BPEI increases antibiotic influx but does not need to disrupt the membrane to be effective. The core oligosaccharides have anionic phosphates that chelate Mg^{2+} ions in the LPS layer.[301, 306-313] LPS is a barrier that hinders drug influx.[179, 314] Cationic PEG-BPEI will bind with these anionic sites to improve diffusion through the LPS. PEG-BPEI could also bind to the phosphates on Lipid A, located near the layer of hydrophobic acyl chains. However, PEG-BPEI is hydrophilic and thus lacks the driving force to enter the hydrophobic regions. This characteristic distinguishes PEG-BPEI from cationic polymyxins and colistin, whose hydrophobic alkyl chains are required for membrane disruption.[182] We reported potentiation across antibiotic classes by lowering LPS barriers, which enhances passive diffusion and porin-mediated drug influx mechanisms.[116, 285] This paradigm applies equally to increasing the influx of β-lactamase inhibitors, such as tazobactam, and should also improve the uptake of efflux-pump inhibitors. These complementary MOAs enhance the value of PEG-BPEI, which also disrupts biofilms,[116-117, 244, 286] an underlying pathology that contributes to delayed healing.[259, 277, 315] We envision PEG-BPEIs used as topical agents for acute and chronic wounds. Future studies will involve further application of these potentiators in biofilm eradication and wound healing. We also hope to observe an improvement in overall wound healing in the presence of these potentiators because PEG-BPEI binds to Gram-positive and Gram-negative pathogen-associate molecular-pattern molecules (PAMPs)[114, 165, 177, 285] to reduce the release of inflammatory cytokines.[285]

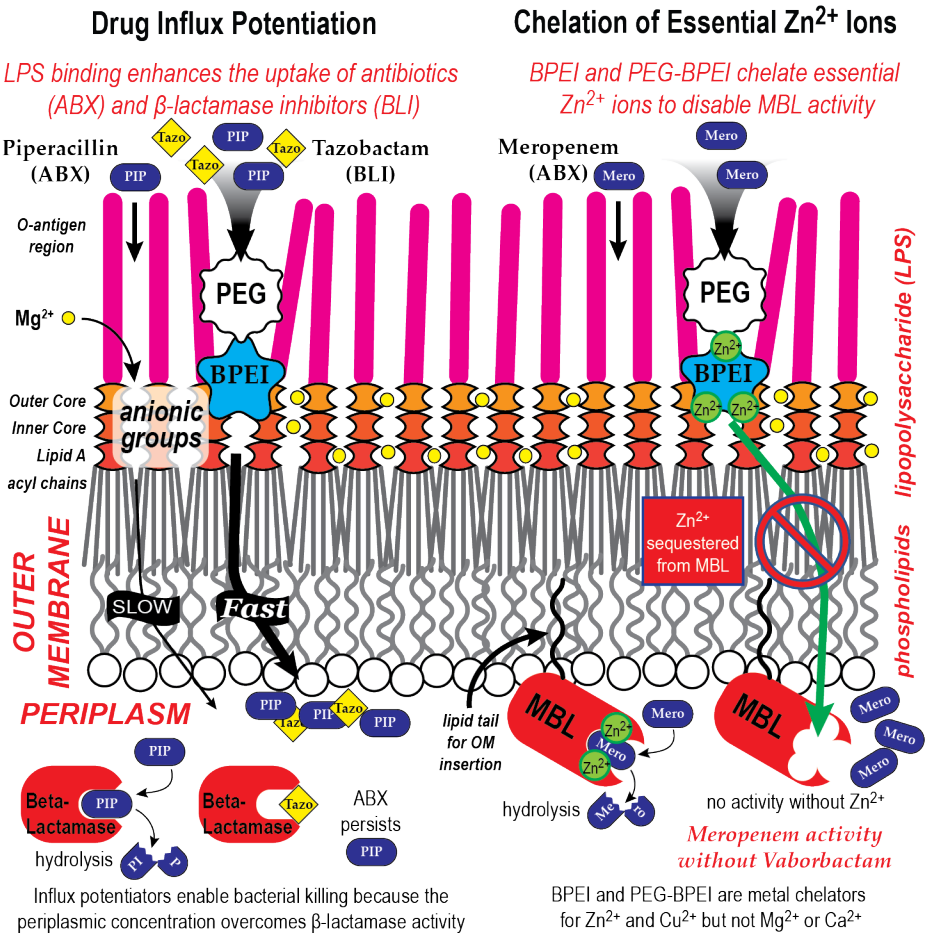

Figure 34. Illustration of mechanism-of-action (MOA) paradigms that allow PEG350-BPEI to overcome resistance factors in carbapenem-resistant Enterobacteriaceae (CRE) expressing the metallo-β-lactamases (MBLs), such as New Delhi MBL (NDM-1).

Final Thoughts

In this work, I emphasized the need to continue the research on biofilms and find new creative approaches in chapter 1. I explained how our lab tries to slow down antibiotic resistance in chapter 2 by developing an antibiotic "enhancer". Chapters 3 and 4 detail how our technology is effective against *P. aeruginosa* and its biofilms while chapter 5 expands to other life-threatening Gram-negative bacteria. Overall, both 600 Da BPEI and PEG-BPEI disrupt biofilms and disable resistance mechanisms of lab-strains and clinical isolates of multi-drug resistant *P. aeruginosa*, methicillin resistant *Staphylococcus aureus*, and methicillin-resistant *S. epidermidis* and counteract resistance mechanisms of life-threatening *E. coli* and *K. pneumoniae*. We foresee 600 Da BPEI and derivative to be a topical agent for wound treatment. It is water-soluble and interacts minimally with other proteins in serum. More studies that explore its other therapeutic uses are underway. Current graduate and undergraduate students in the Rice Lab are working toward a further understanding of the mechanisms of action of 600-Da BPEI across various pathogens as well as other applications of BPEI.

While writing this dissertation, COVID-19 caused a global pandemic. This is a time when scientists all over the world worked together to advance research efforts and find a solution. Backed by many years of groundwork research on related viruses, the COVID-19 vaccine was rolled out only 10 months after the declaration of COVID-19 as a pandemic. A few thoughts come to mind while pondering about this. First is that the pandemic allowed various scientists to focus and work together. The urgency to come up with the solution drove many scientists to develop great science together. The process was challenging but a vaccine was created. This made me think

of the global threat that this dissertation is trying to address—antibiotic resistance, which brings me to my next thought: Another pandemic is already simmering. I have already provided plenty of statistics in this work. However, I want to make sure that the point comes across—one day, all our antibiotics may become *useless*. A simple infection on a minor cut can become deadly. Resistance mechanisms, biofilms, and quickly-evolving bacteria are outcompeting us. My last thought is about generating scientific data in the midst of a pandemic. I was quite impressed with the innovative tools and resources that scientists developed during this time. However, I also do not want to downplay the challenges brought by this pandemic. When research labs shut down, many researchers outside the field of virology had to halt their own work. I was fortunate enough to have collected data prior to shutting down. Hence, my quarantine days were spent conceiving chapters 1 and 5 of this dissertation. Unfortunately, this was a rare case. Plenty of graduate students had to quarantine with not a lot to work with. Writing about resistance during a pandemic was also challenging because all attention went to COVID-19 and the issues it was associated with. Now, why did I include this last thought here? I wanted to show how complex the process of research is. Research is often slowed down by troubleshooting and other various reasons. Then add outside forces, research slows down even more. We cannot keep slowing down and focusing our attention elsewhere. This is a problem now and scientists need to continue working together.

References

1. Silver, L. L., Challenges of antibacterial discovery. *Clin Microbiol Rev* **2011,** *24* (1), 71-109.
2. CDC Biggest Threats and Data. https://www.cdc.gov/drugresistance/biggest-threats.html.
3. Annual report of the European Medicines Agency. https://www.ema.europa.eu/en/documents/annual-report/annual-report-european-medicines-agency-2009_en.pdf (accessed May 2020).
4. Howell, L. In *Global Risks 2013—Eight Edition*, Internet] World Economic Forum, Cologny/Geneva, Switzerland, 2013.
5. Hellen, G.; Molly, M.-P.; Suraj, P.; Sumanth, G.; Jordan, L.; Devra, B.; Andrea, W.; Ramanan, L., State of the World's Antibiotics. *Center for Disease Dynamics, Economics & Policy: Washington, DC* **2015**.
6. Donlan, R. M., Biofilms: microbial life on surfaces. *Emerg Infect Dis* **2002,** *8* (9), 881-890.
7. Kostakioti, M.; Hadjifrangiskou, M.; Hultgren, S. J., Bacterial biofilms: development, dispersal, and therapeutic strategies in the dawn of the postantibiotic era. *Cold Spring Harb Perspect Med* **2013,** *3* (4), a010306-a010306.
8. Dunne, W. M., Jr., Bacterial adhesion: seen any good biofilms lately? *Clin Microbiol Rev* **2002,** *15* (2), 155-166.
9. Koo, H.; Allan, R. N.; Howlin, R. P.; Stoodley, P.; Hall-Stoodley, L., Targeting microbial biofilms: current and prospective therapeutic strategies. *Nature Reviews Microbiology* **2017,** *15* (12), 740-755.
10. Magana, M.; Sereti, C.; Ioannidis, A.; Mitchell, C. A.; Ball, A. R.; Magiorkinis, E.; Chatzipanagiotou, S.; Hamblin, M. R.; Hadjifrangiskou, M.; Tegos, G. P., Options and limitations in clinical investigation of bacterial biofilms. *Clin Microbiol Rev* **2018,** *31* (3), e00084-16.
11. Harrison, F.; Buckling, A., Siderophore production and biofilm formation as linked social traits. *Isme j* **2009,** *3* (5), 632-4.
12. Wood, T. L.; Gong, T.; Zhu, L.; Miller, J.; Miller, D. S.; Yin, B.; Wood, T. K., Rhamnolipids from Pseudomonas aeruginosa disperse the biofilms of sulfate-reducing bacteria. *npj Biofilms and Microbiomes* **2018,** *4* (1), 22.
13. Taylor, P. K.; Van Kessel, A. T.; Colavita, A.; Hancock, R. E.; Mah, T.-F., A novel small RNA is important for biofilm formation and pathogenicity in Pseudomonas aeruginosa. *PloS one* **2017,** *12* (8), e0182582.
14. Fong, J. N.; Yildiz, F. H., Biofilm matrix proteins. *Microbial Biofilms* **2015**, 201-222.
15. Boyd, A.; Chakrabarty, A., Pseudomonas aeruginosa biofilms: role of the alginate exopolysaccharide. *Journal of industrial microbiology* **1995,** *15* (3), 162-168.
16. Lin, M. H.; Shu, J. C.; Lin, L. P.; Chong, K. y.; Cheng, Y. W.; Du, J. F.; Liu, S.-T., Elucidating the Crucial Role of Poly N-Acetylglucosamine from Staphylococcus aureus in Cellular Adhesion and Pathogenesis. *PLOS ONE* **2015,** *10* (4), e0124216.
17. Jennings, L. K.; Storek, K. M.; Ledvina, H. E.; Coulon, C.; Marmont, L. S.; Sadovskaya, I.; Secor, P. R.; Tseng, B. S.; Scian, M.; Filloux, A., Pel is a cationic exopolysaccharide that cross-links extracellular DNA in the Pseudomonas aeruginosa biofilm matrix. *Proceedings of the National Academy of Sciences* **2015,** *112* (36), 11353-11358.
18. Cole, S. J.; Records, A. R.; Orr, M. W.; Linden, S. B.; Lee, V. T., Catheter-associated urinary tract infection by Pseudomonas aeruginosa is mediated by exopolysaccharide-independent biofilms. *Infect Immun* **2014,** *82* (5), 2048-2058.
19. Zetzmann, M.; Okshevsky, M.; Endres, J.; Sedlag, A.; Caccia, N.; Auchter, M.; Waidmann, M. S.; Desvaux, M.; Meyer, R. L.; Riedel, C. U., DNase-Sensitive and -Resistant Modes of Biofilm Formation by Listeria monocytogenes. *Front Microbiol* **2015,** *6*, 1428-1428.

20. Das, T.; Kutty, S. K.; Kumar, N.; Manefield, M., Pyocyanin facilitates extracellular DNA binding to Pseudomonas aeruginosa influencing cell surface properties and aggregation. *PloS one* **2013,** *8* (3), e58299-e58299.
21. Whitchurch, C. B.; Tolker-Nielsen, T.; Ragas, P. C.; Mattick, J. S., Extracellular DNA required for bacterial biofilm formation. *Science* **2002,** *295* (5559), 1487-1487.
22. Okshevsky, M.; Regina, V. R.; Meyer, R. L., Extracellular DNA as a target for biofilm control. *Current opinion in biotechnology* **2015,** *33*, 73-80.
23. Turnbull, L.; Toyofuku, M.; Hynen, A. L.; Kurosawa, M.; Pessi, G.; Petty, N. K.; Osvath, S. R.; Cárcamo-Oyarce, G.; Gloag, E. S.; Shimoni, R.; Omasits, U.; Ito, S.; Yap, X.; Monahan, L. G.; Cavaliere, R.; Ahrens, C. H.; Charles, I. G.; Nomura, N.; Eberl, L.; Whitchurch, C. B., Explosive cell lysis as a mechanism for the biogenesis of bacterial membrane vesicles and biofilms. *Nature Communications* **2016,** *7* (1), 11220.
24. Shehadul Islam, M.; Aryasomayajula, A.; Selvaganapathy, P. R., A Review on Macroscale and Microscale Cell Lysis Methods. *Micromachines (Basel)* **2017,** *8* (3), 83.
25. Deng, B.; Ghatak, S.; Sarkar, S.; Singh, K.; Das Ghatak, P.; Mathew-Steiner, S. S.; Roy, S.; Khanna, S.; Wozniak, D. J.; McComb, D. W.; Sen, C. K., Novel Bacterial Diversity and Fragmented eDNA Identified in Hyperbiofilm-Forming Pseudomonas aeruginosa Rugose Small Colony Variant. *iScience* **2020,** *23* (2), 100827.
26. Wu, J.; Xi, C., Evaluation of different methods for extracting extracellular DNA from the biofilm matrix. *Appl Environ Microbiol* **2009,** *75* (16), 5390-5.
27. Allesen-Holm, M.; Barken, K. B.; Yang, L.; Klausen, M.; Webb, J. S.; Kjelleberg, S.; Molin, S.; Givskov, M.; Tolker-Nielsen, T., A characterization of DNA release in Pseudomonas aeruginosa cultures and biofilms. *Molecular Microbiology* **2006,** *59* (4), 1114-1128.
28. Steinberger, R.; Holden, P., Extracellular DNA in single-and multiple-species unsaturated biofilms. *Appl. Environ. Microbiol.* **2005,** *71* (9), 5404-5410.
29. Sugimoto, S.; Sato, F.; Miyakawa, R.; Chiba, A.; Onodera, S.; Hori, S.; Mizunoe, Y., Broad impact of extracellular DNA on biofilm formation by clinically isolated Methicillin-resistant and -sensitive strains of Staphylococcus aureus. *Scientific Reports* **2018,** *8* (1), 2254.
30. Montanaro, L.; Poggi, A.; Visai, L.; Ravaioli, S.; Campoccia, D.; Speziale, P.; Arciola, C. R., Extracellular DNA in Biofilms. *The International Journal of Artificial Organs* **2011,** *34* (9), 824-831.
31. Zatorska, B.; Groger, M.; Moser, D.; Diab-Elschahawi, M.; Lusignani, L. S.; Presterl, E., Does Extracellular DNA Production Vary in Staphylococcal Biofilms Isolated From Infected Implants versus Controls? *Clinical Orthopaedics and Related Research®* **2017,** *475* (8), 2105-2113.
32. Dusane, D. H., CORR Insights®: Does Extracellular DNA Production Vary in Staphylococcal Biofilms Isolated From Infected Implants versus Controls? *Clinical Orthopaedics and Related Research®* **2017,** *475* (8), 2114-2116.
33. Randrianjatovo-Gbalou, I.; Rouquette, P.; Lefebvre, D.; Girbal-Neuhauser, E.; Marcato-Romain, C.-E., In situ analysis of Bacillus licheniformis biofilms: amyloid-like polymers and eDNA are involved in the adherence and aggregation of the extracellular matrix. *Journal of Applied Microbiology* **2017,** *122* (5), 1262-1274.
34. Petersen, F. C.; Pecharki, D.; Scheie, A. A., Biofilm mode of growth of Streptococcus intermedius favored by a competence-stimulating signaling peptide. *J Bacteriol* **2004,** *186* (18), 6327-6331.
35. Petersen, F. C.; Tao, L.; Scheie, A. A., DNA binding-uptake system: a link between cell-to-cell communication and biofilm formation. *J Bacteriol* **2005,** *187* (13), 4392-4400.
36. Slater, R. T.; Frost, L. R.; Jossi, S. E.; Millard, A. D.; Unnikrishnan, M., Clostridioides difficile LuxS mediates inter-bacterial interactions within biofilms. *Scientific Reports* **2019,** *9* (1), 9903.
37. Whitchurch, C. B.; Tolker-Nielsen, T.; Ragas, P. C.; Mattick, J. S., Extracellular DNA Required for Bacterial Biofilm Formation. *Science* **2002,** *295* (5559), 1487.
38. Matsukawa, M.; Greenberg, E. P., Putative exopolysaccharide synthesis genes influence Pseudomonas aeruginosa biofilm development. *J Bacteriol* **2004,** *186* (14), 4449-56.

39. Pakkulnan, R.; Anutrakunchai, C.; Kanthawong, S.; Taweechaisupapong, S.; Chareonsudjai, P.; Chareonsudjai, S., Extracellular DNA facilitates bacterial adhesion during Burkholderia pseudomallei biofilm formation. *PloS one* **2019,** *14* (3), e0213288-e0213288.
40. Devaraj, A.; Justice, S. S.; Bakaletz, L. O.; Goodman, S. D., DNABII proteins play a central role in UPEC biofilm structure. *Molecular microbiology* **2015,** *96* (6), 1119-1135.
41. Ibáñez de Aldecoa, A. L.; Zafra, O.; González-Pastor, J. E., Mechanisms and Regulation of Extracellular DNA Release and Its Biological Roles in Microbial Communities. *Front Microbiol* **2017,** *8*, 1390-1390.
42. Lackie, J. M., Numerical entries and A. In *The Dictionary of Cell & Molecular Biology (Fifth Edition)*, Lackie, J. M., Ed. Academic Press: Boston, 2013; pp 1-61.
43. Thomas, V. C.; Thurlow, L. R.; Boyle, D.; Hancock, L. E., Regulation of autolysis-dependent extracellular DNA release by Enterococcus faecalis extracellular proteases influences biofilm development. *J Bacteriol* **2008,** *190* (16), 5690-5698.
44. Sahu, P. K.; Iyer, P. S.; Oak, A. M.; Pardesi, K. R.; Chopade, B. A., Characterization of eDNA from the Clinical Strain Acinetobacter baumannii AIIMS 7 and Its Role in Biofilm Formation. *The Scientific World Journal* **2012,** *2012*, 973436.
45. Toyofuku, M.; Nomura, N.; Eberl, L., Types and origins of bacterial membrane vesicles. *Nature Reviews Microbiology* **2019,** *17* (1), 13-24.
46. Carrolo, M.; Frias, M. J.; Pinto, F. R.; Melo-Cristino, J.; Ramirez, M., Prophage spontaneous activation promotes DNA release enhancing biofilm formation in Streptococcus pneumoniae. *PloS one* **2010,** *5* (12), e15678-e15678.
47. Zafra, O.; Lamprecht-Grandío, M.; de Figueras, C. G.; González-Pastor, J. E., Extracellular DNA release by undomesticated Bacillus subtilis is regulated by early competence. *PloS one* **2012,** *7* (11), e48716-e48716.
48. Rutherford, S. T.; Bassler, B. L., Bacterial quorum sensing: its role in virulence and possibilities for its control. *Cold Spring Harb Perspect Med* **2012,** *2* (11), a012427.
49. Qin, Z.; Ou, Y.; Yang, L.; Zhu, Y.; Tolker-Nielsen, T.; Molin, S.; Qu, D., Role of autolysin-mediated DNA release in biofilm formation of Staphylococcus epidermidis. *Microbiology* **2007,** *153* (7), 2083-2092.
50. Tahrioui, A.; Duchesne, R.; Bouffartigues, E.; Rodrigues, S.; Maillot, O.; Tortuel, D.; Hardouin, J.; Taupin, L.; Groleau, M.-C.; Dufour, A.; Déziel, E.; Brenner-Weiss, G.; Feuilloley, M.; Orange, N.; Lesouhaitier, O.; Cornelis, P.; Chevalier, S., Extracellular DNA release, quorum sensing, and PrrF1/F2 small RNAs are key players in Pseudomonas aeruginosa tobramycin-enhanced biofilm formation. *npj Biofilms and Microbiomes* **2019,** *5* (1), 15.
51. Hazan, R.; Que, Y. A.; Maura, D.; Strobel, B.; Majcherczyk, P. A.; Hopper, L. R.; Wilbur, D. J.; Hreha, T. N.; Barquera, B.; Rahme, L. G., Auto poisoning of the respiratory chain by a quorum-sensing-regulated molecule favors biofilm formation and antibiotic tolerance. *Current biology* **2016,** *26* (2), 195-206.
52. Pierson, L. S., 3rd; Pierson, E. A., Metabolism and function of phenazines in bacteria: impacts on the behavior of bacteria in the environment and biotechnological processes. *Appl Microbiol Biotechnol* **2010,** *86* (6), 1659-1670.
53. Das, T.; Manefield, M., Pyocyanin promotes extracellular DNA release in Pseudomonas aeruginosa. *PLoS One* **2012,** *7* (10), e46718.
54. Lin, H.; Wang, C.; Zhao, H.; Chen, G.; Chen, X., Interaction between copper and extracellular nucleic acids in the EPS of unsaturated Pseudomonas putida CZ1 biofilm. *Environmental Science and Pollution Research* **2018,** *25* (24), 24172-24180.
55. Chiang, W.-C.; Nilsson, M.; Jensen, P. Ø.; Høiby, N.; Nielsen, T. E.; Givskov, M.; Tolker-Nielsen, T., Extracellular DNA shields against aminoglycosides in Pseudomonas aeruginosa biofilms. *Antimicrob Agents Chemother* **2013,** *57* (5), 2352-2361.

56. Walker, T. S.; Tomlin, K. L.; Worthen, G. S.; Poch, K. R.; Lieber, J. G.; Saavedra, M. T.; Fessler, M. B.; Malcolm, K. C.; Vasil, M. L.; Nick, J. A., Enhanced Pseudomonas aeruginosa biofilm development mediated by human neutrophils. *Infect Immun* **2005,** *73* (6), 3693-3701.
57. Ikuma, K.; Decho, A. W.; Lau, B. L., The extracellular bastions of bacteria—a biofilm way of life. *Nature Education Knowledge* **2013,** *4* (2), 2-19.10.
58. Alhede, M.; Alhede, M.; Qvortrup, K.; Kragh, K. N.; Jensen, P. Ø.; Stewart, P. S.; Bjarnsholt, T., The origin of extracellular DNA in bacterial biofilm infections in vivo. *Pathog Dis* **2020,** *78* (2), ftaa018.
59. Izano, E. A.; Amarante, M. A.; Kher, W. B.; Kaplan, J. B., Differential roles of poly-N-acetylglucosamine surface polysaccharide and extracellular DNA in Staphylococcus aureus and Staphylococcus epidermidis biofilms. *Appl Environ Microbiol* **2008,** *74* (2), 470-6.
60. Tang, L.; Schramm, A.; Neu, T. R.; Revsbech, N. P.; Meyer, R. L., Extracellular DNA in adhesion and biofilm formation of four environmental isolates: a quantitative study. *FEMS Microbiol Ecol* **2013,** *86* (3), 394-403.
61. Das, T.; Sharma, P. K.; Busscher, H. J.; van der Mei, H. C.; Krom, B. P., Role of Extracellular DNA in Initial Bacterial Adhesion and Surface Aggregation. *Applied and Environmental Microbiology* **2010,** *76* (10), 3405.
62. Okshevsky, M.; Meyer, R. L., The role of extracellular DNA in the establishment, maintenance and perpetuation of bacterial biofilms. *Crit Rev Microbiol* **2015,** *41* (3), 341-52.
63. Berne, C.; Kysela, D. T.; Brun, Y. V., A bacterial extracellular DNA inhibits settling of motile progeny cells within a biofilm. *Molecular microbiology* **2010,** *77* (4), 815-829.
64. Saunders, S. H.; Tse, E. C. M.; Yates, M. D.; Otero, F. J.; Trammell, S. A.; Stemp, E. D. A.; Barton, J. K.; Tender, L. M.; Newman, D. K., Extracellular DNA Promotes Efficient Extracellular Electron Transfer by Pyocyanin in Pseudomonas aeruginosa Biofilms. *Cell* **2020,** *182* (4), 919-932.e19.
65. Johnson, L.; Horsman, S. R.; Charron-Mazenod, L.; Turnbull, A. L.; Mulcahy, H.; Surette, M. G.; Lewenza, S., Extracellular DNA-induced antimicrobial peptide resistance in Salmonella enterica serovar Typhimurium. *BMC Microbiol* **2013,** *13*, 115-115.
66. Mulcahy, H.; Charron-Mazenod, L.; Lewenza, S., Extracellular DNA Chelates Cations and Induces Antibiotic Resistance in Pseudomonas aeruginosa Biofilms. *PLOS Pathogens* **2008,** *4* (11), e1000213.
67. Saxena, P.; Joshi, Y.; Rawat, K.; Bisht, R., Biofilms: Architecture, Resistance, Quorum Sensing and Control Mechanisms. *Indian Journal of Microbiology* **2019,** *59* (1), 3-12.
68. Keeling, P. J.; Palmer, J. D., Horizontal gene transfer in eukaryotic evolution. *Nature Reviews Genetics* **2008,** *9* (8), 605-618.
69. Ussery, D. W., DNA Structure: A-, B-and Z-DNA Helix Families. *e LS* **2001**.
70. Bacolla, A.; Wells, R. D., Non-B DNA conformations, genomic rearrangements, and human disease. *Journal of Biological Chemistry* **2004,** *279* (46), 47411-47414.
71. Basu, H. S.; Feuerstein, B. G.; Zarling, D. A.; Shaffer, R. H.; Marton, L. J., Recognition of Z-RNA and Z-DNA Determinants by Polyamines in Solution: Experimental and Theoretical Studies. *Journal of Biomolecular Structure and Dynamics* **1988,** *6* (2), 299-309.
72. Thomas, T. J.; Messner, R. P., A left-handed (Z) conformation of poly(dA-dC).poly(dG-dT) induced by polyamines. *Nucleic Acids Research* **1986,** *14* (16), 6721-6733.
73. Rosenberg, M.; Azevedo, N. F.; Ivask, A., Propidium iodide staining underestimates viability of adherent bacterial cells. *Scientific Reports* **2019,** *9* (1), 6483.
74. Peterson, B. W.; van der Mei, H. C.; Sjollema, J.; Busscher, H. J.; Sharma, P. K., A Distinguishable Role of eDNA in the Viscoelastic Relaxation of Biofilms. *mBio* **2013,** *4* (5), e00497-13.
75. Ramesh, N.; Brahmachari, S. K., Structural alteration from non-B to B-form could reflect DNase I hypersensitivity. *Journal of Biomolecular Structure and Dynamics* **1989,** *6* (5), 899-906.
76. Blesa, A.; Berenguer, J., Contribution of vesicle-protected extracellular DNA to horizontal gene transfer in Thermus spp. *Int Microbiol* **2015,** *18* (3), 177-187.
77. Alberts, B.; Johnson, A.; Lewis, J.; Raff, M.; Roberts, K.; Walter, P., Protein function. In *Molecular Biology of the Cell. 4th edition*, Garland Science: 2002.

78. Graf, A. C.; Leonard, A.; Schäuble, M.; Rieckmann, L. M.; Hoyer, J.; Maass, S.; Lalk, M.; Becher, D.; Pané-Farré, J.; Riedel, K., Virulence Factors Produced by Staphylococcus aureus Biofilms Have a Moonlighting Function Contributing to Biofilm Integrity. *Molecular & Cellular Proteomics* **2019,** *18* (6), 1036.
79. Skibbens, R. V., Condensins and cohesins – one of these things is not like the other! *Journal of Cell Science* **2019,** *132* (3), jcs220491.
80. Kavanaugh, J. S.; Flack, C. E.; Lister, J.; Ricker, E. B.; Ibberson, C. B.; Jenul, C.; Moormeier, D. E.; Delmain, E. A.; Bayles, K. W.; Horswill, A. R., Identification of Extracellular DNA-Binding Proteins in the Biofilm Matrix. *mBio* **2019,** *10* (3), e01137-19.
81. Arenas, J.; Tommassen, J., Meningococcal Biofilm Formation: Let's Stick Together. *Trends in Microbiology* **2017,** *25* (2), 113-124.
82. Dengler, V.; Foulston, L.; DeFrancesco, A. S.; Losick, R., An Electrostatic Net Model for the Role of Extracellular DNA in Biofilm Formation by Staphylococcus aureus. *J Bacteriol* **2015,** *197* (24), 3779-3787.
83. Devaraj, A.; Buzzo, J.; Rocco, C. J.; Bakaletz, L. O.; Goodman, S. D., The DNABII family of proteins is comprised of the only nucleoid associated proteins required for nontypeable Haemophilus influenzae biofilm structure. *Microbiologyopen* **2018,** *7* (3), e00563-e00563.
84. Novotny, L. A.; Jurcisek, J. A.; Goodman, S. D.; Bakaletz, L. O., Monoclonal antibodies against DNA-binding tips of DNABII proteins disrupt biofilms in vitro and induce bacterial clearance in vivo. *EBioMedicine* **2016,** *10*, 33-44.
85. Goodman, S. D.; Obergfell, K. P.; Jurcisek, J. A.; Novotny, L. A.; Downey, J. S.; Ayala, E. A.; Tjokro, N.; Li, B.; Justice, S. S.; Bakaletz, L. O., Biofilms can be dispersed by focusing the immune system on a common family of bacterial nucleoid-associated proteins. *Mucosal Immunology* **2011,** *4* (6), 625-637.
86. Schwartz, K.; Boles, B. R., Microbial amyloids--functions and interactions within the host. *Curr Opin Microbiol* **2013,** *16* (1), 93-99.
87. Schwartz, K.; Syed, A. K.; Stephenson, R. E.; Rickard, A. H.; Boles, B. R., Functional amyloids composed of phenol soluble modulins stabilize Staphylococcus aureus biofilms. *PLoS pathogens* **2012,** *8* (6), e1002744-e1002744.
88. Schwartz, K.; Ganesan, M.; Payne, D. E.; Solomon, M. J.; Boles, B. R., Extracellular DNA facilitates the formation of functional amyloids in Staphylococcus aureus biofilms. *Molecular Microbiology* **2016,** *99* (1), 123-134.
89. Nwodo, U. U.; Green, E.; Okoh, A. I., Bacterial exopolysaccharides: functionality and prospects. *Int J Mol Sci* **2012,** *13* (11), 14002-14015.
90. Wang, S.; Liu, X.; Liu, H.; Zhang, L.; Guo, Y.; Yu, S.; Wozniak, D. J.; Ma, L. Z., The exopolysaccharide Psl-eDNA interaction enables the formation of a biofilm skeleton in Pseudomonas aeruginosa. *Environ Microbiol Rep* **2015,** *7* (2), 330-340.
91. Kaplan, J. B., Biofilm dispersal: mechanisms, clinical implications, and potential therapeutic uses. *J Dent Res* **2010,** *89* (3), 205-218.
92. Bellin, D. L.; Sakhtah, H.; Zhang, Y.; Price-Whelan, A.; Dietrich, L. E. P.; Shepard, K. L., Electrochemical camera chip for simultaneous imaging of multiple metabolites in biofilms. *Nature Communications* **2016,** *7* (1), 10535.
93. Zhu, K.; Chen, S.; Sysoeva, T. A.; You, L., Universal antibiotic tolerance arising from antibiotic-triggered accumulation of pyocyanin in Pseudomonas aeruginosa. *PLOS Biology* **2019,** *17* (12), e3000573.
94. Schiessl, K. T.; Hu, F.; Jo, J.; Nazia, S. Z.; Wang, B.; Price-Whelan, A.; Min, W.; Dietrich, L. E. P., Phenazine production promotes antibiotic tolerance and metabolic heterogeneity in Pseudomonas aeruginosa biofilms. *Nature Communications* **2019,** *10* (1), 762.
95. Das, T.; Kutty, S. K.; Tavallaie, R.; Ibugo, A. I.; Panchompoo, J.; Sehar, S.; Aldous, L.; Yeung, A. W. S.; Thomas, S. R.; Kumar, N.; Gooding, J. J.; Manefield, M., Phenazine virulence factor binding to

extracellular DNA is important for Pseudomonas aeruginosa biofilm formation. *Scientific reports* **2015,** *5*, 8398-8398.
96. Banin, E.; Brady, K. M.; Greenberg, E. P., Chelator-induced dispersal and killing of Pseudomonas aeruginosa cells in a biofilm. *Appl Environ Microbiol* **2006,** *72* (3), 2064-9.
97. Matsukawa, M.; Greenberg, E. P., Putative Exopolysaccharide Synthesis Genes Influence Pseudomonas aeruginosa Biofilm Development. *J Bacteriol* **2004,** *186* (14), 4449.
98. Eun, H.-M., 3 - Nucleases. In *Enzymology Primer for Recombinant DNA Technology*, Eun, H.-M., Ed. Academic Press: San Diego, 1996; pp 145-232.
99. Hartmann, G., Chapter Four - Nucleic Acid Immunity. In *Advances in Immunology*, Alt, F. W., Ed. Academic Press: 2017; Vol. 133, pp 121-169.
100. Wagener, J. S.; Kupfer, O., Dornase alfa (Pulmozyme). *Current Opinion in Pulmonary Medicine* **2012,** *18* (6).
101. Berends, E. T. M.; Horswill, A. R.; Haste, N. M.; Monestier, M.; Nizet, V.; von Köckritz-Blickwede, M., Nuclease Expression by Staphylococcus aureus Facilitates Escape from Neutrophil Extracellular Traps. *Journal of Innate Immunity* **2010,** *2* (6), 576-586.
102. Nijland, R.; Hall, M. J.; Burgess, J. G., Dispersal of Biofilms by Secreted, Matrix Degrading, Bacterial DNase. *PLOS ONE* **2010,** *5* (12), e15668.
103. Izano, E. A.; Amarante, M. A.; Kher, W. B.; Kaplan, J. B., Differential Roles of Poly-N-Acetylglucosamine Surface Polysaccharide and Extracellular DNA in Staphylococcus aureus and Staphylococcus epidermidis Biofilms. *Applied and Environmental Microbiology* **2008,** *74* (2), 470.
104. Itoh, Y.; Wang, X.; Hinnebusch, B. J.; Preston, J. F., 3rd; Romeo, T., Depolymerization of beta-1,6-N-acetyl-D-glucosamine disrupts the integrity of diverse bacterial biofilms. *J Bacteriol* **2005,** *187* (1), 382-387.
105. Wilton, M.; Charron-Mazenod, L.; Moore, R.; Lewenza, S., Extracellular DNA Acidifies Biofilms and Induces Aminoglycoside Resistance in Pseudomonas aeruginosa. *Antimicrob Agents Chemother* **2016,** *60* (1), 544-53.
106. Zhou, C.; Lehar, S.; Gutierrez, J.; Rosenberger, C. M.; Ljumanovic, N.; Dinoso, J.; Koppada, N.; Hong, K.; Baruch, A.; Carrasco-Triguero, M.; Saad, O.; Mariathasan, S.; Kamath, A. V., Pharmacokinetics and pharmacodynamics of DSTA4637A: A novel THIOMAB™ antibody antibiotic conjugate against Staphylococcus aureus in mice. *MAbs* **2016,** *8* (8), 1612-1619.
107. Zhang, A.; Mu, H.; Zhang, W.; Cui, G.; Zhu, J.; Duan, J., Chitosan Coupling Makes Microbial Biofilms Susceptible to Antibiotics. *Scientific Reports* **2013,** *3* (1), 3364.
108. Beveridge, T. J., Use of the Gram stain in microbiology. *Biotechnic & Histochemistry* **2001,** *76* (3), 111-118.
109. Oliveira, J.; Reygaert, W. C., Gram negative bacteria. **2019**.
110. Waterer, G. W.; Wunderink, R. G., Increasing threat of Gram-negative bacteria. *Critical Care Medicine* **2001,** *29* (4), N75-N81.
111. Silhavy, T. J.; Kahne, D.; Walker, S., The bacterial cell envelope. *Cold Spring Harb Perspect Biol* **2010,** *2* (5), a000414-a000414.
112. López, C. A.; Zgurskaya, H.; Gnanakaran, S., Molecular characterization of the outer membrane of Pseudomonas aeruginosa. *Biochimica et Biophysica Acta (BBA)-Biomembranes* **2020,** *1862* (3), 183151.
113. Lam, A. K.; Hill, M. A.; Moen, E. L.; Pusavat, J.; Wouters, C. L.; Rice, C. V., Cationic Branched Polyethylenimine (BPEI) Disables Antibiotic Resistance in Methicillin-Resistant Staphylococcus epidermidis (MRSE). *ChemMedChem* **2018,** *13* (20), 2240-2248.
114. Hill, M. A.; Lam, A. K.; Reed, P.; Harney, M. C.; Wilson, B. A.; Moen, E. L.; Wright, S. N.; Pinho, M. G.; Rice, C. V., BPEI-Induced Delocalization of PBP4 Potentiates beta-Lactams against MRSA. *Biochemistry* **2019,** *58* (36), 3813-3822.
115. Salton, M. R.; Kim, K.-S.; Baron, S., Medical microbiology. *S. Baron (ed.)* **1996**.

116. Lam, A. K.; Panlilio, H.; Pusavat, J.; Wouters, C. L.; Moen, E. L.; Rice, C. V., Overcoming Multidrug Resistance and Biofilms of Pseudomonas aeruginosa with a Single Dual-Function Potentiator of beta-Lactams. *Acs Infect Dis* **2020**.
117. Lam, A. K.; Wouters, C. L.; Moen, E. L.; Pusavat, J.; Rice, C. V., Antibiofilm Synergy of beta-Lactams and Branched Polyethylenimine against Methicillin-Resistant Staphylococcus epidermidis. *Biomacromolecules* **2019,** *20* (10), 3778-3785.
118. Chaudhary, A. S., A review of global initiatives to fight antibiotic resistance and recent antibiotics′ discovery. *Acta Pharmaceutica Sinica B* **2016,** *6* (6), 552-556.
119. de Kraker, M. E.; Stewardson, A. J.; Harbarth, S., Will 10 million people die a year due to antimicrobial resistance by 2050? *PLoS medicine* **2016,** *13* (11).
120. *Global antimicrobial resistance and use surveillance system (GLASS) report: 2021*; 9240027335; World Health Organization: 2021.
121. Pandey, N.; Cascella, M., Beta lactam antibiotics. *StatPearls [Internet]* **2020**.
122. Wax, R. G.; Lewis, K.; Salyers, A. A.; Taber, H., *Bacterial resistance to antimicrobials*. CRC press: 2007.
123. Gullberg, E.; Cao, S.; Berg, O. G.; Ilbäck, C.; Sandegren, L.; Hughes, D.; Andersson, D. I., Selection of Resistant Bacteria at Very Low Antibiotic Concentrations. *PLOS Pathogens* **2011,** *7* (7), e1002158.
124. Lupo, A.; Coyne, S.; Berendonk, T., Origin and Evolution of Antibiotic Resistance: The Common Mechanisms of Emergence and Spread in Water Bodies. *Front Microbiol* **2012,** *3*.
125. Frankel, G.; Ron, E. Z., *Escherichia Coli, a Versatile Pathogen*. Springer: 2018; Vol. 416.
126. Jang, J.; Hur, H.-G.; Sadowsky, M. J.; Byappanahalli, M. N.; Yan, T.; Ishii, S., Environmental Escherichia coli: ecology and public health implications—a review. *Journal of Applied Microbiology* **2017,** *123* (3), 570-581.
127. Blount, Z. D., The natural history of model organisms: The unexhausted potential of E. coli. *Elife* **2015,** *4*, e05826.
128. Poirel, L.; Madec, J. Y.; Lupo, A.; Schink, A. K.; Kieffer, N.; Nordmann, P.; Schwarz, S., Antimicrobial Resistance in Escherichia coli. *Microbiology spectrum* **2018,** *6* (4).
129. Ashurst, J. V.; Dawson, A., Klebsiella pneumonia. **2018**.
130. Paczosa, M. K.; Mecsas, J., Klebsiella pneumoniae: Going on the Offense with a Strong Defense. *Microbiology and Molecular Biology Reviews* **2016,** *80* (3), 629-661.
131. Mandell, G. L.; Bennett, J. E.; Dolin, R., Mandell, Douglas and Bennett's principles and pratice of infections diseases. In *Mandell, Douglas and Bennett's principles and pratice of infections diseases*, 1995; pp [2916]-[2916].
132. Classics in infectious diseases. On the blue and green coloration that appears on bandages. By Carle Gessard (1850-1925). *Reviews of infectious diseases* **1984,** *6 Suppl 3*, S775-6.
133. Lister, P. D.; Wolter, D. J.; Hanson, N. D., Antibacterial-resistant Pseudomonas aeruginosa: clinical impact and complex regulation of chromosomally encoded resistance mechanisms. *Clin Microbiol Rev* **2009,** *22* (4), 582-610.
134. Wilson, M. G.; Pandey, S., Pseudomonas Aeruginosa. **2020**.
135. Hancock, R. E. W.; Speert, D. P., Antibiotic resistance in Pseudomonas aeruginosa: mechanisms and impact on treatment. *Drug Resistance Updates* **2000,** *3* (4), 247-255.
136. Dongari-Bagtzoglou, A., Pathogenesis of mucosal biofilm infections: challenges and progress. *Expert Rev Anti-Infe* **2008,** *6* (2), 201-8.
137. Durand, G. A.; Raoult, D.; Dubourg, G., Antibiotic discovery: History, methods and perspectives. *International journal of antimicrobial agents* **2019,** *53* (4), 371-382.
138. Hubble, V. B.; Hubbard, B. A.; Minrovic, B. M.; Melander, R. J.; Melander, C., Using Small-Molecule Adjuvants to Repurpose Azithromycin for Use against Pseudomonas aeruginosa. *Acs Infect Dis* **2019,** *5* (1), 141-151.

139. French, S.; Farha, M.; Ellis, M. J.; Sameer, Z.; Cote, J. P.; Cotroneo, N.; Lister, T.; Rubio, A.; Brown, E. D., Potentiation of Antibiotics against Gram-Negative Bacteria by Polymyxin B Analogue SPR741 from Unique Perturbation of the Outer Membrane. *Acs Infect Dis* **2019**.
140. Jammal, J.; Zaknoon, F.; Kaneti, G.; Goldberg, K.; Mor, A., Sensitization of Gram-negative bacteria to rifampin and OAK combinations. *Sci Rep* **2015,** *5* (1), 9216.
141. Zhuk, D. S.; Gembitskii, P. A.; Kargin, V. A., Advances in the chemistry of polyethyleneimine (polyaziridine). *Russian Chemical Reviews* **1965,** *34* (7), 515.
142. Koper, G. J. M.; van Duijvenbode, R. C.; Stam, D. D. P. W.; Steuerle, U.; Borkovec, M., Synthesis and Protonation Behavior of Comblike Poly(ethyleneimine). *Macromolecules* **2003,** *36* (7), 2500-2507.
143. Xn, H. C.; Germany, W., Polyethylenimine Basic information.
144. Glaser, H. T.; Edzwald, J. K., Coagulation and direct filtration of humic substances with polyethylenimine. *Environ Sci Technol* **1979,** *13* (3), 299-305.
145. Dai, Z.; Gjetting, T.; Mattebjerg, M. A.; Wu, C.; Andresen, T. L., Elucidating the interplay between DNA-condensing and free polycations in gene transfection through a mechanistic study of linear and branched PEI. *Biomaterials* **2011,** *32* (33), 8626-8634.
146. Panzarasa, G.; Dübner, M.; Soliveri, G.; Edler, M.; Griesser, T., Branched poly(ethyleneimine): a versatile scaffold for patterning polymer brushes by means of remote photocatalytic lithography. *Nanotechnology* **2017,** *28* (39), 395302.
147. Chung, Y. J.; Kim, K.; Lee, B. I.; Park, C. B., Carbon Nanodot-Sensitized Modulation of Alzheimer's β-Amyloid Self-Assembly, Disassembly, and Toxicity. *Small* **2017,** *13* (34), 1700983.
148. Kim, W. J.; Chang, C.-W.; Lee, M.; Kim, S. W., Efficient siRNA delivery using water soluble lipopolymer for anti-angiogenic gene therapy. *Journal of Controlled Release* **2007,** *118* (3), 357-363.
149. Kleemann, E.; Dailey, L. A.; Abdelhady, H. G.; Gessler, T.; Schmehl, T.; Roberts, C. J.; Davies, M. C.; Seeger, W.; Kissel, T., Modified polyethylenimines as non-viral gene delivery systems for aerosol gene therapy: investigations of the complex structure and stability during air-jet and ultrasonic nebulization. *Journal of Controlled Release* **2004,** *100* (3), 437-450.
150. Thomas, K. Interactions of Metal Ions with the Polyanionic Gram-positve cell wall and the Effect of Antimicrobial Cationic Branched Polyethylenimine on Metal Binding and Cell Viability. University of Oklahoma, Norman, OK, 2014.
151. Myhre, A. E.; Aasen, A. O.; Thiemermann, C.; Wang, J. E., Peptidoglycan--an endotoxin in its own right? *Shock (Augusta, Ga.)* **2006,** *25* (3), 227-35.
152. Wiegand, C.; Bauer, M.; Hipler, U.-C.; Fischer, D., Poly (ethyleneimines) in dermal applications: biocompatibility and antimicrobial effects. *International journal of pharmaceutics* **2013,** *456* (1), 165-174.
153. Lyczak, J. B.; Cannon, C. L.; Pier, G. B., Establishment of Pseudomonas aeruginosa infection: lessons from a versatile opportunist1*Address for correspondence: Channing Laboratory, 181 Longwood Avenue, Boston, MA 02115, USA. *Microbes and Infection* **2000,** *2* (9), 1051-1060.
154. Branski, L. K.; Al-Mousawi, A.; Rivero, H.; Jeschke, M. G.; Sanford, A. P.; Herndon, D. N., Emerging infections in burns. *Surg Infect (Larchmt)* **2009,** *10* (5), 389-97.
155. Davies, D., Understanding biofilm resistance to antibacterial agents. *Nat Rev Drug Discov* **2003,** *2* (2), 114-22.
156. Drenkard, E.; Ausubel, F. M., Pseudomonas biofilm formation and antibiotic resistance are linked to phenotypic variation. *Nature* **2002,** *416* (6882), 740-3.
157. Fazli, M.; Bjarnsholt, T.; Kirketerp-Moller, K.; Jorgensen, B.; Andersen, A. S.; Krogfelt, K. A.; Givskov, M.; Tolker-Nielsen, T., Nonrandom distribution of Pseudomonas aeruginosa and Staphylococcus aureus in chronic wounds. *J Clin Microbiol* **2009,** *47* (12), 4084-9.
158. Malic, S.; Hill, K. E.; Hayes, A.; Percival, S. L.; Thomas, D. W.; Williams, D. W., Detection and identification of specific bacteria in wound biofilms using peptide nucleic acid fluorescent in situ hybridization (PNA FISH). *Microbiology* **2009,** *155* (Pt 8), 2603-11.

159. Vermote, A.; Van Calenbergh, S., Small-Molecule Potentiators for Conventional Antibiotics against Staphylococcus aureus. *Acs Infect Dis* **2017,** *3* (11), 780-796.
160. (USCAST)., T. U. S. C. o. A. S. T. Breakpoint tables for interpretation of MICs and zone diameters Version 3.0. http://www.uscast.org.
161. Ceri, H.; Olson, M.; Morck, D.; Storey, D.; Read, R.; Buret, A.; Olson, B., [25] The MBEC assay system: Multiple equivalent biofilms for antibiotic and biocide susceptibility testing. In *Methods in Enzymology*, Doyle, R. J., Ed. Academic Press: 2001; Vol. 337, pp 377-385.
162. Goldstein, J., *Practical scanning electron microscopy: electron and ion microprobe analysis*. Springer Science & Business Media: 2012.
163. Ceri, H.; Olson, M.; Stremick, C.; Read, R.; Morck, D.; Buret, A., The Calgary Biofilm Device: new technology for rapid determination of antibiotic susceptibilities of bacterial biofilms. *Journal of clinical microbiology* **1999,** *37* (6), 1771-1776.
164. ATCC BAA-47 Pseudomonas aeruginosa (Schroeter) Migula. https://www.atcc.org/products/all/BAA-47.aspx.
165. Foxley, M. A.; Friedline, A. W.; Jensen, J. M.; Nimmo, S. L.; Scull, E. M.; King, J. B.; Strange, S.; Xiao, M. T.; Smith, B. E.; Thomas Iii, K. J.; Glatzhofer, D. T.; Cichewicz, R. H.; Rice, C. V., Efficacy of ampicillin against methicillin-resistant Staphylococcus aureus restored through synergy with branched poly(ethylenimine). *The Journal of antibiotics* **2016,** *69* (12), 871-878.
166. Lam, A. K.; Panlilio, H.; Pusavat, J.; Wouters, C. L.; Moen, E. L.; Rice, C. V., Overcoming Multidrug Resistance and Biofilms of Pseudomonas aeruginosa with a Single Dual-Function Potentiator of β-Lactams. *ACS Infectious Diseases* **2020,** *6* (5), 1085-1097.
167. Kojima, S.; Nikaido, H., Permeation rates of penicillins indicate that Escherichia coli porins function principally as nonspecific channels. *Proc Natl Acad Sci U S A* **2013,** *110* (28), E2629-34.
168. Zgurskaya, H. I.; Lopez, C. A.; Gnanakaran, S., Permeability Barrier of Gram-Negative Cell Envelopes and Approaches To Bypass It. *Acs Infect Dis* **2015,** *1* (11), 512-522.
169. Nascimento, A., Jr.; Pontes, F. J.; Lins, R. D.; Soares, T. A., Hydration, ionic valence and cross-linking propensities of cations determine the stability of lipopolysaccharide (LPS) membranes. *Chem Commun (Camb)* **2014,** *50* (2), 231-3.
170. Srimal, S.; Surolia, N.; Balasubramanian, S.; Surolia, A., Titration calorimetric studies to elucidate the specificity of the interactions of polymyxin B with lipopolysaccharides and lipid A. *Biochemical journal* **1996,** *315* (2), 679-686.
171. Jo, S.; Wu, E. L.; Stuhlsatz, D.; Klauda, J. B.; MacKerell, A. D.; Widmalm, G.; Im, W., Lipopolysaccharide Membrane Building and Simulation. In *Glycoinformatics*, Lütteke, T.; Frank, M., Eds. Springer New York: New York, NY, 2015; pp 391-406.
172. Dias, R. P.; Lin, L.; Soares, T. A.; Alexov, E., Modeling the electrostatic potential of asymmetric lipopolysaccharide membranes: the MEMPOT algorithm implemented in DelPhi. *J Comput Chem* **2014,** *35* (19), 1418-1429.
173. Knirel, Y. A.; Bystrova, O. V.; Kocharova, N. A.; Zahringer, U.; Pier, G. B., Conserved and variable structural features in the lipopolysaccharide of Pseudomonas aeruginosa. *J Endotoxin Res* **2006,** *12* (6), 324-36.
174. Barkleit, A.; Moll, H.; Bernhard, G., Interaction of uranium(VI) with lipopolysaccharide. *Dalton Trans* **2008,** (21), 2879-86.
175. Krishnamoorthy, G.; Leus, I. V.; Weeks, J. W.; Wolloscheck, D.; Rybenkov, V. V.; Zgurskaya, H. I., Synergy between Active Efflux and Outer Membrane Diffusion Defines Rules of Antibiotic Permeation into Gram-Negative Bacteria. *MBio* **2017,** *8* (5).
176. Rampersad, S. N., Multiple Applications of Alamar Blue as an Indicator of Metabolic Function and Cellular Health in Cell Viability Bioassays. *Sensors-Basel* **2012,** *12* (9), 12347-12360.
177. Foxley, M. A.; Wright, S. N.; Lam, A. K.; Friedline, A. W.; Strange, S. J.; Xiao, M. T.; Moen, E. L.; Rice, C. V., Targeting Wall Teichoic Acid in Situ with Branched Polyethylenimine Potentiates beta-Lactam Efficacy against MRSA. *ACS Med. Chem. Let.* **2017,** *8* (10), 1083-1088.

178. Westfall, D. A.; Krishnamoorthy, G.; Wolloscheck, D.; Sarkar, R.; Zgurskaya, H. I.; Rybenkov, V. V., Bifurcation kinetics of drug uptake by Gram-negative bacteria. *PLoS One* **2017,** *12* (9), e0184671.
179. Clifton, L. A.; Ciesielski, F.; Skoda, M. W.; Paracini, N.; Holt, S. A.; Lakey, J. H., The Effect of Lipopolysaccharide Core Oligosaccharide Size on the Electrostatic Binding of Antimicrobial Proteins to Models of the Gram Negative Bacterial Outer Membrane. *Langmuir* **2016,** *32* (14), 3485-94.
180. Hancock, R. E.; Farmer, S. W.; Li, Z. S.; Poole, K., Interaction of aminoglycosides with the outer membranes and purified lipopolysaccharide and OmpF porin of Escherichia coli. *Antimicrob Agents Chemother* **1991,** *35* (7), 1309-14.
181. Gill, E. E.; Franco, O. L.; Hancock, R. E., Antibiotic adjuvants: diverse strategies for controlling drug-resistant pathogens. *Chem Biol Drug Des* **2015,** *85* (1), 56-78.
182. Trimble, M. J.; Mlynarcik, P.; Kolar, M.; Hancock, R. E., Polymyxin: Alternative Mechanisms of Action and Resistance. *Cold Spring Harb Perspect Med* **2016,** *6* (10).
183. Humphries, R. M.; Ambler, J.; Mitchell, S. L.; Castanheira, M.; Dingle, T.; Hindler, J. A.; Koeth, L.; Sei, K.; Development, C. M.; Standardization Working Group of the Subcommittee on Antimicrobial Susceptibility, T., CLSI Methods Development and Standardization Working Group Best Practices for Evaluation of Antimicrobial Susceptibility Tests. *J Clin Microbiol* **2018,** *56* (4).
184. Helander, I. M.; Latva-Kala, K.; Lounatmaa, K., Permeabilizing action of polyethyleneimine on Salmonella typhimurium involves disruption of the outer membrane and interactions with lipopolysaccharide. *Microbiol-Uk* **1998,** *144*, 385-390.
185. Loh, B.; Grant, C.; Hancock, R., Use of the fluorescent probe 1-N-phenylnaphthylamine to study the interactions of aminoglycoside antibiotics with the outer membrane of Pseudomonas aeruginosa. *Antimicrob Agents Chemother* **1984,** *26* (4), 546-551.
186. Hancock, R. E. W.; Wong, P. G. W., Compounds Which Increase the Permeability of the Pseudomonas-Aeruginosa Outer-Membrane. *Antimicrob Agents Chemother* **1984,** *26* (1), 48-52.
187. Lutkenhaus, J.; Pichoff, S.; Du, S., Bacterial cytokinesis: From Z ring to divisome. *Cytoskeleton* **2012,** *69* (10), 778-90.
188. de Boer, P. A., Advances in understanding E. coli cell fission. *Curr Opin Microbiol* **2010,** *13* (6), 730-7.
189. Lavery, L. A.; Armstrong, D. G.; Murdoch, D. P.; Peters, E. J.; Lipsky, B. A., Validation of the Infectious Diseases Society of America's diabetic foot infection classification system. *Clin Infect Dis* **2007,** *44* (4), 562-5.
190. Swanson, T.; Wolcott, R. D.; Wallis, H.; Woodmansey, E. J., Understanding biofilm in practice: a global survey of health professionals. *J Wound Care* **2017,** *26* (8), 426-440.
191. Stevens, D. L.; Bisno, A. L.; Chambers, H. F.; Dellinger, E. P.; Goldstein, E. J.; Gorbach, S. L.; Hirschmann, J. V.; Kaplan, S. L.; Montoya, J. G.; Wade, J. C., Practice guidelines for the diagnosis and management of skin and soft tissue infections: 2014 update by the infectious diseases society of America. *Clin Infect Dis* **2014,** *59* (2), 147-59.
192. Jennings, L. K.; Storek, K. M.; Ledvina, H. E.; Coulon, C.; Marmont, L. S.; Sadovskaya, I.; Secor, P. R.; Tseng, B. S.; Scian, M.; Filloux, A.; Wozniak, D. J.; Howell, P. L.; Parsek, M. R., Pel is a cationic exopolysaccharide that cross-links extracellular DNA in the Pseudomonas aeruginosa biofilm matrix. *Proc Natl Acad Sci U S A* **2015,** *112* (36), 11353-8.
193. Holland, L. M.; Conlon, B.; O'Gara, J. P., Mutation of tagO reveals an essential role for wall teichoic acids in Staphylococcus epidermidis biofilm development. *Microbiology* **2011,** *157* (Pt 2), 408-18.
194. Joo, H. S.; Otto, M., Mechanisms of resistance to antimicrobial peptides in staphylococci. *Biochim Biophys Acta* **2015,** *1848* (11 Pt B), 3055-61.
195. Krismer, B.; Weidenmaier, C.; Zipperer, A.; Peschel, A., The commensal lifestyle of Staphylococcus aureus and its interactions with the nasal microbiota. *Nat Rev Microbiol* **2017,** *15* (11), 675-687.

196. Sadovskaya, I.; Vinogradov, E.; Li, J.; Jabbouri, S., Structural elucidation of the extracellular and cell-wall teichoic acids of Staphylococcus epidermidis RP62A, a reference biofilm-positive strain. *Carbohydr Res* **2004,** *339* (8), 1467-73.
197. Vinogradov, E.; Sadovskaya, I.; Li, J.; Jabbouri, S., Structural elucidation of the extracellular and cell-wall teichoic acids of Staphylococcus aureus MN8m, a biofilm forming strain. *Carbohydr Res* **2006,** *341* (6), 738-43.
198. Wagstaff, J. L.; Sadovskaya, I.; Vinogradov, E.; Jabbouri, S.; Howard, M. J., Poly-N-acetylglucosamine and poly(glycerol phosphate) teichoic acid identification from staphylococcal biofilm extracts using excitation sculptured TOCSY NMR. *Mol Biosyst* **2008,** *4* (2), 170-4.
199. Arciola, C. R.; Campoccia, D.; Speziale, P.; Montanaro, L.; Costerton, J. W., Biofilm formation in Staphylococcus implant infections. A review of molecular mechanisms and implications for biofilm-resistant materials. *Biomaterials* **2012,** *33* (26), 5967-82.
200. Bucher, T.; Oppenheimer-Shaanan, Y.; Savidor, A.; Bloom-Ackermann, Z.; Kolodkin-Gal, I., Disturbance of the bacterial cell wall specifically interferes with biofilm formation. *Environ Microbiol Rep* **2015,** *7* (6), 990-1004.
201. Laverty, G.; Gorman, S. P.; Gilmore, B. F., Biomolecular mechanisms of staphylococcal biofilm formation. *Future Microbiol* **2013,** *8* (4), 509-24.
202. O'Neill, E.; Pozzi, C.; Houston, P.; Smyth, D.; Humphreys, H.; Robinson, D. A.; O'Gara, J. P., Association between methicillin susceptibility and biofilm regulation in Staphylococcus aureus isolates from device-related infections. *J Clin Microbiol* **2007,** *45* (5), 1379-88.
203. Gibney, K. A.; Sovadinova, I.; Lopez, A. I.; Urban, M.; Ridgway, Z.; Caputo, G. A.; Kuroda, K., Poly(ethylene imine)s as antimicrobial agents with selective activity. *Macromol Biosci* **2012,** *12* (9), 1279-89.
204. Khalil, H.; Chen, T.; Riffon, R.; Wang, R.; Wang, Z., Synergy between polyethylenimine and different families of antibiotics against a resistant clinical isolate of Pseudomonas aeruginosa. *Antimicrob Agents Chemother* **2008,** *52* (5), 1635-1641.
205. Helander, I. M.; Mattila-Sandholm, T., Fluorometric assessment of Gram-negative bacterial permeabilization. *Journal of Applied Microbiology* **2000,** *88* (2), 213-219.
206. Fleeman, R. M.; Debevec, G.; Antonen, K.; Adams, J. L.; Santos, R. G.; Welmaker, G. S.; Houghten, R. A.; Giulianotti, M. A.; Shaw, L. N., Identification of a Novel Polyamine Scaffold With Potent Efflux Pump Inhibition Activity Toward Multi-Drug Resistant Bacterial Pathogens. *Front Microbiol* **2018,** *9*, 1301.
207. Wang, B.; Pachaiyappan, B.; Gruber, J. D.; Schmidt, M. G.; Zhang, Y. M.; Woster, P. M., Antibacterial Diamines Targeting Bacterial Membranes. *J Med Chem* **2016,** *59* (7), 3140-51.
208. Kwon, D. H.; Lu, C. D., Polyamine effects on antibiotic susceptibility in bacteria. *Antimicrob Agents Chemother* **2007,** *51* (6), 2070-7.
209. Costerton, J. W.; Stewart, P. S.; Greenberg, E. P., Bacterial biofilms: a common cause of persistent infections. *Science* **1999,** *284* (5418), 1318-22.
210. Lim, H. W.; Collins, S. A. B.; Resneck, J. S., Jr.; Bolognia, J. L.; Hodge, J. A.; Rohrer, T. A.; Van Beek, M. J.; Margolis, D. J.; Sober, A. J.; Weinstock, M. A.; Nerenz, D. R.; Smith Begolka, W.; Moyano, J. V., The burden of skin disease in the United States. *J Am Acad Dermatol* **2017,** *76* (5), 958-972 e2.
211. Jones, R. E.; Foster, D. S.; Longaker, M. T., Management of chronic wounds—2018. *Jama* **2018,** *320* (14), 1481-1482.
212. Sen, C. K.; Gordillo, G. M.; Roy, S.; Kirsner, R.; Lambert, L.; Hunt, T. K.; Gottrup, F.; Gurtner, G. C.; Longaker, M. T., Human skin wounds: a major and snowballing threat to public health and the economy. *Wound repair and regeneration* **2009,** *17* (6), 763-771.
213. Omar, A.; Wright, J. B.; Schultz, G.; Burrell, R.; Nadworny, P., Microbial biofilms and chronic wounds. *Microorganisms* **2017,** *5* (1), 9.
214. Wolcott, R., Disrupting the biofilm matrix improves wound healing outcomes. *Journal of wound care* **2015,** *24* (8), 366-371.

215. Schultz, G.; Bjarnsholt, T.; James, G. A.; Leaper, D. J.; McBain, A. J.; Malone, M.; Stoodley, P.; Swanson, T.; Tachi, M.; Wolcott, R. D., Consensus guidelines for the identification and treatment of biofilms in chronic nonhealing wounds. *Wound Repair and Regeneration* **2017,** *25* (5), 744-757.
216. Zhao, G.; Usui, M. L.; Lippman, S. I.; James, G. A.; Stewart, P. S.; Fleckman, P.; Olerud, J. E., Biofilms and inflammation in chronic wounds. *Advances in wound care* **2013,** *2* (7), 389-399.
217. Frykberg, R. G.; Banks, J., Challenges in the treatment of chronic wounds. *Advances in wound care* **2015,** *4* (9), 560-582.
218. Nussbaum, S. R.; Carter, M. J.; Fife, C. E.; DaVanzo, J.; Haught, R.; Nusgart, M.; Cartwright, D., An Economic Evaluation of the Impact, Cost, and Medicare Policy Implications of Chronic Nonhealing Wounds. *Value in Health* **2018,** *21* (1), 27-32.
219. Bhargava, A.; Hayakawa, K.; Silverman, E.; Haider, S.; Alluri, K. C.; Datla, S.; Diviti, S.; Kuchipudi, V.; Muppavarapu, K. S.; Lephart, P. R.; Marchaim, D.; Kaye, K. S., Risk factors for colonization due to carbapenem-resistant Enterobacteriaceae among patients exposed to long-term acute care and acute care facilities. *Infect Control Hosp Epidemiol* **2014,** *35* (4), 398-405.
220. Marchaim, D.; Chopra, T.; Bogan, C.; Bheemreddy, S.; Sengstock, D.; Jagarlamudi, R.; Malani, A.; Lemanek, L.; Moshos, J.; Lephart, P. R.; Ku, K.; Hasan, A.; Lee, J.; Khandker, N.; Blunden, C.; Geffert, S. F.; Moody, M.; Hiro, R.; Wang, Y.; Ahmad, F.; Mohammadi, T.; Faruque, O.; Patel, D.; Pogue, J. M.; Hayakawa, K.; Dhar, S.; Kaye, K. S., The burden of multidrug-resistant organisms on tertiary hospitals posed by patients with recent stays in long-term acute care facilities. *Am J Infect Control* **2012,** *40* (8), 760-5.
221. Henig, O.; Cober, E.; Richter, S. S.; Perez, F.; Salata, R. A.; Kalayjian, R. C.; Watkins, R. R.; Marshall, S.; Rudin, S. D.; Domitrovic, T. N.; Hujer, A. M.; Hujer, K. M.; Doi, Y.; Evans, S.; Fowler, V. G., Jr.; Bonomo, R. A.; van Duin, D.; Kaye, K. S.; Antibacterial Resistance Leadership, G., A Prospective Observational Study of the Epidemiology, Management, and Outcomes of Skin and Soft Tissue Infections Due to Carbapenem-Resistant Enterobacteriaceae. *Open Forum Infect Dis* **2017,** *4* (3), ofx157.
222. Pseudomonas aeruginosa Infection | HAI | CDC. https://www.cdc.gov/hai/organisms/pseudomonas.html (accessed December 23, 2020).
223. Ruffin, M.; Brochiero, E., Repair Process Impairment by Pseudomonas aeruginosa in Epithelial Tissues: Major Features and Potential Therapeutic Avenues. *Frontiers in Cellular and Infection Microbiology* **2019,** *9* (182).
224. Panlilio, H.; Rice, C. V., The role of extracellular DNA in the formation, architecture, stability, and treatment of bacterial biofilms. *Biotechnol Bioeng* **2021**.
225. Lam, A. K.; Hill, M. A.; Moen, E. L.; Pusavat, J.; Wouters, C. L.; Rice, C. V., Cationic Branched Polyethylenimine (BPEI) Disables Antibiotic Resistance in Methicillin-Resistant Staphylococcus epidermidis (MRSE). *ChemMedChem* **2018,** *13* (20), 2240-2248.
226. Lam, A. K.; Wouters, C. L.; Moen, E. L.; Pusavat, J.; Rice, C. V., Antibiofilm Synergy of β-Lactams and Branched Polyethylenimine against Methicillin-Resistant Staphylococcus epidermidis. *Biomacromolecules* **2019,** *20* (10), 3778-3785.
227. Panlilio, H.; Lam, A. K.; Heydarian, N.; Haight, T.; Wouters, C. L.; Moen, E. L.; Rice, C. V., Dual-Function Potentiation by PEG-BPEI Restores Activity of Carbapenems and Penicillins against Carbapenem-Resistant Enterobacteriaceae. *ACS Infectious Diseases* **2021**.
228. Lam, A. K.; Moen, E. L.; Pusavat, J.; Wouters, C. L.; Panlilio, H.; Ferrell, M. J.; Houck, M. B.; Glatzhofer, D. T.; Rice, C. V., PEGylation of Polyethylenimine Lowers Acute Toxicity while Retaining Anti-Biofilm and β-Lactam Potentiation Properties against Antibiotic-Resistant Pathogens. *ACS Omega* **2020,** *5* (40), 26262-26270.
229. Merritt, J. H.; Kadouri, D. E.; O'Toole, G. A., Growing and analyzing static biofilms. *Curr Protoc Microbiol* **2005,** *Chapter 1*, Unit-1B.1.
230. Stoffel, J. J.; Kohler Riedi, P. L.; Hadj Romdhane, B., A multimodel regime for evaluating effectiveness of antimicrobial wound care products in microbial biofilms. *Wound repair and regeneration : official publication of the Wound Healing Society [and] the European Tissue Repair Society* **2020,** *28* (4), 438-447.

231. Feoktistova, M.; Geserick, P.; Leverkus, M., Crystal violet assay for determining viability of cultured cells. *Cold Spring Harbor Protocols* **2016,** *2016* (4), pdb. prot087379.
232. Silfies, J.; Schwartz, S.; Davidson, M., The diffraction barrier in optical microscopy. *Nikon Inc.,[Online]. Available: https://www. microscopyu. com/articles/superresolution/diffractionbarrier. html.[Accessed 28. 10. 2015]* **2019**.
233. Wang, J.; Woo, M.; Yan, C., Spot plating assay for the determination of survival and plating efficiency of Escherichia coli in sub-MIC levels of antibiotics. *JEMI Methods* **2017,** *1*, 26-29.
234. Mann, E. E.; Wozniak, D. J., Pseudomonas biofilm matrix composition and niche biology. *FEMS Microbiology Reviews* **2012,** *36* (4), 893-916.
235. Lam, A. K.; Panlilio, H.; Pusavat, J.; Wouters, C. L.; Moen, E. L.; Neel, A. J.; Rice, C. V., Low-Molecular-Weight Branched Polyethylenimine Potentiates Ampicillin against MRSA Biofilms. *ACS Medicinal Chemistry Letters* **2020,** *11* (4), 473-478.
236. Franklin, M. J.; Nivens, D. E.; Weadge, J. T.; Howell, P. L., Biosynthesis of the Pseudomonas aeruginosa Extracellular Polysaccharides, Alginate, Pel, and Psl. *Front Microbiol* **2011,** *2*, 167-167.
237. Colvin, K. M.; Gordon, V. D.; Murakami, K.; Borlee, B. R.; Wozniak, D. J.; Wong, G. C. L.; Parsek, M. R., The pel polysaccharide can serve a structural and protective role in the biofilm matrix of Pseudomonas aeruginosa. *PLoS Pathog* **2011,** *7* (1), e1001264-e1001264.
238. Billings, N.; Millan, M.; Caldara, M.; Rusconi, R.; Tarasova, Y.; Stocker, R.; Ribbeck, K., The extracellular matrix Component Psl provides fast-acting antibiotic defense in Pseudomonas aeruginosa biofilms. *PLoS Pathog* **2013,** *9* (8), e1003526-e1003526.
239. Haas, D.; Holloway, B. W.; Schamböck, A.; Leisinger, T., The genetic organization of arginine biosynthesis in Pseudomonas aeruginosa. *Molecular & general genetics : MGG* **1977,** *154* (1), 7-22.
240. HOLLOWAY, B. W., Genetic Recombination in Pseudomonas aeruginosa. *Microbiology* **1955,** *13* (3), 572-581.
241. Cao, H.; Lai, Y.; Bougouffa, S.; Xu, Z.; Yan, A., Comparative genome and transcriptome analysis reveals distinctive surface characteristics and unique physiological potentials of Pseudomonas aeruginosa ATCC 27853. *BMC genomics* **2017,** *18* (1), 1-17.
242. Rumbaugh, K. P.; Sauer, K., Biofilm dispersion. *Nature Reviews Microbiology* **2020,** *18* (10), 571-586.
243. Lam, A. K.; Panlilio, H.; Pusavat, J.; Wouters, C. L.; Moen, E. L.; Rice, C. V., Overcoming Multidrug Resistance and Biofilms of Pseudomonas aeruginosa with a Single Dual-Function Potentiator of beta-Lactams. *ACS Infect Dis* **2020,** *6* (5), 1085-1097.
244. Lam, A. K.; Panlilio, H.; Pusavat, J.; Wouters, C. L.; Moen, E. L.; Neel, A. J.; Rice, C. V., Low-Molecular-Weight Branched Polyethylenimine Potentiates Ampicillin against MRSA Biofilms. *ACS Med. Chem. Let.* **2020,** *11* (4), 473-478.
245. Lam, A. K.; Moen, E. L.; Pusavat, J.; Wouters, C. L.; Panlilio, H.; Ferrell, M. J.; Houck, M. B.; Glatzhofer, D. T.; Rice, C. V., PEGylation of Polyethylenimine Lowers Acute Toxicity while Retaining Anti-Biofilm and beta-Lactam Potentiation Properties against Antibiotic-Resistant Pathogens. *ACS Omega* **2020,** *5* (40), 26262-26270.
246. Dabiri, G.; Damstetter, E.; Phillips, T., Choosing a Wound Dressing Based on Common Wound Characteristics. *Adv Wound Care (New Rochelle)* **2016,** *5* (1), 32-41.
247. Bernier, S. P.; Ha, D.-G.; Khan, W.; Merritt, J. H.; O'Toole, G. A., Modulation of Pseudomonas aeruginosa surface-associated group behaviors by individual amino acids through c-di-GMP signaling. *Res Microbiol* **2011,** *162* (7), 680-688.
248. O'Toole, G. A., Microtiter dish biofilm formation assay. *J Vis Exp* **2011,** (47), 2437.
249. Baker, A.; Saltik, M.; Lehrmann, H.; Killisch, I.; Mautner, V.; Lamm, G.; Christofori, G.; Cotten, M., Polyethylenimine (PEI) is a simple, inexpensive and effective reagent for condensing and linking plasmid DNA to adenovirus for gene delivery. *Gene therapy* **1997,** *4* (8), 773-782.
250. Utsuno, K.; Uludağ, H., Thermodynamics of Polyethylenimine-DNA Binding and DNA Condensation. *Biophysical Journal* **2010,** *99* (1), 201-207.

251. Rozenbaum, R. T.; Andrén, O. C. J.; van der Mei, H. C.; Woudstra, W.; Busscher, H. J.; Malkoch, M.; Sharma, P. K., Penetration and Accumulation of Dendrons with Different Peripheral Composition in Pseudomonas aeruginosa Biofilms. *Nano Letters* **2019,** *19* (7), 4327-4333.
252. Richards, L. A. Spatial heterogeneity in Pseudomonas aeruginosa biofilms and how it affects antibiotic tolerance. Montana State University-Bozeman, College of Engineering, 2006.
253. Rooney, L. M.; Amos, W. B.; Hoskisson, P. A.; McConnell, G., Intra-colony channels in E. coli function as a nutrient uptake system. *The ISME Journal* **2020,** *14* (10), 2461-2473.
254. Gloag, E. S.; Turnbull, L.; Huang, A.; Vallotton, P.; Wang, H.; Nolan, L. M.; Mililli, L.; Hunt, C.; Lu, J.; Osvath, S. R.; Monahan, L. G.; Cavaliere, R.; Charles, I. G.; Wand, M. P.; Gee, M. L.; Prabhakar, R.; Whitchurch, C. B., Self-organization of bacterial biofilms is facilitated by extracellular DNA. *P Natl Acad Sci USA* **2013,** *110* (28), 11541-6.
255. Cavaliere, R.; Ball, J. L.; Turnbull, L.; Whitchurch, C. B., The biofilm matrix destabilizers, EDTA and DNaseI, enhance the susceptibility of nontypeable Hemophilus influenzae biofilms to treatment with ampicillin and ciprofloxacin. *Microbiologyopen* **2014,** *3* (4), 557-67.
256. Musken, M.; Pawar, V.; Schwebs, T.; Bahre, H.; Felgner, S.; Weiss, S.; Haussler, S., Breaking the Vicious Cycle of Antibiotic Killing and Regrowth of Biofilm-Residing Pseudomonas aeruginosa. *Antimicrob Agents Ch* **2018,** *62* (12).
257. Jones, R. E.; Foster, D. S.; Longaker, M. T., Management of Chronic Wounds-2018. *JAMA* **2018,** *320* (14), 1481-1482.
258. Gurtner, G. C.; Werner, S.; Barrandon, Y.; Longaker, M. T., Wound repair and regeneration. *Nature* **2008,** *453* (7193), 314-21.
259. Zhao, G.; Usui, M. L.; Lippman, S. I.; James, G. A.; Stewart, P. S.; Fleckman, P.; Olerud, J. E., Biofilms and Inflammation in Chronic Wounds. *Adv Wound Care (New Rochelle)* **2013,** *2* (7), 389-399.
260. Schultz, G.; Bjarnsholt, T.; James, G. A.; Leaper, D. J.; McBain, A. J.; Malone, M.; Stoodley, P.; Swanson, T.; Tachi, M.; Wolcott, R. D.; Global Wound Biofilm Expert, P., Consensus guidelines for the identification and treatment of biofilms in chronic nonhealing wounds. *Wound Repair Regen* **2017,** *25* (5), 744-757.
261. Tacconelli, E.; Carrara, E.; Savoldi, A.; Harbarth, S.; Mendelson, M.; Monnet, D. L.; Pulcini, C.; Kahlmeter, G.; Kluytmans, J.; Carmeli, Y.; Ouellette, M.; Outterson, K.; Patel, J.; Cavaleri, M.; Cox, E. M.; Houchens, C. R.; Grayson, M. L.; Hansen, P.; Singh, N.; Theuretzbacher, U.; Magrini, N.; Aboderin, A. O.; Al-Abri, S. S.; Awang Jalil, N.; Benzonana, N.; Bhattacharya, S.; Brink, A. J.; Burkert, F. R.; Cars, O.; Cornaglia, G.; Dyar, O. J.; Friedrich, A. W.; Gales, A. C.; Gandra, S.; Giske, C. G.; Goff, D. A.; Goossens, H.; Gottlieb, T.; Guzman Blanco, M.; Hryniewicz, W.; Kattula, D.; Jinks, T.; Kanj, S. S.; Kerr, L.; Kieny, M.-P.; Kim, Y. S.; Kozlov, R. S.; Labarca, J.; Laxminarayan, R.; Leder, K.; Leibovici, L.; Levy-Hara, G.; Littman, J.; Malhotra-Kumar, S.; Manchanda, V.; Moja, L.; Ndoye, B.; Pan, A.; Paterson, D. L.; Paul, M.; Qiu, H.; Ramon-Pardo, P.; Rodríguez-Baño, J.; Sanguinetti, M.; Sengupta, S.; Sharland, M.; Si-Mehand, M.; Silver, L. L.; Song, W.; Steinbakk, M.; Thomsen, J.; Thwaites, G. E.; van der Meer, J. W. M.; Van Kinh, N.; Vega, S.; Villegas, M. V.; Wechsler-Fördös, A.; Wertheim, H. F. L.; Wesangula, E.; Woodford, N.; Yilmaz, F. O.; Zorzet, A., Discovery, research, and development of new antibiotics: the WHO priority list of antibiotic-resistant bacteria and tuberculosis. *The Lancet Infectious Diseases* **2018,** *18* (3), 318-327.
262. CDC, Antibiotic Resistance Threats in the United States, 2019. U.S. Department of Health and Human Services. **2019**.
263. Logan, L. K.; Weinstein, R. A., The Epidemiology of Carbapenem-Resistant Enterobacteriaceae: The Impact and Evolution of a Global Menace. *J Infect Dis* **2017,** *215* (suppl_1), S28-S36.
264. Satlin, M. J.; Chen, L.; Patel, G.; Gomez-Simmonds, A.; Weston, G.; Kim, A. C.; Seo, S. K.; Rosenthal, M. E.; Sperber, S. J.; Jenkins, S. G.; Hamula, C. L.; Uhlemann, A. C.; Levi, M. H.; Fries, B. C.; Tang, Y. W.; Juretschko, S.; Rojtman, A. D.; Hong, T.; Mathema, B.; Jacobs, M. R.; Walsh, T. J.; Bonomo, R. A.; Kreiswirth, B. N., Multicenter Clinical and Molecular Epidemiological Analysis of Bacteremia Due to Carbapenem-Resistant Enterobacteriaceae (CRE) in the CRE Epicenter of the United States. *Antimicrob Agents Chemother* **2017,** *61* (4).

265. Tamma, P. D.; Aitken, S. L.; Bonomo, R. A.; Mathers, A. J.; van Duin, D.; J., C. C. Infectious Diseases Society of America Antimicrobial Resistant Treatment Guidance: Gram-Negative Bacterial Infections 2020. https://www.idsociety.org/practice-guideline/amr-guidance/.
266. Conlan, S.; Thomas, P. J.; Deming, C.; Park, M.; Lau, A. F.; Dekker, J. P.; Snitkin, E. S.; Clark, T. A.; Luong, K.; Song, Y.; Tsai, Y. C.; Boitano, M.; Dayal, J.; Brooks, S. Y.; Schmidt, B.; Young, A. C.; Thomas, J. W.; Bouffard, G. G.; Blakesley, R. W.; Program, N. C. S.; Mullikin, J. C.; Korlach, J.; Henderson, D. K.; Frank, K. M.; Palmore, T. N.; Segre, J. A., Single-molecule sequencing to track plasmid diversity of hospital-associated carbapenemase-producing Enterobacteriaceae. *Sci Transl Med* **2014,** *6* (254), 254ra126.
267. Potter, R. F.; D'Souza, A. W.; Dantas, G., The rapid spread of carbapenem-resistant Enterobacteriaceae. *Drug Resist Updat* **2016,** *29*, 30-46.
268. Chavda, K. D.; Chen, L.; Jacobs, M. R.; Bonomo, R. A.; Kreiswirth, B. N., Molecular Diversity and Plasmid Analysis of KPC-Producing Escherichia coli. *Antimicrob Agents Chemother* **2016,** *60* (7), 4073-81.
269. Sheu, C. C.; Chang, Y. T.; Lin, S. Y.; Chen, Y. H.; Hsueh, P. R., Infections Caused by Carbapenem-Resistant Enterobacteriaceae: An Update on Therapeutic Options. *Front Microbiol* **2019,** *10*, 80.
270. Paterson, D. L.; Isler, B.; Stewart, A., New treatment options for multiresistant gram negatives. *Curr Opin Infect Dis* **2020,** *33* (2), 214-223.
271. Sorli, L.; Luque, S.; Li, J.; Campillo, N.; Danes, M.; Montero, M.; Segura, C.; Grau, S.; Horcajada, J. P., Colistin for the treatment of urinary tract infections caused by extremely drug-resistant Pseudomonas aeruginosa: Dose is critical. *J Infect* **2019,** *79* (3), 253-261.
272. van Duin, D.; Perez, F.; Rudin, S. D.; Cober, E.; Hanrahan, J.; Ziegler, J.; Webber, R.; Fox, J.; Mason, P.; Richter, S. S.; Cline, M.; Hall, G. S.; Kaye, K. S.; Jacobs, M. R.; Kalayjian, R. C.; Salata, R. A.; Segre, J. A.; Conlan, S.; Evans, S.; Fowler, V. G., Jr.; Bonomo, R. A., Surveillance of carbapenem-resistant Klebsiella pneumoniae: tracking molecular epidemiology and outcomes through a regional network. *Antimicrob Agents Chemother* **2014,** *58* (7), 4035-41.
273. Gupta, V.; Ye, G.; Olesky, M.; Lawrence, K.; Murray, J.; Yu, K., Trends in resistant Enterobacteriaceae and Acinetobacter species in hospitalized patients in the United States: 2013-2017. *BMC Infect Dis* **2019,** *19* (1), 742.
274. McCann, E.; Srinivasan, A.; DeRyke, C. A.; Ye, G.; DePestel, D. D.; Murray, J.; Gupta, V., Carbapenem-Nonsusceptible Gram-Negative Pathogens in ICU and Non-ICU Settings in US Hospitals in 2017: A Multicenter Study. *Open Forum Infect Dis* **2018,** *5* (10), ofy241.
275. Jabbour, J. F.; Sharara, S. L.; Kanj, S. S., Treatment of multidrug-resistant Gram-negative skin and soft tissue infections. *Curr Opin Infect Dis* **2020,** *33* (2), 146-154.
276. Sen, C. K.; Gordillo, G. M.; Roy, S.; Kirsner, R.; Lambert, L.; Hunt, T. K.; Gottrup, F.; Gurtner, G. C.; Longaker, M. T., Human skin wounds: a major and snowballing threat to public health and the economy. *Wound Repair Regen* **2009,** *17* (6), 763-71.
277. Omar, A.; Wright, J. B.; Schultz, G.; Burrell, R.; Nadworny, P., Microbial Biofilms and Chronic Wounds. *Microorganisms* **2017,** *5* (1).
278. Bowler, P. G., Antibiotic resistance and biofilm tolerance: a combined threat in the treatment of chronic infections. *J Wound Care* **2018,** *27* (5), 273-277.
279. Gjodsbol, K.; Christensen, J. J.; Karlsmark, T.; Jorgensen, B.; Klein, B. M.; Krogfelt, K. A., Multiple bacterial species reside in chronic wounds: a longitudinal study. *Int Wound J* **2006,** *3* (3), 225-31.
280. Frykberg, R. G.; Banks, J., Challenges in the Treatment of Chronic Wounds. *Adv Wound Care (New Rochelle)* **2015,** *4* (9), 560-582.
281. Hackel, M. A.; Tsuji, M.; Yamano, Y.; Echols, R.; Karlowsky, J. A.; Sahm, D. F., In Vitro Activity of the Siderophore Cephalosporin, Cefiderocol, against a Recent Collection of Clinically Relevant Gram-Negative Bacilli from North America and Europe, Including Carbapenem-Nonsusceptible Isolates (SIDERO-WT-2014 Study). *Antimicrob Agents Chemother* **2017,** *61* (9).

282. Hackel, M. A.; Tsuji, M.; Yamano, Y.; Echols, R.; Karlowsky, J. A.; Sahm, D. F., In Vitro Activity of the Siderophore Cephalosporin, Cefiderocol, against Carbapenem-Nonsusceptible and Multidrug-Resistant Isolates of Gram-Negative Bacilli Collected Worldwide in 2014 to 2016. *Antimicrob Agents Chemother* **2018,** *62* (2).
283. Hudson, C. M.; Bent, Z. W.; Meagher, R. J.; Williams, K. P., Resistance determinants and mobile genetic elements of an NDM-1-encoding Klebsiella pneumoniae strain. *PLoS One* **2014,** *9* (6), e99209.
284. Sun, Y.; Liao, X.; Huang, Z.; Xie, Y.; Liu, Y.; Ma, C.; Jiang, B.; Zhang, L.; Yan, Y.; Li, G.; Cheng, X.; Yin, Q.; Ding, C. Z.; Shen, L.; Li, J.; Chen, S.; Wei, Y.; Wang, Z.; Wei, X., Therapeutic effect and mechanisms of the novel monosulfactam 0073. *Antimicrob Agents Chemother* **2020**.
285. Lam, A. K.; Panlilio, H.; Pusavat, J.; Wouters, C. L.; Moen, E. L.; Brennan, R. E.; Rice, C. V., Expanding the Spectrum of Antibiotics Capable of Killing Multidrug-Resistant Staphylococcus aureus and Pseudomonas aeruginosa. *ChemMedChem* **2020,** *15* (15), 1421-1428.
286. Lam, A. K.; Moen, E. L.; Pusavat, J.; Wouters, C. L.; Panlilio, H.; Ferrell, M. J.; Houck, M. B.; Glatzhofer, D. T.; Rice, C. V., PEGylation of Polyethylenimine Lowers Acute Toxicity while Retaining Anti-Biofilm and β-Lactam Potentiation Properties against Antibiotic-Resistant Pathogens. *ACS Omega* **2020**.
287. (EUCAST)., E. C. o. A. S. T. The European Committee on Antimicrobial Susceptibility Testing. Breakpoint tables for interpretation of MICs and zone diameters. Version 10.0, 2020. http://www.eucast.org.
288. Terminology relating to methods for the determination of susceptibility of bacteria to antimicrobial agents. *Clinical Microbiology and Infection* **2000,** *6* (9), 503-508.
289. Falconer, S. B.; Reid-Yu, S. A.; King, A. M.; Gehrke, S. S.; Wang, W.; Britten, J. F.; Coombes, B. K.; Wright, G. D.; Brown, E. D., Zinc Chelation by a Small-Molecule Adjuvant Potentiates Meropenem Activity in Vivo against NDM-1-Producing Klebsiella pneumoniae. *Acs Infect Dis* **2015,** *1* (11), 533-43.
290. Schnaars, C.; Kildahl-Andersen, G.; Prandina, A.; Popal, R.; Radix, S.; Le Borgne, M.; Gjoen, T.; Andresen, A. M. S.; Heikal, A.; Okstad, O. A.; Frohlich, C.; Samuelsen, O.; Lauksund, S.; Jordheim, L. P.; Rongved, P.; Astrand, O. A. H., Synthesis and Preclinical Evaluation of TPA-Based Zinc Chelators as Metallo-beta-lactamase Inhibitors. *Acs Infect Dis* **2018,** *4* (9), 1407-1422.
291. Tehrani, K.; Bruchle, N. C.; Wade, N.; Mashayekhi, V.; Pesce, D.; van Haren, M. J.; Martin, N. I., Small Molecule Carboxylates Inhibit Metallo-beta-lactamases and Resensitize Carbapenem-Resistant Bacteria to Meropenem. *Acs Infect Dis* **2020,** *6* (6), 1366-1371.
292. Linciano, P.; Cendron, L.; Gianquinto, E.; Spyrakis, F.; Tondi, D., Ten Years with New Delhi Metallo-beta-lactamase-1 (NDM-1): From Structural Insights to Inhibitor Design. *Acs Infect Dis* **2019,** *5* (1), 9-34.
293. Prunotto, A.; Bahr, G.; Gonzalez, L. J.; Vila, A. J.; Dal Peraro, M., Molecular Bases of the Membrane Association Mechanism Potentiating Antibiotic Resistance by New Delhi Metallo-beta-lactamase 1. *Acs Infect Dis* **2020**.
294. Chen, A. Y.; Thomas, C. A.; Thomas, P. W.; Yang, K.; Cheng, Z.; Fast, W.; Crowder, M. W.; Cohen, S. M., Iminodiacetic Acid as a Novel Metal-Binding Pharmacophore for New Delhi Metallo-beta-lactamase Inhibitor Development. *ChemMedChem* **2020,** *15* (14), 1272-1282.
295. Kildahl-Andersen, G.; Schnaars, C.; Prandina, A.; Radix, S.; Le Borgne, M.; Jordheim, L. P.; Gjoen, T.; Andresen, A. M. S.; Lauksund, S.; Frohlich, C.; Samuelsen, O.; Rongved, P.; Astrand, O. A. H., Synthesis and biological evaluation of zinc chelating compounds as metallo-beta-lactamase inhibitors. *Medchemcomm* **2019,** *10* (4), 528-537.
296. Proschak, A.; Kramer, J.; Proschak, E.; Wichelhaus, T. A., Bacterial zincophore [S,S]-ethylenediamine-N,N'-disuccinic acid is an effective inhibitor of MBLs. *J Antimicrob Chemother* **2018,** *73* (2), 425-430.
297. Baker, K. R.; Jana, B.; Hansen, A. M.; Vissing, K. J.; Nielsen, H. M.; Franzyk, H.; Guardabassi, L., Repurposing azithromycin and rifampicin against Gram-negative pathogens by combination with peptide potentiators. *Int J Antimicrob Agents* **2019,** *53* (6), 868-872.

298. Bush, K., Game Changers: New beta-Lactamase Inhibitor Combinations Targeting Antibiotic Resistance in Gram-Negative Bacteria. *Acs Infect Dis* **2018,** *4* (2), 84-87.
299. Song, M.; Liu, Y.; Huang, X.; Ding, S.; Wang, Y.; Shen, J.; Zhu, K., A broad-spectrum antibiotic adjuvant reverses multidrug-resistant Gram-negative pathogens. *Nat Microbiol* **2020,** *5* (8), 1040-1050.
300. Vaara, M., Polymyxin Derivatives that Sensitize Gram-Negative Bacteria to Other Antibiotics. *Molecules* **2019,** *24* (2).
301. Lopez, C. A.; Zgurskaya, H.; Gnanakaran, S., Molecular characterization of the outer membrane of Pseudomonas aeruginosa. *Biochim Biophys Acta Biomembr* **2020,** *1862* (3), 183151.
302. Takagishi, T.; Okuda, S.; Kuroki, N.; Kozuka, H., Binding of Metal-Ions by Polyethylenimine and Its Derivatives. *J Polym Sci Pol Chem* **1985,** *23* (8), 2109-2116.
303. Paul, P.; Slayton, R. B.; Kallen, A. J.; Walters, M. S.; Jernigan, J. A., Modeling Regional Transmission and Containment of a Healthcare-associated Multidrug-resistant Organism. *Clin Infect Dis* **2020,** *70* (3), 388-394.
304. Doi, Y.; Bonomo, R. A.; Hooper, D. C.; Kaye, K. S.; Johnson, J. R.; Clancy, C. J.; Thaden, J. T.; Stryjewski, M. E.; van Duin, D.; Gram-Negative Committee of the Antibacterial Resistance Leadership Group, a., Gram-Negative Bacterial Infections: Research Priorities, Accomplishments, and Future Directions of the Antibacterial Resistance Leadership Group. *Clin Infect Dis* **2017,** *64* (suppl_1), S30-S35.
305. Barbier, F.; Timsit, J. F., Risk stratification for multidrug-resistant bacteria in patients with skin and soft tissue infection. *Curr Opin Infect Dis* **2020,** *33* (2), 137-145.
306. Abraham, T.; Schooling, S. R.; Nieh, M. P.; Kucerka, N.; Beveridge, T. J.; Katsaras, J., Neutron diffraction study of Pseudomonas aeruginosa lipopolysaccharide bilayers. *J Phys Chem B* **2007,** *111* (10), 2477-83.
307. Clifton, L. A.; Skoda, M. W.; Le Brun, A. P.; Ciesielski, F.; Kuzmenko, I.; Holt, S. A.; Lakey, J. H., Effect of divalent cation removal on the structure of gram-negative bacterial outer membrane models. *Langmuir* **2015,** *31* (1), 404-12.
308. Kucerka, N.; Papp-Szabo, E.; Nieh, M. P.; Harroun, T. A.; Schooling, S. R.; Pencer, J.; Nicholson, E. A.; Beveridge, T. J.; Katsaras, J., Effect of cations on the structure of bilayers formed by lipopolysaccharides isolated from Pseudomonas aeruginosa PAO1. *J Phys Chem B* **2008,** *112* (27), 8057-62.
309. Langley, S.; Beveridge, T. J., Effect of O-side-chain-lipopolysaccharide chemistry on metal binding. *Appl Environ Microbiol* **1999,** *65* (2), 489-98.
310. Parikh, S. J.; Chorover, J., Infrared spectroscopy studies of cation effects on lipopolysaccharides in aqueous solution. *Colloids Surf B Biointerfaces* **2007,** *55* (2), 241-50.
311. Schneck, E.; Schubert, T.; Konovalov, O. V.; Quinn, B. E.; Gutsmann, T.; Brandenburg, K.; Oliveira, R. G.; Pink, D. A.; Tanaka, M., Quantitative determination of ion distributions in bacterial lipopolysaccharide membranes by grazing-incidence X-ray fluorescence. *Proc Natl Acad Sci U S A* **2010,** *107* (20), 9147-51.
312. Shephard, J.; McQuillan, A. J.; Bremer, P. J., Mechanisms of Cation Exchange by Pseudomonas aeruginosa PAO1 and PAO1 wbpL, a Strain with a Truncated Lipopolysaccharide. *Appl Environ Microbiol* **2008,** *74* (22), 6980-6.
313. Texier, A. C.; Andres, Y.; Le Cloirec, P., Selective biosorption of lanthanide (La, Eu, Yb) ions by Pseudomonas aeruginosa. *Environ Sci Technol* **1999,** *33* (3), 489-495.
314. Goldberg, J. B.; Hatano, K.; Pier, G. B., Synthesis of lipopolysaccharide O side chains by Pseudomonas aeruginosa PAO1 requires the enzyme phosphomannomutase. *J Bacteriol* **1993,** *175* (6), 1605-11.
315. Wolcott, R., Disrupting the biofilm matrix improves wound healing outcomes. *J Wound Care* **2015,** *24* (8), 366-71.

Appendix: Supplemental Information

Table S1. Antibiotic susceptibility table for *P. aeruginosa* clinical isolates										
	minimum inhibitory concentration (ug/mL)									
	R = resistant, I = intermediate, S = susceptible									
ANTIBIOTIC	**OU1**		**OU12**		**OU15**		**OU19**		**OU22**	
aztreonam	16	R	16	R	16	R	16	R	16	R
cefepime	16	I	16	R	32	R	16	R	32	R
ceftazidime	16	R	16	R	16	R	16	R	16	R
ciprofloxacin	2	R	2	I	2	R	2	R	0.5	S
gentamicin	2	S	8	I	2	S	4	S	2	S
meropenem	4	I	1	S	8	R	8	R	8	R
pip/tazobactam	128	R	64	R	128	R	64	R	128	R
tobramycin	2	S	2	S	2	S	4	S	2	S

Table S2. MIC and FICI values for *P. aeruginosa* treated with 600-Da BPEI, cefepime, and their combination.

Strain	**MIC**					**FICI**	**Outcome**
	600-Da BPEI	Cefepime	Cefepime	+	600-Da BPEI		
PA OU15	32	32	0.5	+	16 µg/mL	0.52	Additivity
PA OU19	64	64	8	+	16 µg/mL	0.38	Synergy
PA OU22	64	128	8	+	16 µg/mL	0.31	Synergy

Table S3. MIC and FICI values for *P. aeruginosa* treated with 600-Da BPEI, meropenem, and their combination.

Strain	MIC					FICI	Outcome
	600-Da BPEI	Meropenem	Meropenem	+	600-Da BPEI		
PA OU15	32	64	16	+	8 µg/mL	0.75	Additivity
PA OU19	64	16	1	+	16 µg/mL	0.56	Additivity
PA OU22	64	16	2	+	8 µg/mL	0.63	Additivity

Table S4. MIC and FICI values for *P. aeruginosa* treated with 600-Da BPEI, erythromycin, and their combination.

Strain	MIC					FICI	Outcome
	600-Da BPEI	Erythromycin	Erythromycin	+	600-Da BPEI		
PA OU15	32	256	64	+	8 µg/mL	0.5	Synergy
PA OU19	64	256	2	+	16 µg/mL	0.26	Synergy
PA OU22	64	256	64	+	16 µg/mL	0.5	Synergy

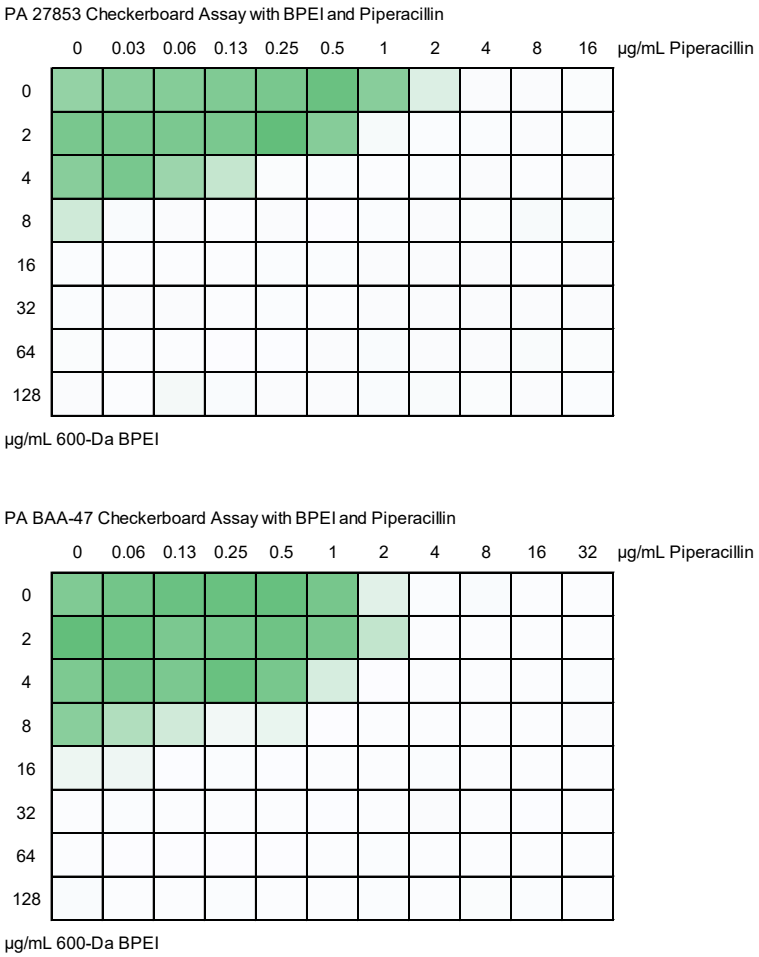

Figure S1. Checkerboard assay data demonstrating that sub-lethal amounts of 600-Da BPEI lower the antibiotic MIC against *Pseudomonas aeruginosa* ATCC 27853 and BAA-47.

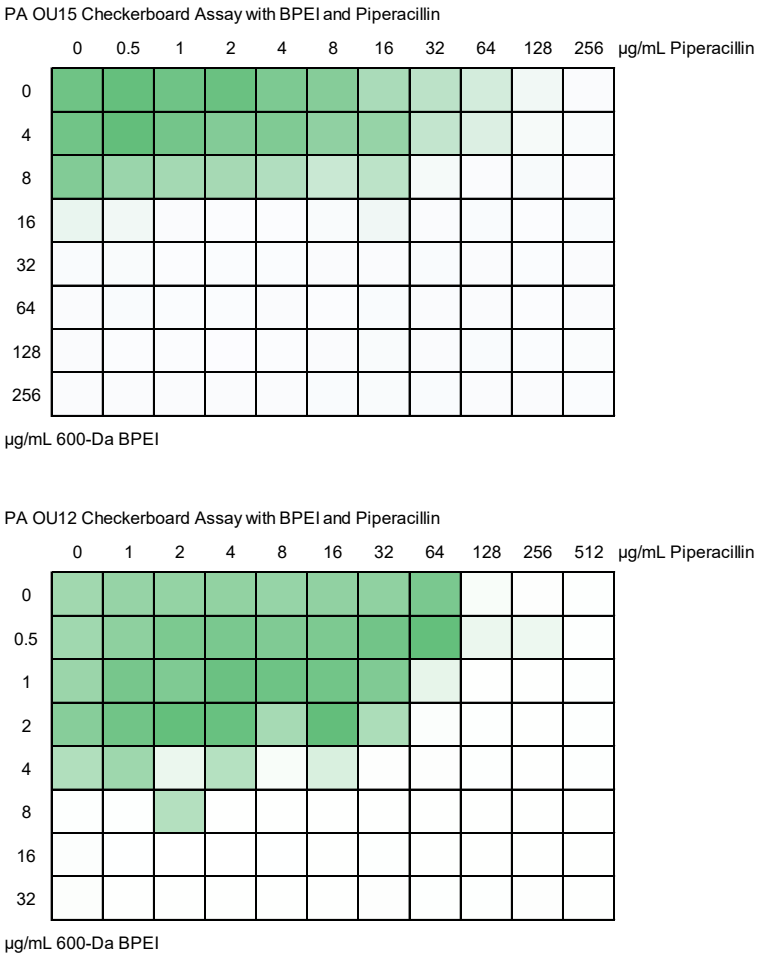

Figure S2. Checkerboard assay data demonstrating that sub-lethal amounts of 600-Da BPEI lower the antibiotic MIC against *Pseudomonas aeruginosa*

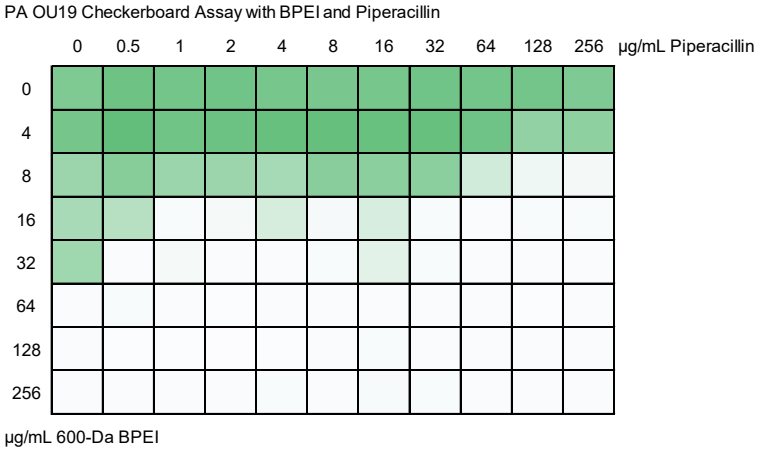

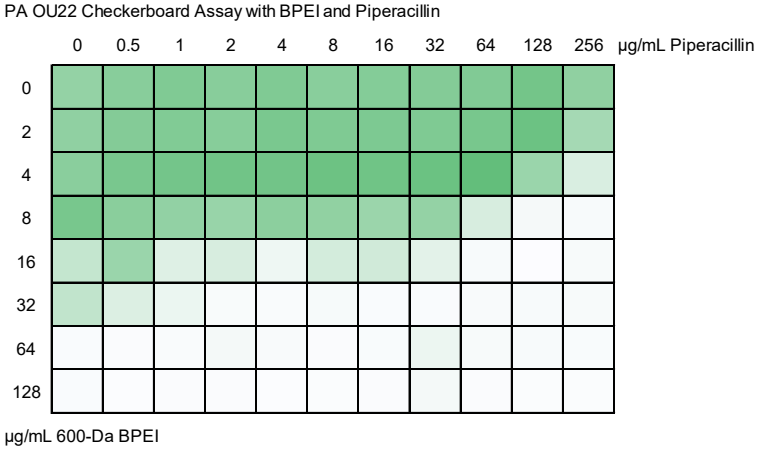

Figure S2 (continued). Checkerboard assay data demonstrating that sub-lethal amounts of 600-Da BPEI lower the antibiotic MIC against *Pseudomonas aeruginosa*

PA OU15 Checkerboard Assay with BPEI and Cefepime

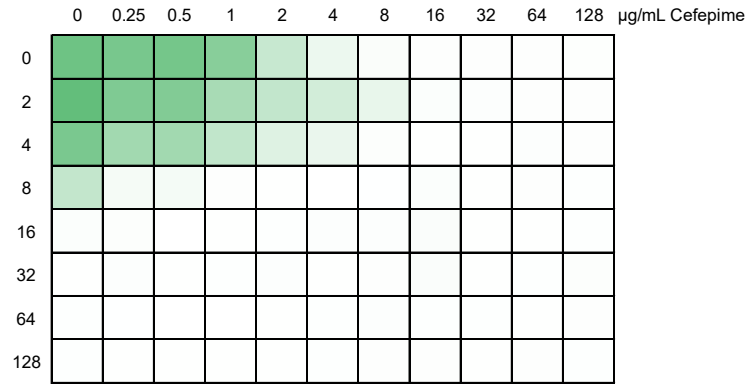

PA OU15 Checkerboard Assay with BPEI and Cefepime

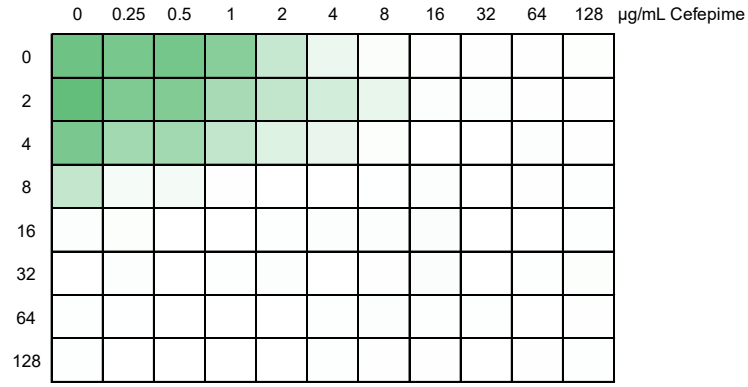

PA OU19 Checkerboard Assay with BPEI and Cefepime

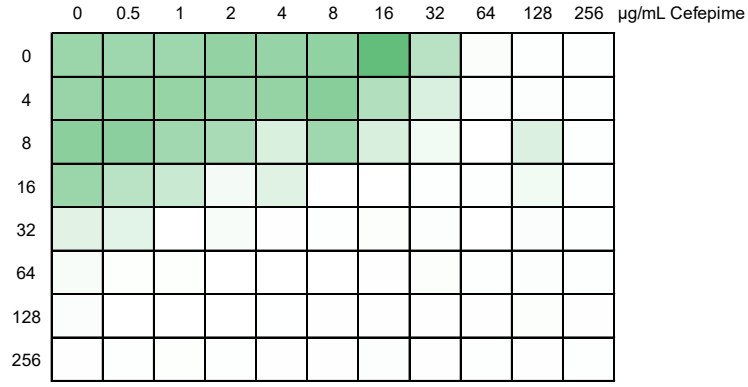

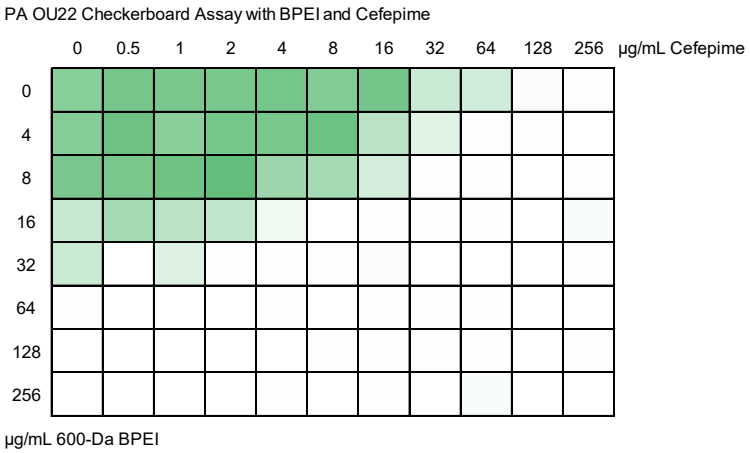

Figure S3. Checkerboard assay data demonstrating that sub-lethal amounts of 600-Da BPEI lower the antibiotic MIC against *Pseudomonas aeruginosa*

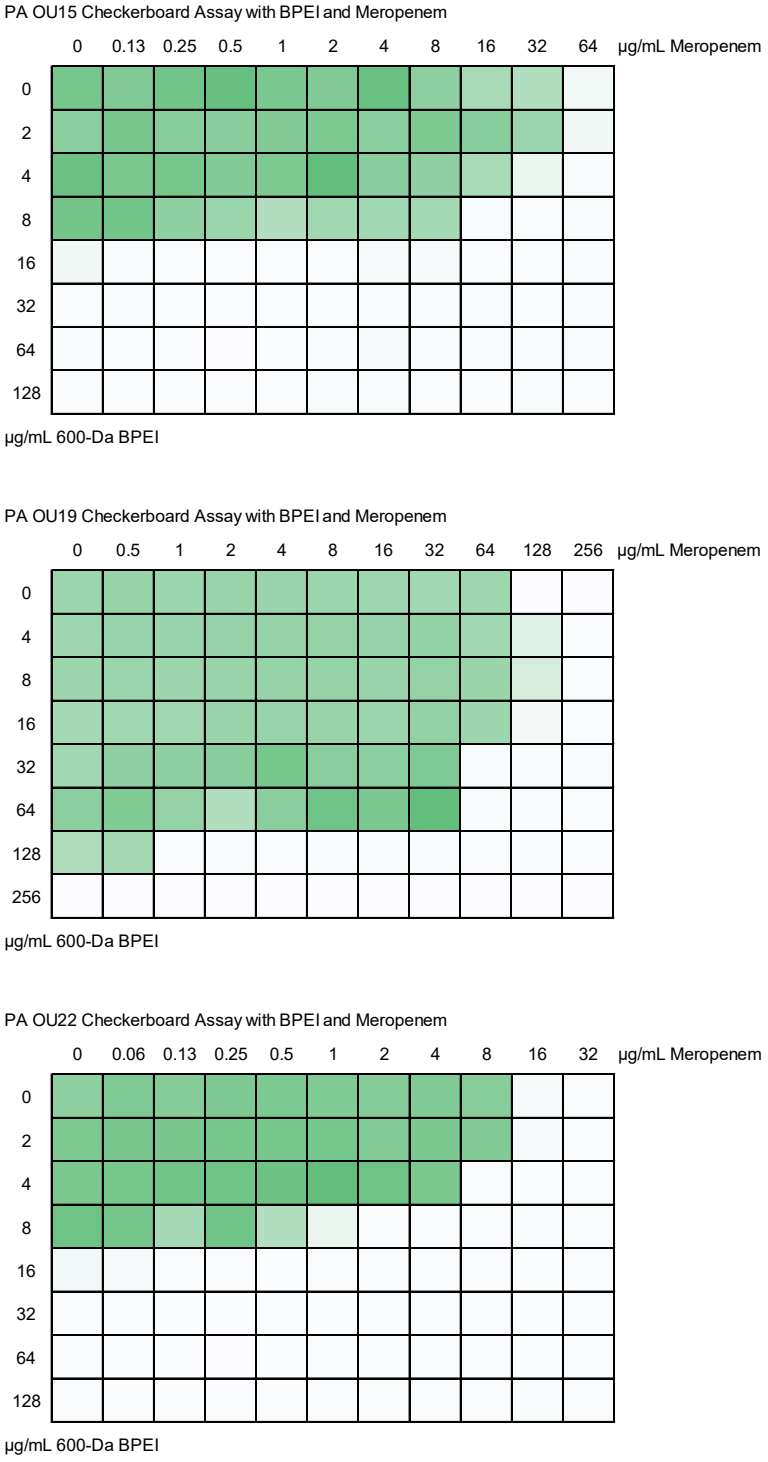

Figure S4. Checkerboard assay data demonstrating that sub-lethal amounts of 600-Da BPEI lower the antibiotic MIC against *Pseudomonas aeruginosa*

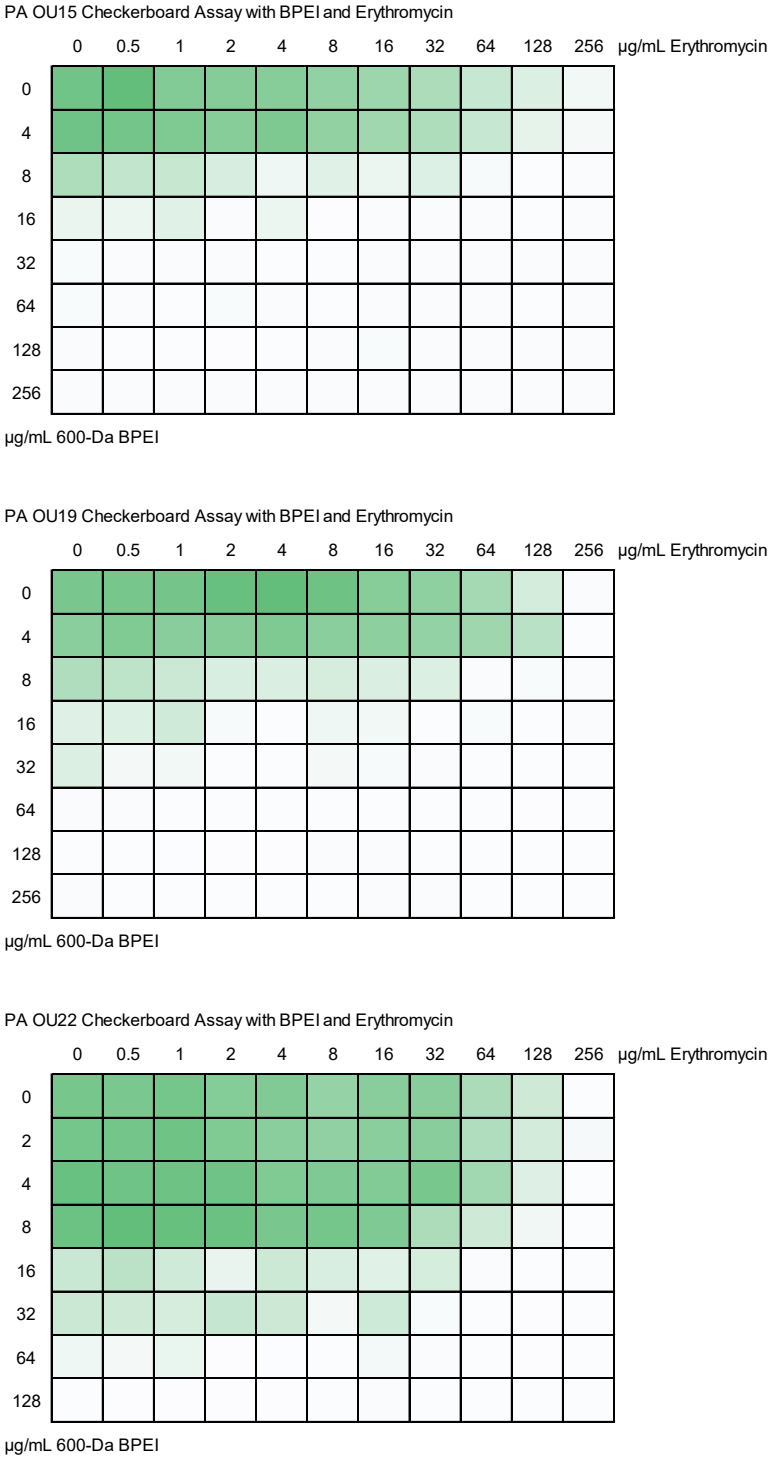

Figure S5. Checkerboard assay data demonstrating that sub-lethal amounts of 600-Da BPEI lower the antibiotic MIC against *Pseudomonas aeruginosa*

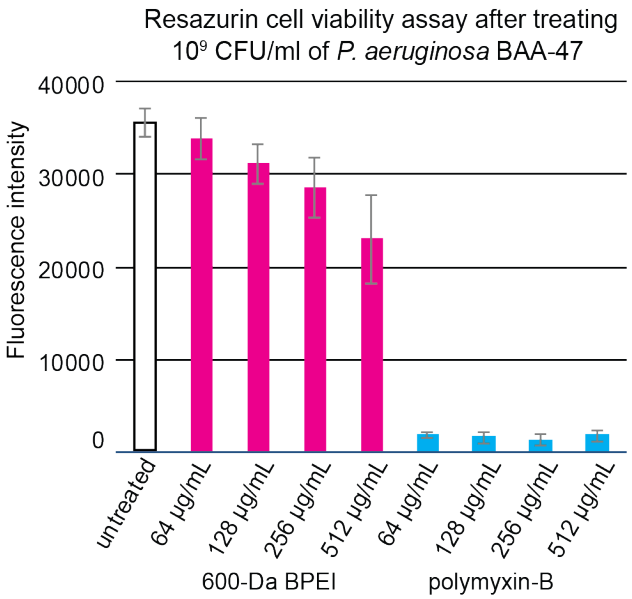

Figure S6. Incubation of PA BAA-47 cells at high cell density (~6x10^9 CFU/mL) with resazurin produces the fluorescence molecule resorufin via cellular metabolism. Treating these cells with 600-Da BPEI prior to resazurin addition results in lower emission that indicates (a) the cells are alive, (b) BPEI has affected the growth rate in a concentration-dependent manner, and (c) the cells are not depolarized. This contrasts with cells treated with polymyxin-B, which kills the cell culture at all concentrations tested.

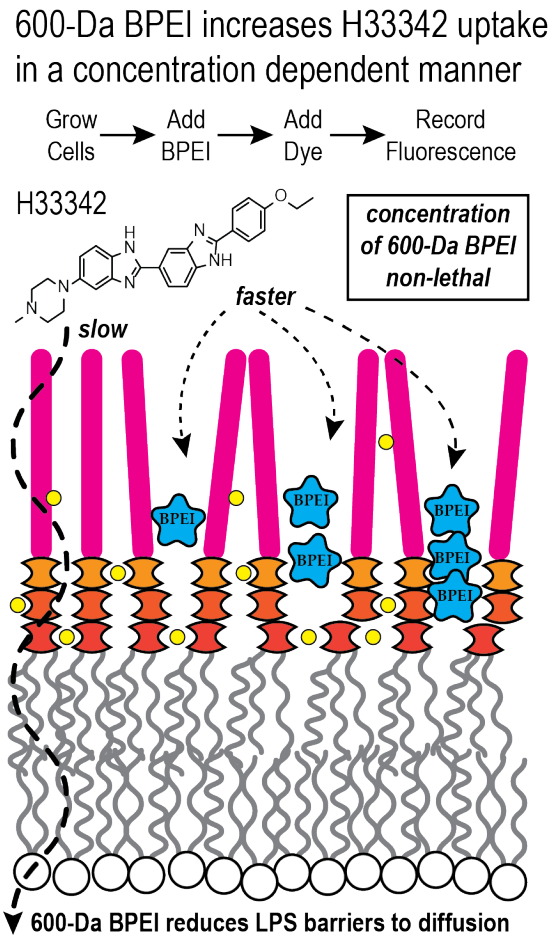

Figure S7. The uptake of H33342 is a multi-step process with exponential kinetics. This illustration is used to explain the concentration dependence of dye uptake. The rate of influx increases as the passive diffusion barriers are lowered from 600-Da BPEI binding to additional anionic sites on LPS molecules.

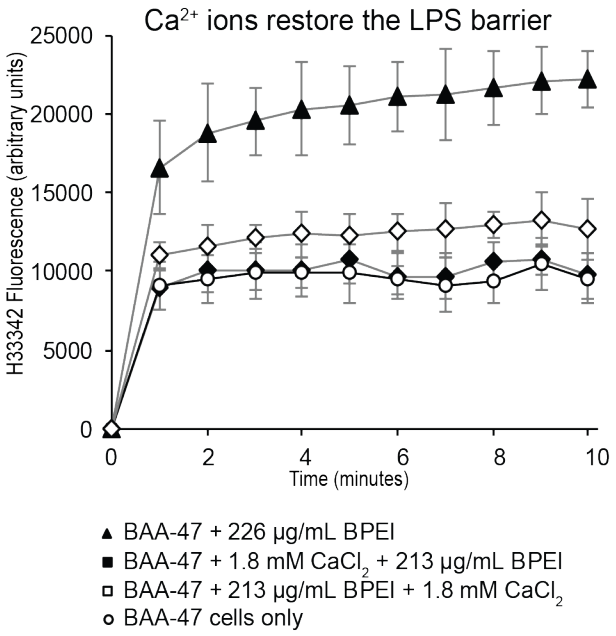

Figure S8. Calcium ions occupy LPS binding sites that would attract BPEI molecules. 600-Da BPEI binds with LPS and increase H33342 influx (triangles) compared to untreated cells (open circles). However, adding 1.8 mM $CaCl_2$ to BPEI-treated cells results in a reduction of dye influx (open squares) as the metals ions occupy remaining anionic sites and restore LPS barriers to diffusion. Likewise, if the metal ions are added first (closed squares), all LPS anionic sites are occupied, preventing the binding of 600-Da BPEI that would otherwise increase dye influx.

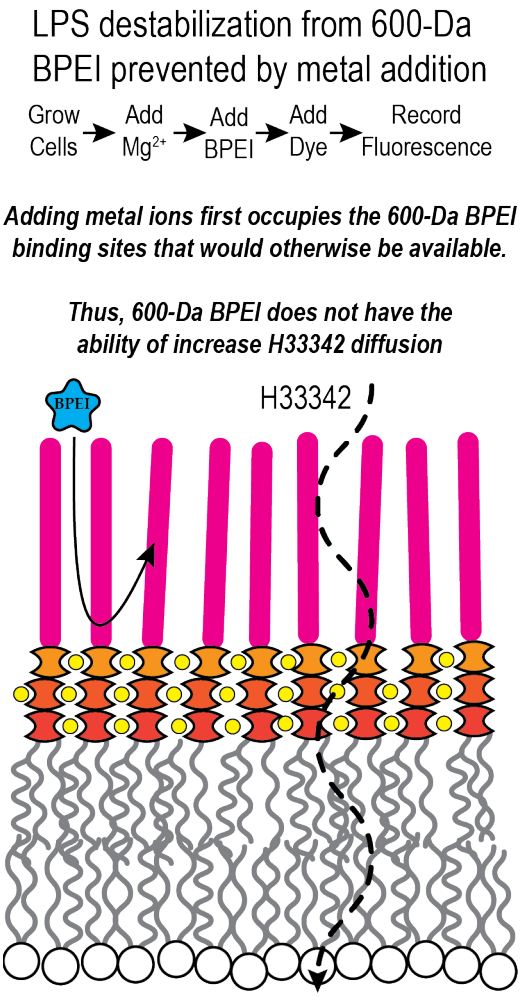

Figure S9. Illustration of using excess metal ions (yellow circles) to occupy the anionic site of LPS and prevent the binding of 600-Da BPEI. In this way, the diffusion barrier of LPS remains intact and BPEI is unable to assist with the uptake of the H33342 dye.

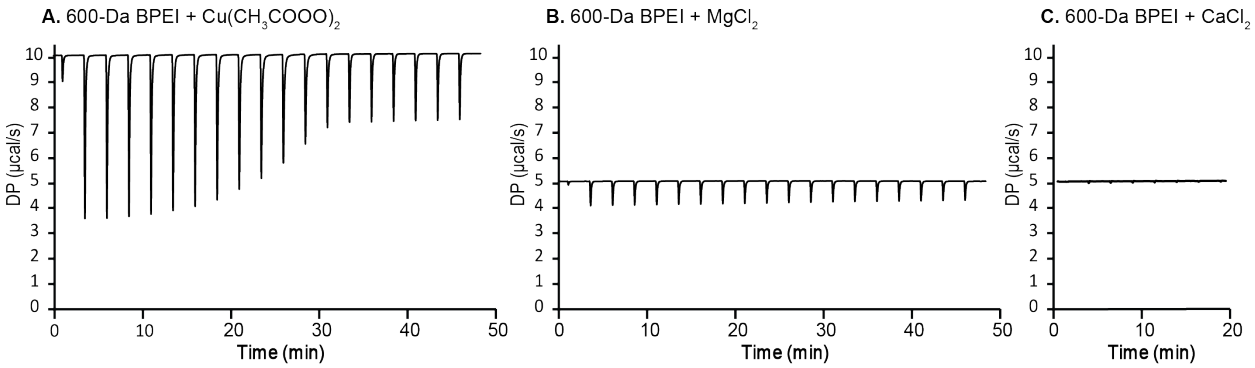

Figure S10. ITC data confirm that 600-Da BPEI can bind with copper ions (A) but there is no binding or chelation with magnesium (B) or calcium ions (C). This contrasts with EDTA, a well-known chelator of these divalent metal ions.

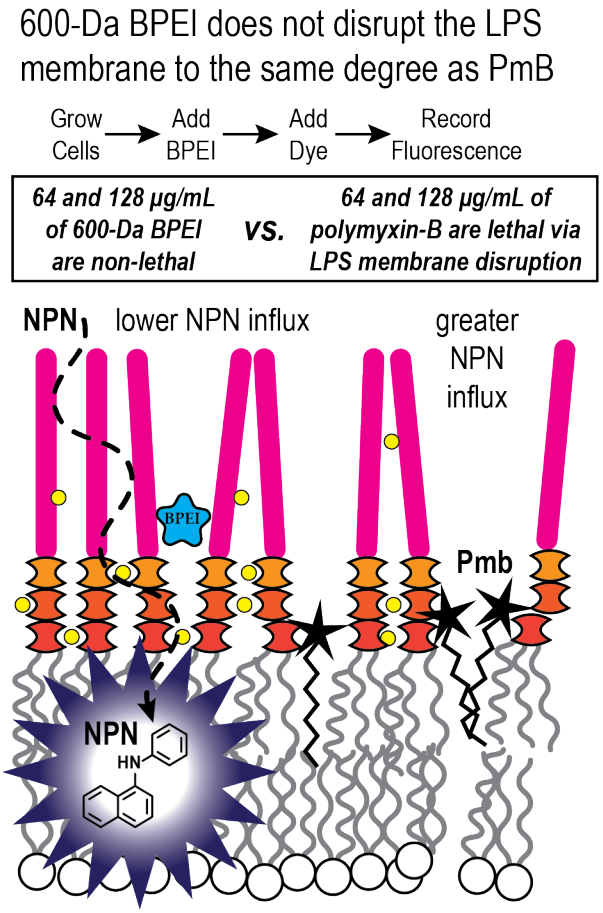

Figure S11. Illustration of the dye 1-*N*-phenylnaphthylamine (NPN), which accumulates in hydrophobic regions and fluoresces when bound to phosphate groups. Polymyxin-B (PmB) allows greater uptake of NPN than 600-Da BPEI. The sub-lethal concentrations of 600-Da BPEI allow NPN access to the membrane but the resazurin assay data in Figure S6 show that the cell membranes are not disrupted, a process that would kill the bacterium To the contrary, similar amounts of polymyxin-B increases the NPN intensity by disrupting the membrane and killing the bacterial cells.

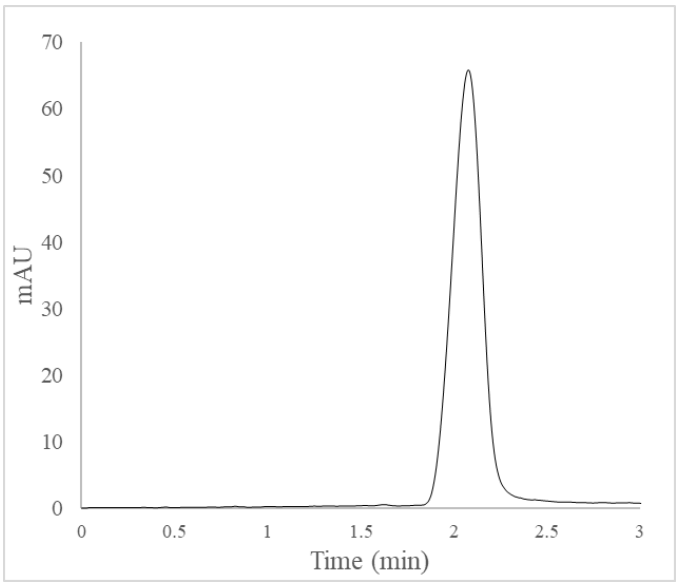

Figure S12. HPLC chromatogram of aqueous 600-Da BPEI (2.56 mg/mL). Retention time of BPEI peaks at 2.09 min. This only peak indicates that the BPEI stock solution does not contain other contaminants.

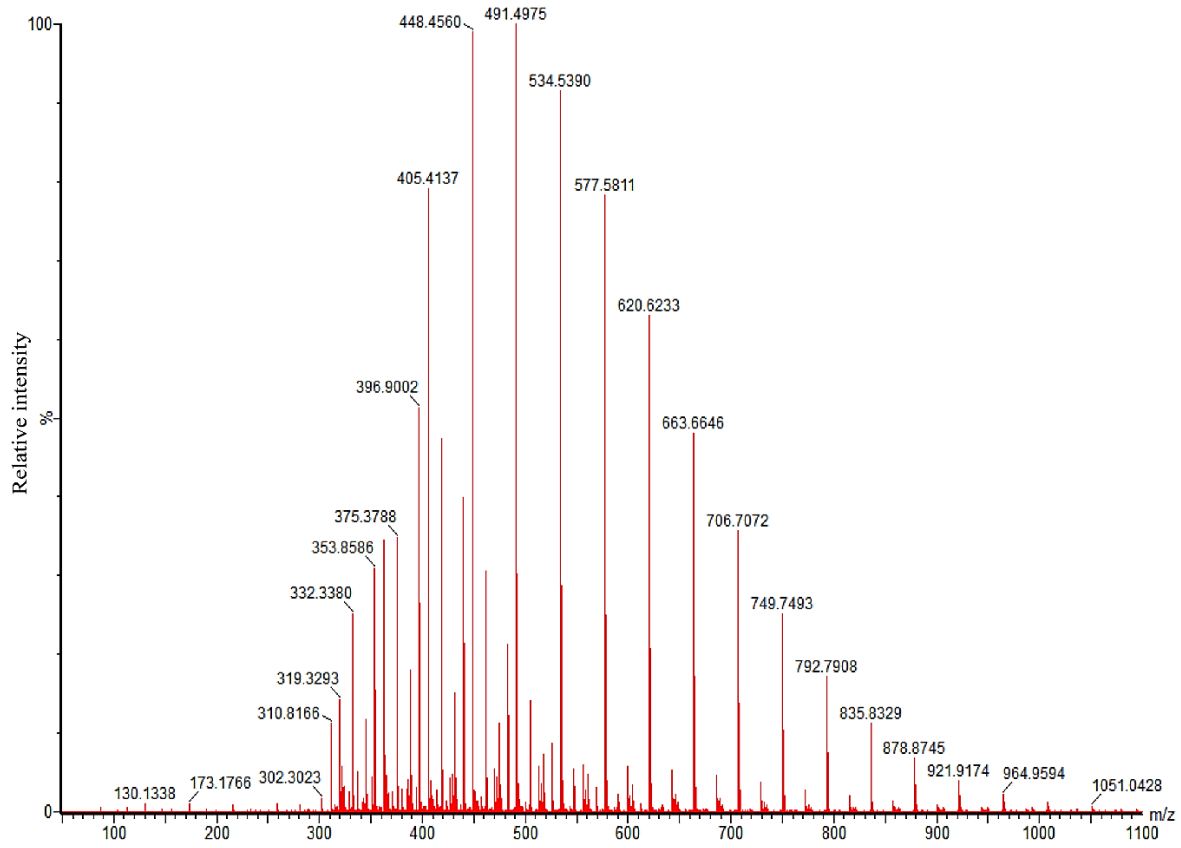

Figure S13. Mass spectrum of 600-Da BPEI. Most abundant peaks are around ~500 m/z which are the most ionized fragments of 600-Da BPEI. Each peak has a similar difference of 43 m/z from the adjacent peak, which is equal to the mass ratio of one amine and an ethyl repeating unit of the polymer (i.e. 534.5 – 491.5 = 43 m/z).

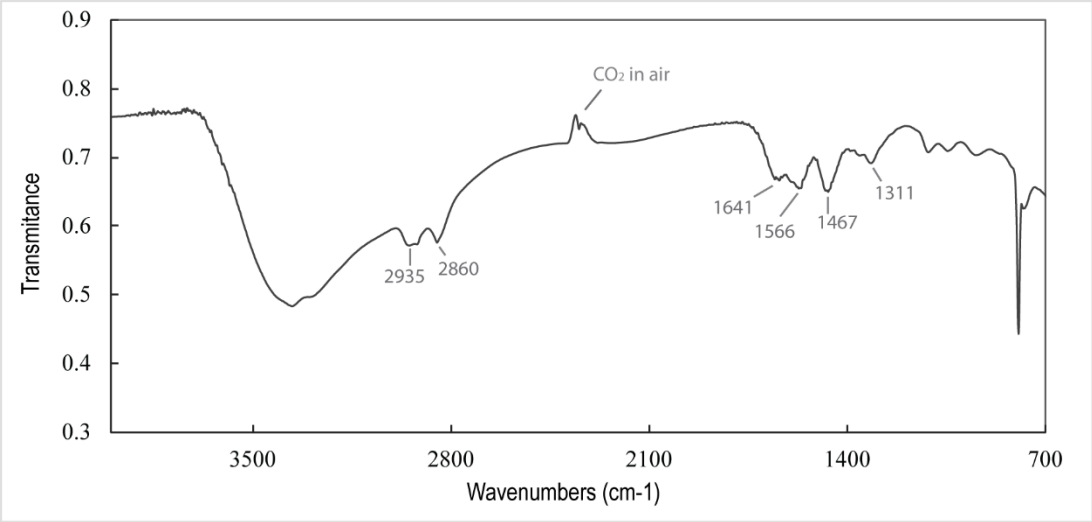

Figure S14. FTIR spectrum of 600-Da BPEI (in CCl_4). Broad peak at 3300-3500 cm^{-1} indicates the N-H bond of amines in BPEI. Peaks of 2935 and 2860 and 1467 cm^{-1} are from alkane C-H stretches of the alkyl spacers. The two peaks at 1641 and 1566 cm^{-1} are from the C-C stretch of polymeric BPEI. Peak of 1311 cm^{-1} indicates the C-N bond.

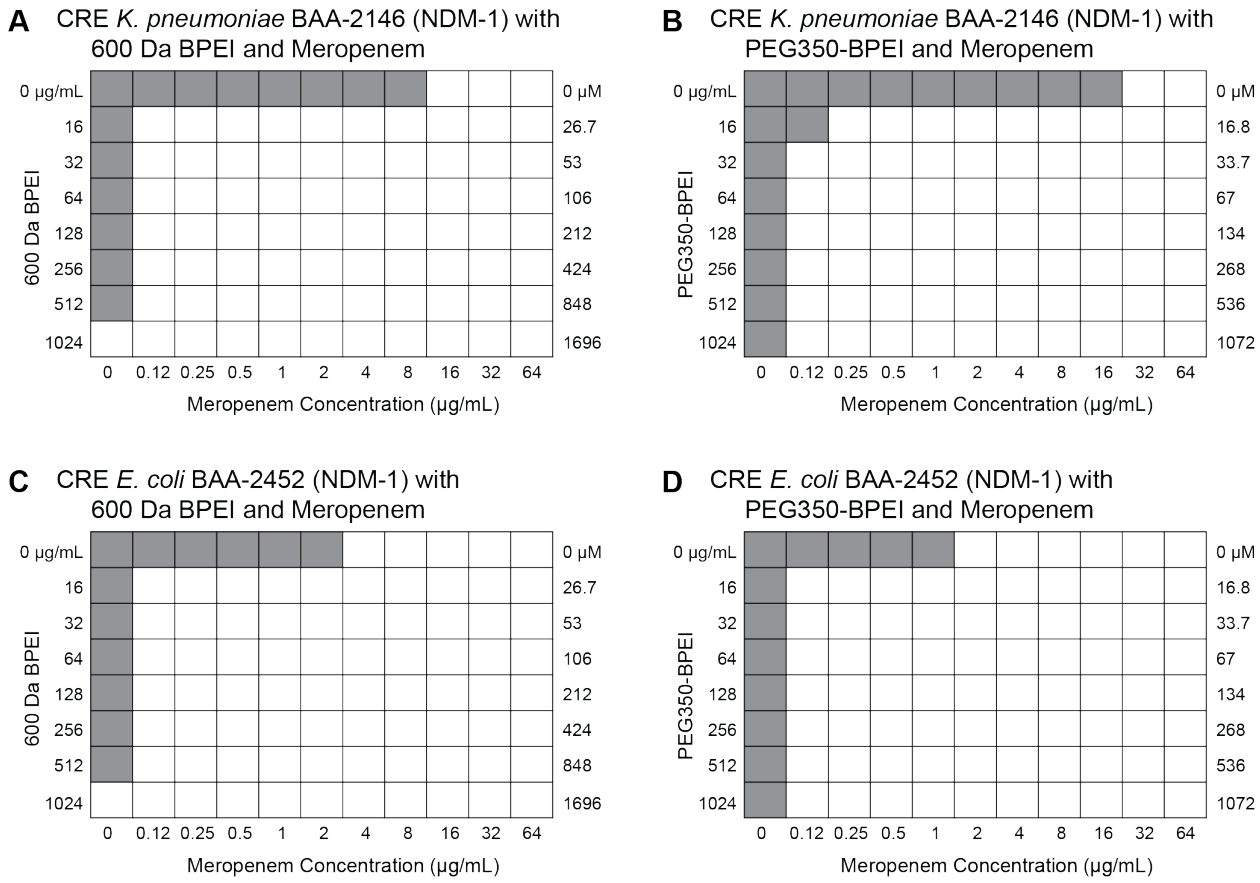

Figure S15. Checkerboard assay data for killing carbapenem-resistant *Enterobacteriaceae* (CRE) with meropenem (MER) antibiotic. The range of 600 Da BPEI or PEG350-BPEI used in the assay ranged from 0 to 1024 µg/mL.

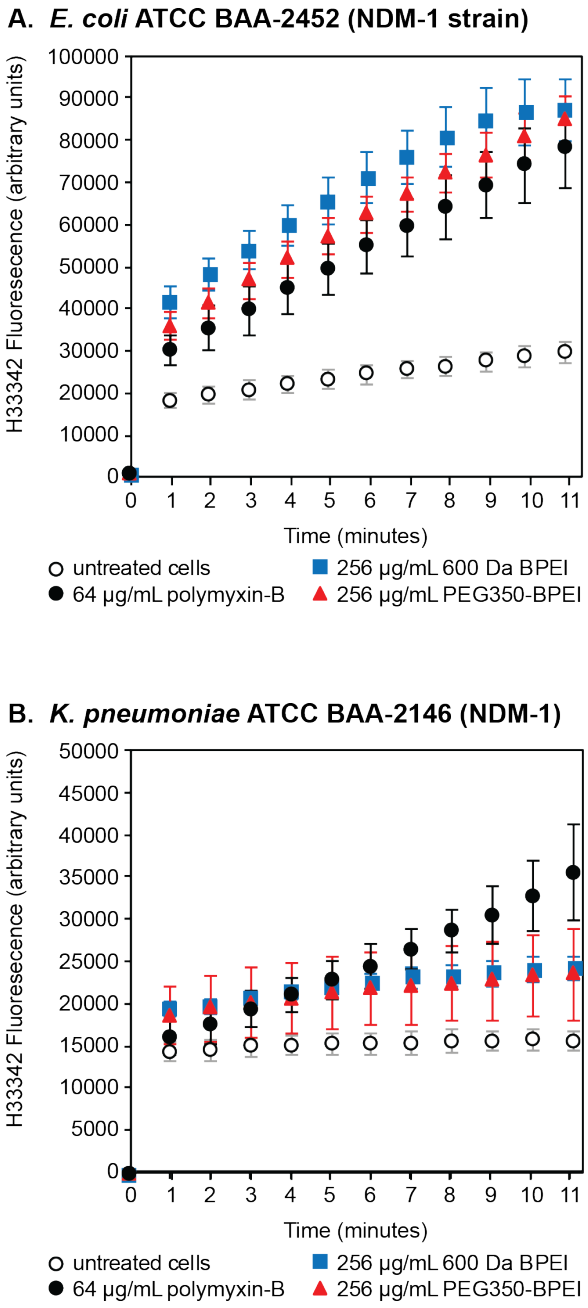

Figure S16. Fluorescence intensity data for the intracellular accumulation of the DNA-binding compounds H33342 with error bars (n = 5). Both 600-Da BPEI (blue squares) and PEG350-BPEI (red triangles) increase the uptake of H33342 by *E. coli* BAA-2452 (A), but the effect is lower with *K. pneumoniae* BAA-2146 (B).

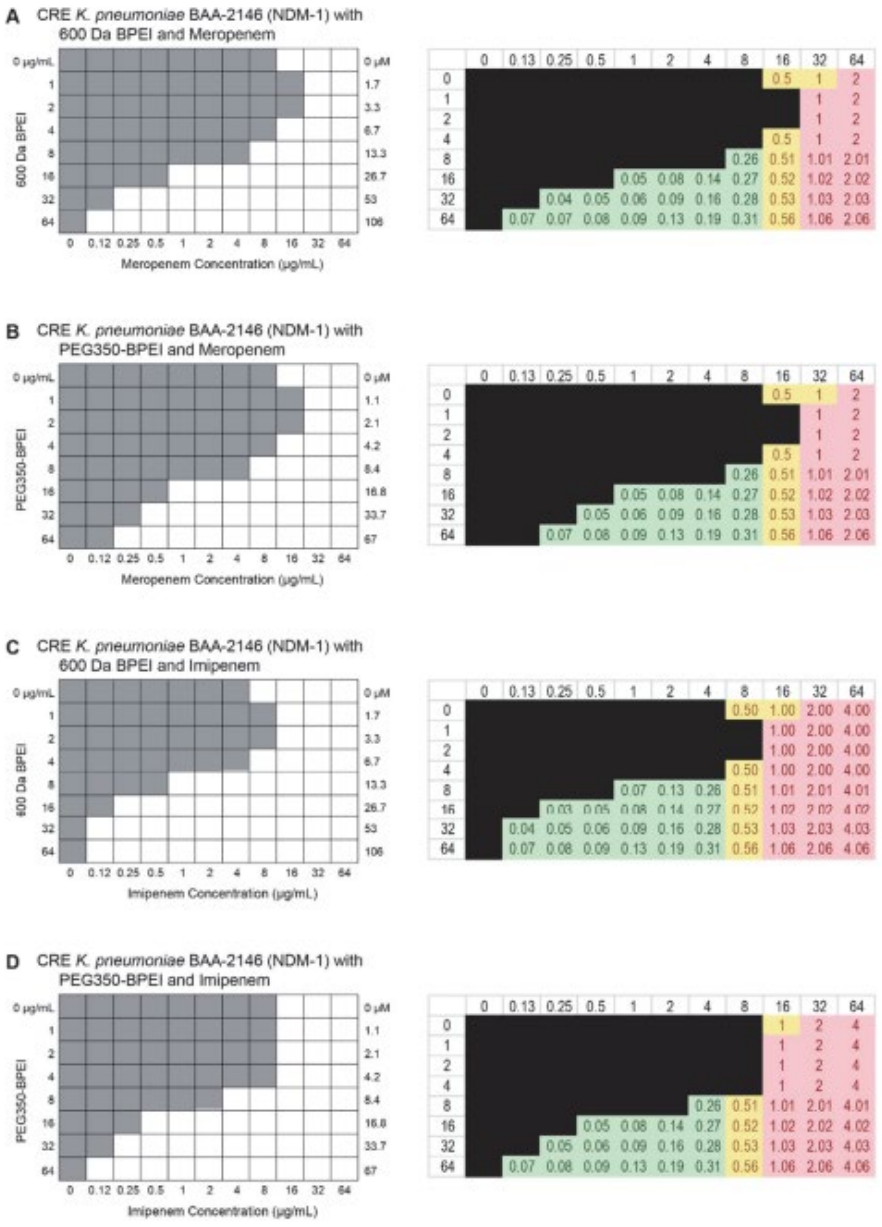

Figure S17a. Reproduction of the checkerboard assay data in Figure 31 with the fractional inhibitory concentration indices (FICI). The FICI is calculated using the MIC of the antibiotics and potentiators determined from Figure S15. MIC for 600 Da BPEI = 1024 µg/mL; MIC for PEG350-BPEI = 1024 µg/mL. An FICI lower than 0.5 indicates synergy between the treatments, while an FICI between 0.5 and 1 represents additivity (from the reference "Terminology relating to methods for the determination of susceptibility of bacteria to antimicrobial agents", Clinical Microbiology and Infection **2000**, 6 (9), pp. 503-508).

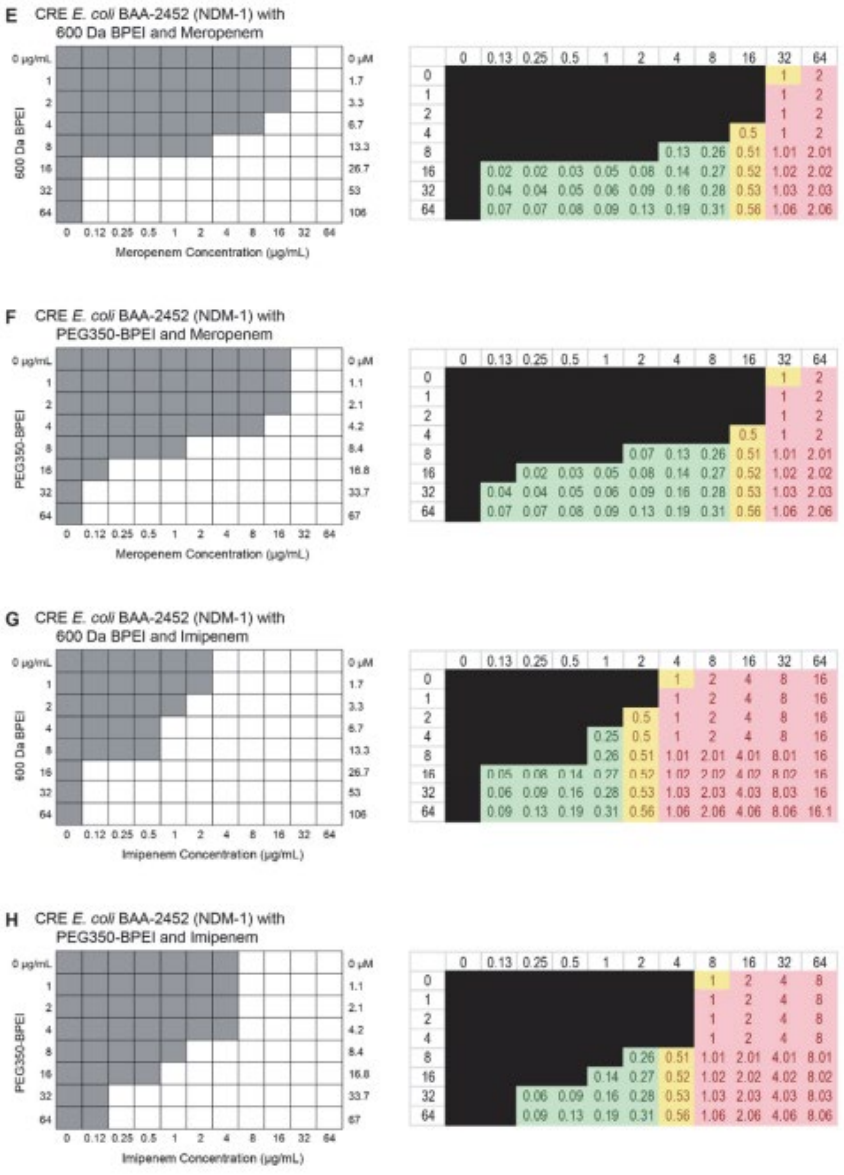

Figure S17b. Reproduction of the checkerboard assay data in Figure 31 with the fractional inhibitory concentration indices (FICI). The FICI is calculated using the MIC of the antibiotics and potentiators determined from Figure S15. MIC for 600 Da BPEI = 1024 µg/mL; MIC for PEG350-BPEI = 1024 µg/mL. An FICI lower than 0.5 indicates synergy between the treatments, while an FICI between 0.5 and 1 represents additivity (from the reference "Terminology relating to methods for the determination of susceptibility of bacteria to antimicrobial agents", Clinical Microbiology and Infection **2000**, *6 (9)*, pp. 503-508).

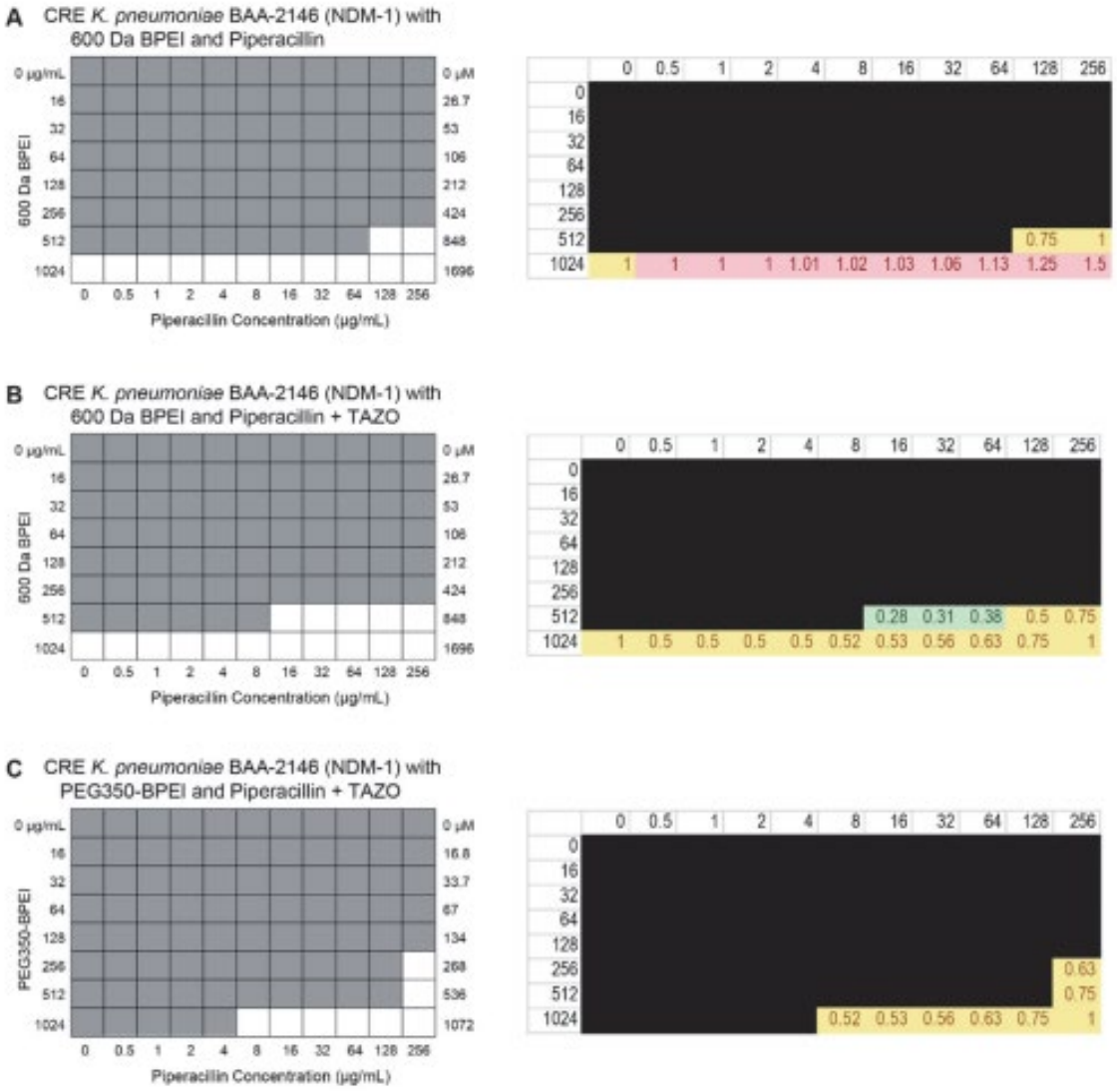

Figure S17c. Reproduction of the checkerboard assay data in Figure 31 with the fractional inhibitory concentration indices (FICI). The FICI is calculated using the MIC of the antibiotics and potentiators determined from Figure S15. MIC for 600 Da BPEI = 1024 µg/mL; MIC for PEG350-BPEI = 1024 µg/mL. An FICI lower than 0.5 indicates synergy between the treatments, while an FICI between 0.5 and 1 represents additivity (from the reference "Terminology relating to methods for the determination of susceptibility of bacteria to antimicrobial agents", Clinical Microbiology and Infection **2000**, *6 (9),* pp. 503-508).

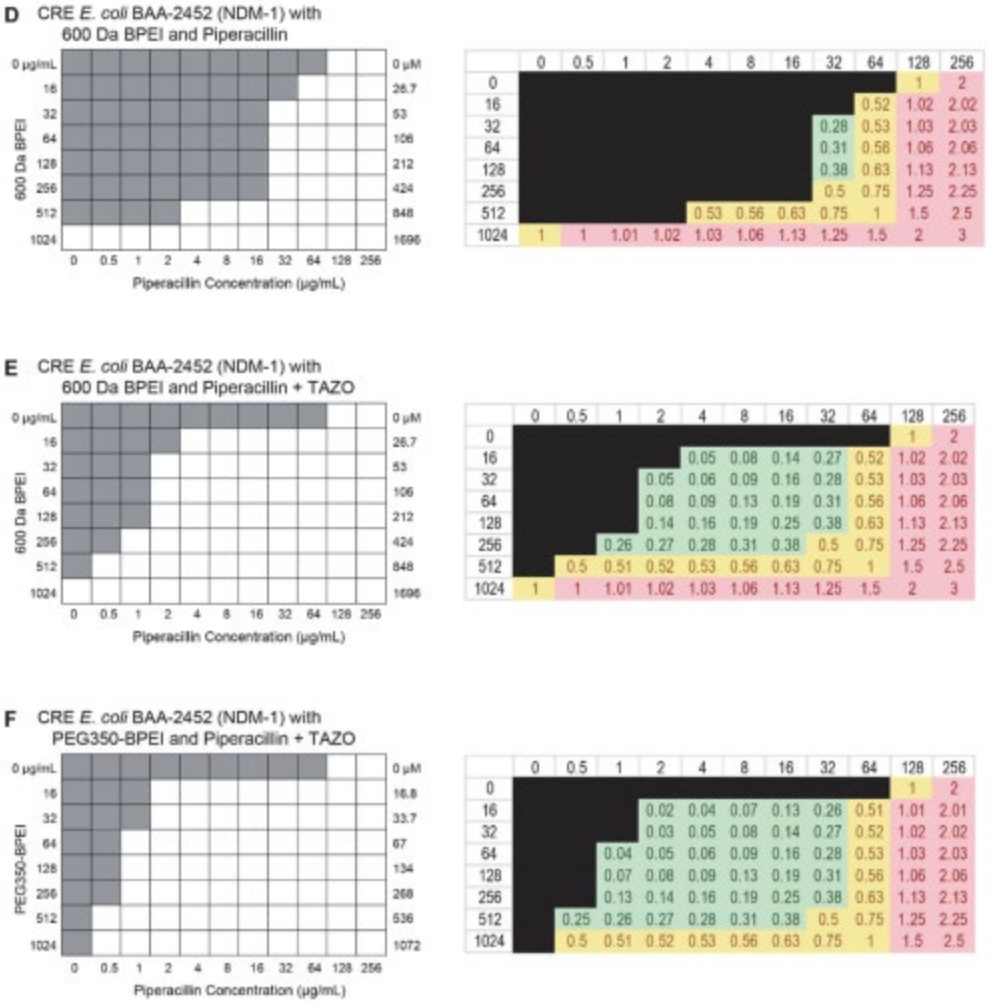

Figure S18. Reproduction of the checkerboard assay data in Figure 34 with the fractional inhibitory concentration indices (FICI). The FICI is calculated using the MIC of the antibiotics and potentiators determined from Figure S15. MIC for 600 Da BPEI = 1024 µg/mL; MIC for PEG350-BPEI = 1024 µg/mL. An FICI lower than 0.5 indicates synergy between the treatments, while an FICI between 0.5 and 1 represents additivity (from the reference "Terminology relating to methods for the determination of susceptibility of bacteria to antimicrobial agents", Clinical Microbiology and Infection **2000**, *6 (9),* pp. 503-508).